DESIGN AND ANALYSIS OF HELICAL COIL SPRING FORMS FOR INDEPENDENT SUSPENSIONS OF AUTOMOBILES

A THESIS SUBMITTED TO
THE GRADUATE SCHOOL OF NATURAL AND APPLIED SCIENCES
OF
MIDDLE EAST TECHNICAL UNIVERSITY

BY

GÖKHAN YAZAR

IN PARTIAL FULFILLMENT OF THE REQUIREMENTS
FOR
THE DEGREE OF MASTER OF SCIENCE
IN
MECHANICAL ENGINEERING

DECEMBER 2015

Approval of the thesis:

DESIGN AND ANALYSIS OF HELICAL COIL SPRING FORMS FOR INDEPENDENT SUSPENSIONS OF AUTOMOILES

submitted by **GÖKHAN YAZAR** in partial fulfillment of the requirements for the degree of **Master of Science in Mechanical Engineering Department, Middle East Technical University** by,

Prof. Dr. M.Gülbin Dural Ünver
Dean, Graduate School of **Natural and Applied Sciences** _____

Prof. Dr. Tuna Balkan
Head of Department, **Mechanical Engineering** _____

Prof. Dr. Y.Samim Ünlüsoy
Supervisor, **Mechanical Engineering Dept., METU** _____

Examining Committee Members:

Prof. Dr. Metin Akkök
Mechanical Engineering Dept., METU _____

Prof. Dr. Y.Samim Ünlüsoy
Mechanical Engineering Dept., METU _____

Prof. Dr. Tuna Balkan
Mechanical Engineering Dept., METU _____

Prof. Dr. Suat Kadıoğlu
Mechanical Engineering Dept., METU _____

Asst. Prof. Dr. Kutluk Bilge Arıkan
Mechatronics Engineering Dept., Atılım University _____

Date: **11.12.2015**

I hereby declare that all information in this document has been obtained and presented in accordance with academic rules and ethical conduct. I also declare that, as required by these rules and conduct, I have fully cited and referenced all material and results that are not original to this work.

Name, Last Name : Gökhan YAZAR

Signature :

ABSTRACT

DESIGN AND ANALYSIS OF HELICAL COIL SPRING FORMS FOR INDEPENDENT SUSPENSIONS OF AUTOMOBILES

Yazar, Gökhan
M. S., Department of Mechanical Engineering
Supervisor: Prof. Dr. Y.Samim Ünlüsoy
December 2015, 129 pages

Suspension system is one of the major and indispensable subsystems for land vehicles and has functions of providing better road holding, handling, and ride comfort. There are many suspension system types used for automobiles, and MacPherson strut suspension is one of the most widely used suspension system type due to its favorable features like simplicity, low cost, and high performance. However, there exists a drawback of this suspension type; since the coil springs have no ability to absorb lateral forces, undesired dry friction effects on the damper may degrade the ride comfort. As remedy to this drawback, the most popular and contemporary application is the use of coil spring forms which are called side load springs.

In this study, a procedure for the design of a class of side load springs to be used in MacPherson strut type suspension to reduce the side loads on the damper is developed. The procedure starts with the analysis of the suspension system to estimate the side force required. The next step is the determination of the side load

spring form to provide the required side force. Then a finite element model of the spring is prepared and the side force provided by the designed spring is obtained. A graphical user interface is developed to consider various design alternatives by varying design parameters.

Keywords: MacPherson strut suspension, side load spring, lateral force, ride comfort, finite element analysis

ÖZ

BAĞIMSIZ SÜSPANSİYONLU OTOMOBİLLER İÇİN SARMAL YAY FORMLARININ TASARIMI VE ANALİZİ

Yazar, Gökhan
Yüksek Lisans, Makina Mühendisliği Bölümü
Tez Yöneticisi: Prof. Dr. Y.Samim Ünlüsoy
Aralık 2015, 129 sayfa

Süspansiyon sistemi kara araçlarının en önemli ve vazgeçilmez alt sistemlerinden biridir ve süspansiyon sistemlerinin temel fonksiyonları arasında yol tutuşu, direksiyon hakimiyeti ve sürüş konforu gibi fonksiyonlar önde gelmektedir. Otomobillerde bir çok süspansiyon tipi kullanılmakla beraber, MacPherson süspansiyon sistemi basit yapısı, düşük maliyeti, yüksek performansı gibi olumlu özellikleri nedeniyle en yaygın şekilde kullanılan süspansiyon sistemlerinden biridir. Ancak, bu süspansiyon sisteminin bir kusuru bulunmaktadır; sarmal yayların yanal kuvvetleri sönümleme kabiliyeti olmadığı için amortisör üzerinde istenmeyen yan kuvvetler oluşarak kuru sürtünme etkisiyle sürüş konforunun azalmasına neden olur. Bu kusuru ortadan kaldırmak için en güncel uygulama ise yan yük yayı olarak isimlendirilen sarmal yay formlarının kullanılmasıdır.

Bu çalışmada, MacPherson süspansiyonlarında kullanılan ve amörtisör üzerindeki yanal yükleri azaltan yan yük yayları için bir tasarım prosedürü geliştirilmiştir. Prosedür süspansiyon sisteminin çözümlenerek gerekli yan kuvvetin bulunması ile

başlamaktadır. İkinci adım ise istenen yan kuvveti sağlayabilecek yan yük yayı formunun hesaplanmasıdır. Elde edilen tasarımın bir sonlu elemanlar modeli hazırlanarak, tasarlanan yayın sağladığı yan kuvvet elde edilir. Yayın tasarım parametrelerinin kolayca değiştirilerek farklı tasarım alternatiflerinin elde edilmesi için bir kullanıcı arayüzü de geliştirilmiştir.

Anahtar kelimeler: MacPherson süspansiyon sistemi, yan yük yayı, yanal yük, sürüş konforu, sonlu elemanlar analizi

ACKNOWLEDGEMENTS

I would like to express my deepest gratitude to my supervisor Prof. Dr. Y.Samim Ünlüsoy for his guidance, advice, criticism, encouragements and insight throughout this thesis study.

I would like to acknowledge TÜBİTAK (BİDEB 2228 Scholarship) for funding this thesis work.

I would like to thank Emre Dede and Kemal Uçan for their gentle supports to my study.

Also, completion of this project could not have been accomplished without the support of my family; my parents Dilek and Ali, my brothers ‘Balık’ Furkan and Nuri.

TABLE OF CONTENTS

LIST OF TABLES

TABLES

LIST OF FIGURES

FIGURES

LIST OF SYMBOLS

n'	Total number of coils
n	Number of active coils
$d\ or\ d_w$	Diameter of the wire
δ_{max}	Maximum compression(deflection)
$D\ or\ D_m$	Mean diameter of the coil
k	Spring rate (stiffness)
W	Axial load
L_S	Solid length of the coil spring
L_{f_i}	Free length of inner side of the coil spring
L_{f_o}	Free length of outer side of the coil spring
L_F	Free length of the coil spring
L_w	Working length of the coil spring
Δh_i	Deflection at the inner side of the coil spring
Δh_o	Deflection at the outer side of the coil spring
F_{inner}	Vertical spring force at the inner side of the coil spring
F_{outer}	Vertical spring force at the outer side of the coil spring
F_v	Total vertical spring force
c	Displacement of spring centerline
c_u	Displacement of spring centerline at the top of the coil spring
α	Angle between the spring centerline and direction of the force on the damper top, and angle of the spring force action line

p	Pitch of the coils
$\tau \; or \; \tau_{max}$	Maximum shear stress
τ_1	Torsional shear stress
τ_2	Direct shear stress
G	Rigidity of the spring material
E	Elastic Modulus of the spring material
C	Spring index
δ	Deflection of the spring(as a result of W)
T	Twisting moment
K_S	Shear stress factor
$K \; or \; K_w$	Wahl's stress factor
θ	Angular deflection of the wire when upon by the torque T
l	Total active length
F	Force on the top of damper
F_L	Force on the LCA
F_A	Force exerted from the road
F_Q	Lateral force on the damper
R	Radius of curvature
ρ	Amount of curvature
J	Polar moment of inertia of the spring wire
γ	End condition constant (buckling)
F_{LD}	Desired lateral force

LIST OF ABBREVIATIONS

FEA	Finite Element Analysis
LCA	Lower Control Arm
CAD	Computer Aided Design
GUI	Graphical User Interface
DOF	Degree of Freedom

CHAPTER 1

INTRODUCTION

If roads were perfectly flat and had no irregularities, suspensions would not be necessary. However, roads are far away from being perfectly flat, and for this reason suspension systems have been developed. A suspension system is one of the indispensable structures of land vehicles with the main functions of isolating the body from road excitations for good ride comfort and maintaining contact between road surface and tires to get better road holding and steering ability.

Many types of suspension systems have been designed over the years. MacPherson strut type suspension is the most widely used suspension system type with its advantages like simplicity, low manufacturing and maintenance cost, high performance, low unsprung weight, and so forth. The MacPherson strut suspension combines simply a coil spring and a damper coaxially into a single unit that makes contribution to its simplicity and thus provides a compact and light suspension system. Unfortunately there exists a drawback of this suspension type. Since the coil springs have no ability to absorb lateral forces, side forces are developed on the strut and undesired dry friction occurs between the damper piston and the cylinder as well as between the damper piston rod and cylinder bearing. This effect results in stick-slip type action and degrades ride comfort. Further undue damage to piston and piston rod seals occurs. To eliminate this drawback, the suspension spring is mounted on the damper with an offset. However, the modern approach is the use of coil spring forms which are called side load springs.

1.1. OVERVIEW OF THE THESIS

In the first and second chapters of this study, the vehicle suspension systems and special features of MacPherson type of suspension are explained; recent studies and patents related to the thesis study are examined; and general information on coil springs are given. Before going into the analyses of side load springs, static analyses of conventional helical coil springs are investigated to validate the finite element analysis presented in the third chapter. While validating the analysis model; mesh type, mesh size, spring end connection types, and spring seat types are examined. After static analysis results are validated, analyses of some intuitively designed side load springs are carried out and the results of conventional springs and side load springs are compared. Then, mathematical aspect of the side load spring is investigated and formulations are obtained for the spring centerline curvature of the side load spring that can take lateral forces in the early sections of the fourth chapter. These equations are used in side load spring modeling which is done in CATIA by importing data from MATLAB. Finally, the study is concluded, results are evaluated and finalized and possible extensions of the study in future are discussed.

1.2. SUSPENSION SYSTEM

Suspension is the system of mechanical components that connects the wheels and axles to the vehicle body. The requirements of ride comfort, road holding, and handling are to be satisfied as the main functions of a suspension system. A well designed suspension system should meet all of the above mentioned requirements. However, ride comfort is generally assumed to be the most important task of the suspension system and designs mostly start with this function in mind. Therefore, many different suspension systems have been designed, manufactured, and used since the early days of automobiles.

Suspension systems can be classified in general into two groups as dependent and independent wheel suspensions. Dependent suspensions have a configuration of the wheels that are connected by a rigid axle and the motion of each wheel is affected by the motion of the other; while in independent suspensions, wheels can move independently. The MacPherson strut, double wishbone, and multi-link suspensions are the most popular independent suspension types used in automobiles.

1.3. MACPHERSON STRUT SUSPENSION

MacPherson strut suspension is very popular due to its simple structure, performance, low cost, small unsprung mass, and small lateral space requirement which leaves more compartment place in the vehicle. It has a strut structure that consists of coaxially mounted coil spring and damper which controls the vertical location of the wheel, while lateral motion of the wheel is controlled by a control arm which is connected to the wheel hub and the body. The structure of a typical MacPherson strut suspension can be seen in Figure 1-1.

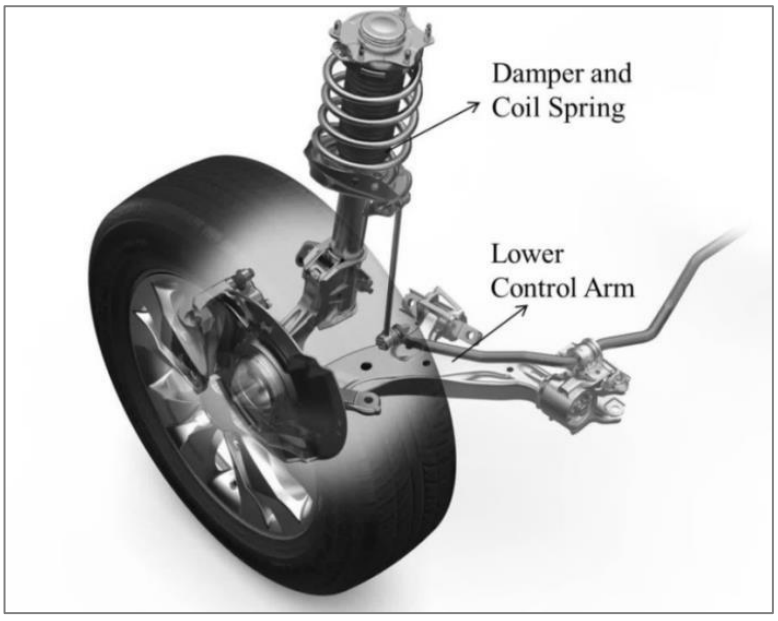

Figure 1-1: MacPherson Strut Suspension [1]

However, MacPherson strut type suspension has some disadvantages also, like the requirement of relatively more space in the vertical direction, and incapability of absorbing lateral forces on the strut. The second disadvantage will be emphasized and will be the main subject in this study.

Lateral forces have a negative impact on the ride comfort by increasing the damper dry friction. This disadvantage can be handled by inclining the spring axis relative to the damper axis as a traditional solution. However, installation space of suspension limits this angle; it can be seen in Figure 1-2. For this reason, the side load may not be eliminated totally. This has led to the development of new types of coil springs.

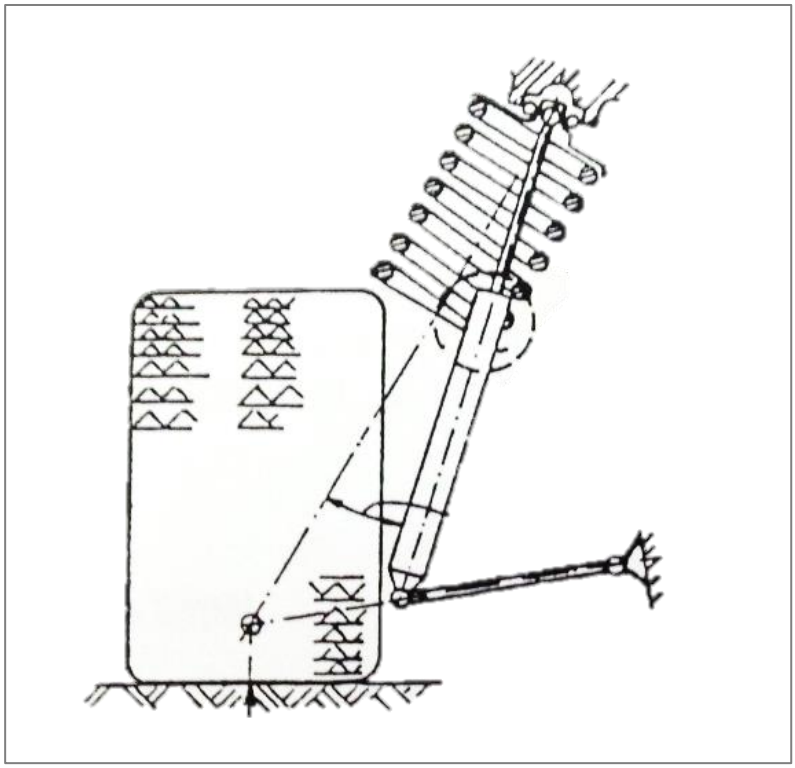

Figure 1-2: Installation Space Limitation of Inclined Coil Spring [2]

A recent development is the use of side load coil springs which can absorb lateral forces, unlike conventional coil springs. Side load coil springs have a curved centerline and proper design of the centerline curvature allows the side load spring take lateral loads. The side load coil spring is mounted on the damper like a conventional coil spring and form the strut. The main advantage of side load spring is that force action line has an angle with respect to strut axis while the force action line of standard coil spring is axial. This results in reduced side force, increased ride comfort, and extended life of damper parts.

Side load coil springs are also called ‘S-shaped’, ’C-shaped’, or ‘Banana’ springs due to their curved shape. A typical form of a side load coil spring can be seen in Figure 1-3. Side load springs has become popular because of their benefits with respect to packaging of the suspension system. Side load springs are examined in more detail in the following sections.

Figure 1-3: Form of Side Load Spring [3]

CHAPTER 2

LITERATURE REVIEW

2.1. PREVIOUS STUDIES

As introduced in the first chapter; simple structure, low cost, and compact design have led MacPherson strut suspension to become one of the most popular suspension types. Main disadvantage of the MacPherson suspension is the side force on the damper that increases friction between damper parts and resulting in degraded ride comfort. The traditional method to eliminate this drawback is to incline the spring axis with respect to the damper axis; however the packaging size of inclined spring is limited and this solution restricts the elimination of lateral forces at the desired level. Therefore, a new spring type which is called side load spring was developed in the early 1990's. Side load springs are special type of springs which prevent the reduced ride comfort and increased wear of damper parts by generating anti side forces.

There are certain publications about the reduction of side load on the damper in MacPherson suspension and the design and analysis procedures about the side load spring. In this part, researchers who have contributed to the topic and their studies are examined.

In 1994, Muhr, Wünscche, Biecker, and Schnaubelt introduced advantages of side load spring to reduce the lateral force in MacPherson strut suspension [2]. Their research was based on physical models and results of experimental studies showed the improvement in body acceleration and damper stroke which proved the effect of the new spring in ride comfort performance. However, their research was about only

an existing side load spring and objective of their research is to determine the performance character of this side load spring. Further they did not provide any information about how to design a side load spring with desired characteristics.

In 1996, Suzuki, Kamiya, and Imaizumi introduced the FEA model for the side load spring and investigated the effects of structural parameters like number of free coils and slenderness ratio to the spring characteristics [4]. They also discussed the methods of the arrangement of setting position of spring and the arrangement of tilting angle of spring seat for reducing side force. There were many FEA models and experiments to validate the analyses, however, the research was still limited within the analysis of performance characteristics and did not cover the design methods.

In 2000, Gotoh and Imaizumi used mechanical dynamics and FEA software in common to perform the design procedure and analysis of friction of the damper in their study [5]. In their paper, a FEA model for the side load spring and spring seats were built to study the effects of spring end coil angles and seat angles on the reaction force line of the side load spring. Then a new design procedure combining mechanical dynamics with FEA software was introduced. Finally, they compared the reaction force axis and frictions of suspension of new design with conventional springs to show the advantage of side load spring. However, the design procedure was not represented fully, and some improvements still need to be discussed for the design procedure part of this paper, especially to design a side load spring for an existing MacPherson suspension.

In 2001, Hamano and Nakamura offered L-shaped coil spring to reduce the friction on the MacPherson strut suspension system [6]. They explained the calculation method to determine the load axis firstly and applied to L-shaped spring. Then, they tried to validate the calculations by experimentally and using FEA and to see the effects of L-shaped coil spring to reduce the friction. However, their study was about only L-shaped form of side load springs and was not including the other shape forms and design methods, besides the offered FEA model was primitive.

In 2002, Nishizawa, Ikeda, Logsdon, Enomoto, Sato, and Hamano investigated the effects of rubber seats on coil spring force line [7]. They used FEA models for comparing the metal and rubber seats. This paper was only about the spring seat effects on the side load and can be accepted as a supportive study for the design and analysis of side load springs.

In 2006, Nishizawa, Ruiz, Sakai, and Ikeda introduced a parametric study which investigated the effect of spring force line on vehicle self-steer for a MacPherson strut suspension system [8]. Their study was not directly related to side load spring and reducing lateral forces but it was helpful for the controlling of the spring force line. They developed a mathematical model of suspension system to obtain ideal force action line which minimizes self-steer of vehicle. Their study did not cover any aspects of designing side load spring; on the other hand, their mathematical model and calculations may be useful while developing the mathematical model for side load springs.

In 2008, Liu, Zhuang, Yu, and Lou represented the combination of multi body dynamics and finite element analysis for the design optimization of MacPherson strut suspension system with side load spring [9]. They used multi-body dynamics software ADAMS/CAR to examine the forces on the suspension system and then analyzed lateral and vertical characteristics of the side load spring using FEA analysis software ANSYS. Although this study just covered the study of only one spring and did not include detailed analyses, it can be accepted one of the most sophisticated study in this research field and was taken as basis for this thesis study, especially for mathematical modeling and benefited from it affluently.

In 2010, Ryu, Kang, Heo, Yim, and Jeon developed analytical processes for the design of a coil spring to reduce side load in MacPherson strut type suspension [10]. They constructed a kinematic model of the suspension to calculate and optimize spring force line to minimize the side load. At last, some experiments were carried out to validate the analysis results for spring force line and some other parameters like stiffness, stress and fatigue life. In their study, they investigated an S-shaped coil

spring and focused on fatigue life of side load spring; however no mathematical model was offered for the centerline curvature of S-shaped coil spring.

In 2010, Choi, An, and Won introduced a study that included the design of pigtail coil springs [11]. This study was not directly about side load springs; however design of pigtail may be combined with side load springs.

In 2012, Joshi and Chhabra developed a mathematical model to find piercing points and design the profile of side load springs [12]. Their model was very useful particularly for the determination of upper and bottom piercing points. On the other hand, mathematical model to design the center curve of the side load spring was just an extension of the study of Liu [9].

2.2. PATENTS

There are many patents on the side load spring design and related to reduction of side loads on the damper of the MacPherson suspension. However, details of the most of these patents which include the design studies are not accessible. Therefore, the accessible information about these patents will be mentioned in this section.

In 1989, the U.S. patent with the number of 4883288 is one of the oldest studies about side force problem on suspension strut and aims to eliminate bending moments caused by side forces on the suspension strut rod; however, the method in this invention is the usage of bracket as a lateral support and side load spring phenomena was not an option in those years yet [13].

The U.S. patent with the number of 4903985, whose invention year is 1990, is possibly the first study which offers to use spring with a curved or “S-shaped” spring centerline as a solution of lateral forces on the MacPherson strut. Inventors explain the situation very clearly and this invention can be assumed the oldest guiding study for side load spring works [14].

In 1992, the European patent with No 0225271 B1 is another study that addresses the problem of side load on the MacPherson strut and it offers the solution of using air spring for reducing side load. However, this invention is no more than a similar method of mounting coil spring with and offset or angle to the damper rod. This invention is the modified version of U.S. patent with the number of 4688774, and there are some extensions when compared to previous version [15][16].

In 1995, the U.S. patent with the number of 5467971 is another one of the studies about side load compensation in MacPherson strut suspensions. The inventors used the inclined spring seat to reduce not only the suspension strut friction and also steering friction caused by side loads on the suspension. The reduced steering friction is the main aspect of this invention. U.S. Patent with the number of 5454585 A was published just a few months ago from US 5467971 and proposes nearly the same design [17][18].

In 2001, the design of coil spring with curved centerline is offered in patent US 6328290 B1. In this invention, helical spring with a curved coil axis at a predetermined radius of curvature in unloaded state is proposed and various additional options are also added this curved coil spring like tilted end coils or pigtail end coils. This patent is one of the most inclusive studies that give information about side load spring and its design. Later, this invention is modified a little bit and published as US 6712346 B2 [19][20].

The U.S. patent with the number of 6375174 B2, which is offered as an invention in 2002, is another study that covers the design steps and options of a side load spring that enables to reduce side force on the damper rod. Side load spring is defined as C-shaped coil spring in this study [21].

In 2002, the U.S. patent with the number of 6481701 B2 offers a coil spring with varying coil diameter. In this study, inventors took the advantage of compactness of varying coil diameter when compressed and side load absorbing capability due its shape [22].

In 2003, side load spring design is proposed in a U.S. patent No 6616131 B2 by using pigtail coil springs on the end coils and tilting these end coils to provide a centerline which has an offset to coil axis. Also, the effects of changing the tilting angles on the upper and lower end coils are investigated in this invention. This patent application was done by the one of the inventors of U.S. patent with No 6328290 B1 and invention is also very similar to that invention [23][19].

In 2004, the patent with publication number of US 2004/0169324 A1 proposes an invention that offers a strut assembly which minimizes the lateral load and undesired moment that causes sticking suspension. In this invention, inventors used the C-shaped coil spring to eliminate lateral forces on the suspension. The patent with the publication number of US 2004/0169323 A1 patent is also taken by the same inventors and nearly the same invention is proposed in this study. In 2005, same inventors published another invention similar to previous study with the U.S. Patent No 6883790 B2 [24][25][26].

In 2004, in the patent with the number of US 20040178601 A1, a method that uses a second spring for absorbing lateral forces is invented. Inventors also mentioned curved helical coil spring as a solution for eliminating lateral loads, however difficulty of altering the shape of the spring and probability of insufficient results push them to solve this situation in a different way [27].

In 2013, in the patent number of CN 103310047 A, inventor proposes an optimization method for elimination of lateral force by establishing a multi rigid body simulation model which regulates the coordinates of hard points and determines the force action line of coil spring by changing the geometrical parameters of the spring seat to optimize lateral force on the strut rod [28].

2.3. SCOPE AND MOTIVATION

Numerous suspension systems have been developed so far to absorb shocks and vibrations that are transferred from roads for good ride comfort and many advantageous features made the MacPherson strut suspension system the most popular one, especially at front of the vehicles. The structure of MacPherson strut suspension consists of coaxially mounted a coil spring and a damper unit. Coil springs cannot absorb lateral forces and this cause to degrade the ride comfort because of generated side forces and thus undesired friction on the damper. This situation can be assumed the most significant disadvantage for the MacPherson strut suspensions.

When literature is researched about this topic, it is observed that coil spring forms which have capability of absorbing lateral forces can solve this problem. Researchers made contributions about the design of side load springs; however, no one has offered a simple and complete solution which contains the combination of mathematical model for centerline curvature of the coil spring and a detailed finite element analysis for coil spring generated with the centerline curvature which is obtained from that mathematical model and covers all type of coil springs.

In this study, an algorithm which gives the centerline curvature of the coil spring that can absorb lateral forces at any desired level is offered and characteristics of all type coil springs can be investigated by changing simply changing the parameters of the coil spring.

The design flowchart is as follows; desired lateral force that will be absorbed is defined and according to that side force, a spring centerline curvature is obtained in MATLAB. Then this centerline is exported to Excel file as points which generate the spring centerline curvature. Finally, these points are imported to the CATIA for modeling of the coil spring and analysis of this modeled coil spring is done by using ANSYS software.

To carry out the proposed procedure easily, a MATLAB GUI is designed to give the centerline curvature of the coil spring when required inputs are provided. The GUI enables user to save the data of the centerline curvature for later use in modeling and analyses. A general appearance of the designed GUI can be seen in Figure 2-1.

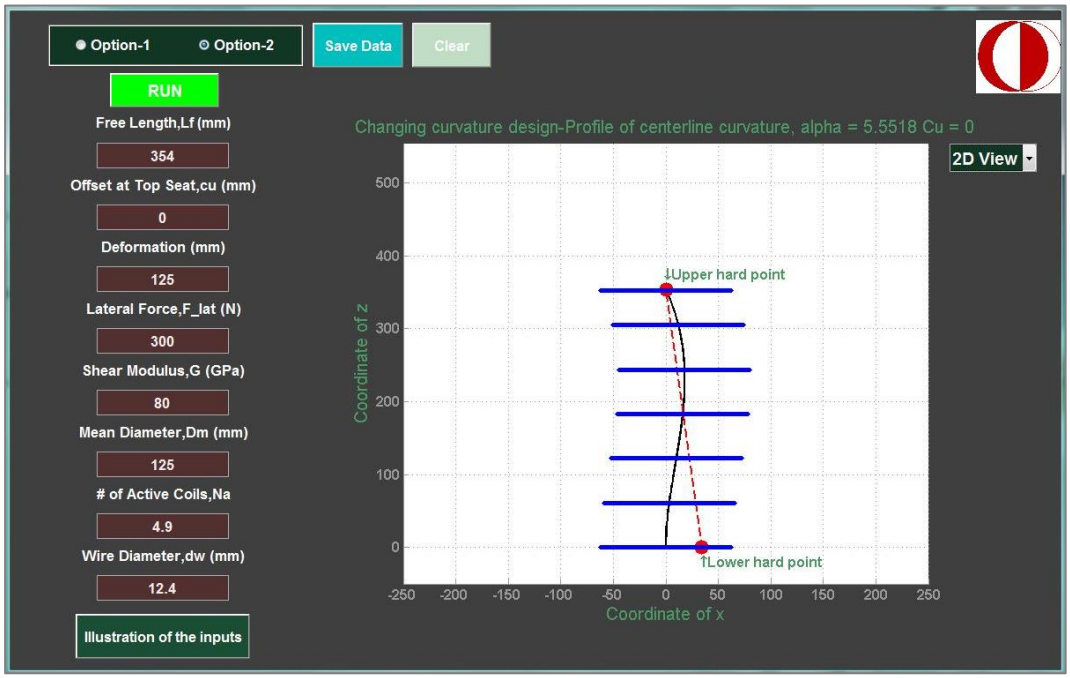

Figure 2-1: General Appearance of the GUI

CHAPTER 3

STATIC ANALYSIS OF CONVENTIONAL HELICAL COIL SPRINGS

In this chapter, theoretical information about conventional coil springs is given and static analyses of a number of helical coil springs are illustrated. Specifications for a typical coil spring are given in Table 3-3. Before carrying out analyses in finite element software ANSYS, theoretical calculations are done according to formulations in section 3.1. In the ANSYS analyses, some considerations like spring end connection type, seat types, etc. are also modeled and examined. The spring properties, theoretical calculations, and analysis results of the conventional spring models can be found in APPENDIX A. After the analyses of the conventional helical coil springs, some intuitive methods are applied to coil spring forms to obtain side load springs, and then these intuitively designed side load springs are examined and these modified springs are also analyzed and their side force generation is investigated.

3.1. BACKGROUND THEORY OF HELICAL COIL SPRINGS

In this part, not only the general information is given about the springs and also term definitions together with equations for the terms that will be used frequently in this study are given [29]. The helical coil springs are made up of a wire coiled in the form of a helix and are intended for compressive or tensile loads. The cross-section of the wire of the spring is generally circular and the two main types of helical coil springs are compression and tension helical springs. Only the compression springs will be of interest in this study. A typical compression coil spring can be seen in Figure 3-1.

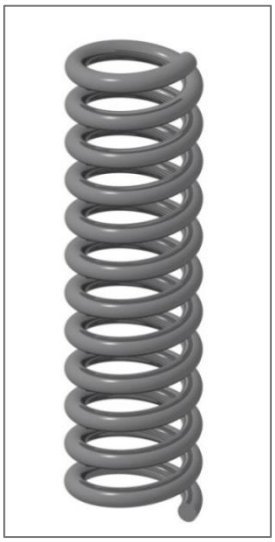

Figure 3-1: Compression Helical Coil Spring

- **Definitions of the Some Terms Used in Compression Coil Springs**

Solid Length: That is the length when the spring is compressed until the coils come in contact with each other.

$$L_S = n'.d \quad \textbf{(1)}$$

Free length: It is the length of the spring in the free or unloaded condition.

$$L_F = n'.d + \delta_{max} + 0.15\,\delta_{max} \quad \textbf{(2)}$$

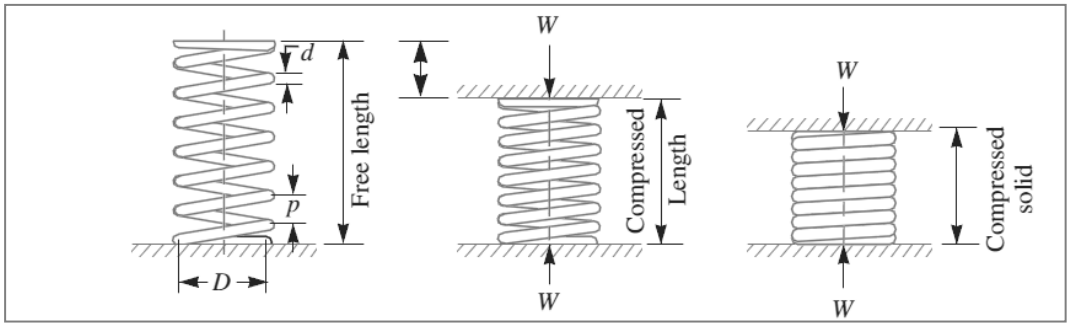

Figure 3-2: Free and Solid Length of the Helical Coil Spring [29]

Spring index: The ratio of the mean diameter of the coil to the diameter of the wire.

$$C = \frac{D}{d} \tag{3}$$

Spring rate (stiffness): The load required per unit deflection of the spring.

$$k = \frac{W}{\delta} \tag{4}$$

Pitch: The axial distance between adjacent coils in uncompressed state.

$$p = \frac{Free\ length - Solid\ Lenth}{n' - 1}\ or\ p = \frac{L_F - L_S}{n'} + d \tag{5}$$

- **End connections for compression springs**

The end connections are suitably formed to apply the load. Commonly used forms are shown in Figure 3-3.

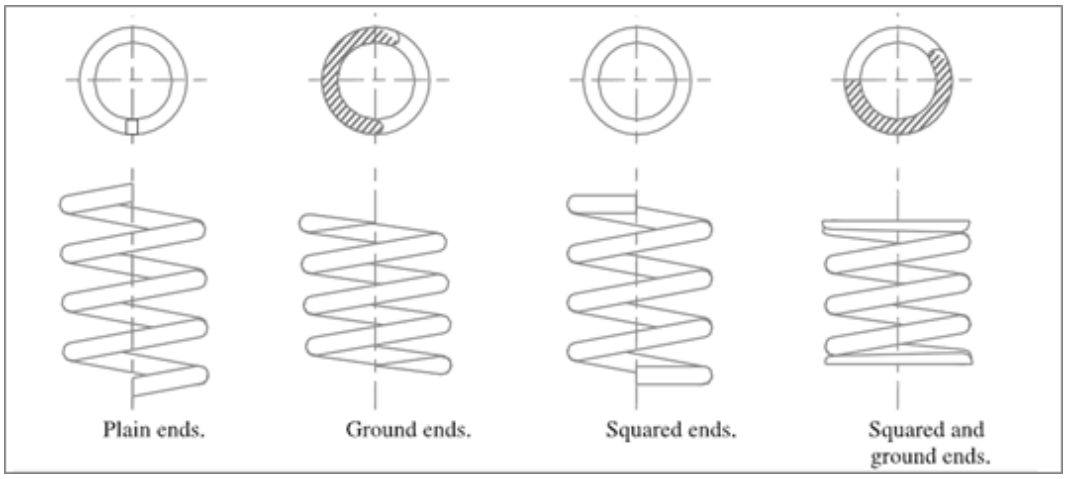

Figure 3-3: End Connection Types of Compression Springs [29]

Table 3-1: Formulations for End Connection Types

Type of End	Total number of turns (n')	Solid Length (L_s)	Free Length (L_f)
Plain Ends	n	(n+1).d	p.n+d
Ground ends	n+1	(n+1).d	p.(n+1)
Squared ends	n+2	(n+3).d	p.n+3d
Squared and ground ends	n+2	(n+2).d	p.n+2d

- **Stresses in Helical Springs of Coil Wire**

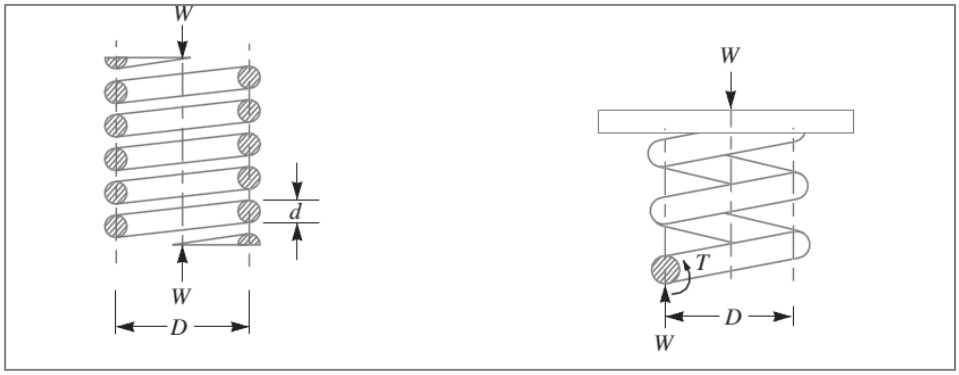

Figure 3-4: Axially Loaded Spring and Free Body Diagram [29]

The spring is under the action of two forces; the axial force (W) and the twisting moment (T) which can be seen in Figure 3-4.

$$T = W \cdot \frac{D}{2} = \frac{\pi}{16} . \tau_1 . d^3 \quad \textbf{(6)}$$

The torsional shear stress;

$$\tau_1 = \frac{8W.D}{\pi.d^3} \tag{7}$$

The direct shear stress due to axial load W;

$$\tau_2 = \frac{4W}{\pi.d^2} \tag{8}$$

The resultant shear stress in the wire becomes;

$$\tau = \tau_1 \pm \tau_2 = \frac{8W.D}{\pi.d^3} \pm \frac{4W}{\pi.d^2} \tag{9}$$

Positive sign is for the inner edge and negative sign is for the outer edge of the wire.

As a result, the maximum shear stress;

$$\tau = \frac{8W.D}{\pi.d^3} + \frac{4W}{\pi.d^2} = \frac{8W.D}{\pi.d^3}\left(1 + \frac{d}{2D}\right) = \frac{8W.D}{\pi.d^3} \cdot K_S \tag{10}$$

$$K_S: Shear\ stress\ factor = 1 + \frac{1}{2C} \tag{11}$$

The shear stress diagrams according to Eq**.** (9);

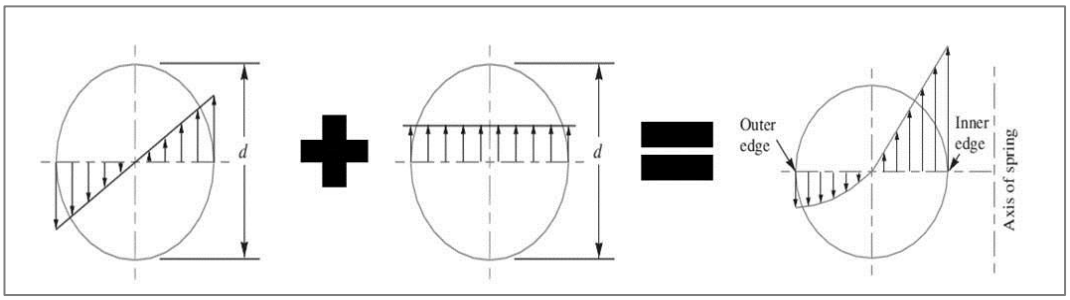

Figure 3-5: Torsional Shear, Direct Shear and Resultant Shear Stress Diagrams

In order to include the effect of the curvature of the wire, Wahl's stress factor (K) can be used. Then, the maximum shear stress induced in the wire;

$$\tau = K \cdot \frac{8W.D}{\pi.d^3} = K \cdot \frac{8W.C}{\pi.d^2} \quad \textbf{(12)}$$

$$K = \frac{4C-1}{4C-4} + \frac{0.615}{C} \quad \textbf{(13)}$$

The maximum shear stress equation has importance, because, while doing the static analysis validation of the analysis model in ANSYS, the results will be checked according to maximum shear stress value and deformation according to applied load.

- **Deflection of Helical Springs of Circular Wire**

The total active length of the coil spring;

$$l = Length\ of\ one\ coil \cdot number\ of\ active\ coils = \pi D \cdot n \quad \textbf{(14)}$$

The axial deflection of the spring;

$$\delta = \theta \cdot \frac{D}{2} \quad \textbf{(15)}$$

It is known that;

$$\theta = \frac{T.l}{J.G} \quad \textbf{(16)}$$

$$J = \frac{\pi}{32} \cdot d^4 \quad \textbf{(17)}$$

After substitutions, the deflection for an applied load becomes;

$$\delta = \frac{8W.D^3.n}{G.d^4} = \frac{8W.C^3.n}{G.d} \quad \textbf{(18)}$$

Then, the stiffness of the spring can be written as;

$$\frac{W}{\delta} = \frac{G.d^4}{8D^3.n} = \frac{G.d}{8C^3.n} = constant \rightarrow k \quad \textbf{(19)}$$

- **Buckling of Compression Coil Springs**

Large deformations may cause buckling in compression coil springs. The condition for stability of steel springs can be investigated by checking the relation which is given in Eq. (20).

$$L_f < 2.63\frac{D}{\gamma} \quad \textbf{(20)}$$

Where γ is a constant related to end condition and γ values for usual end conditions can be seen in Table 3-2.

Table 3-2: End Condition Constants for Compression Coil Springs

End Condition	End Condition Constant, γ
Spring supported between flat parallel surfaces (fixed ends)	0.5
One end supported by flat surface perpendicular to spring axis (fixed) ; other end pivoted (hinged)	0.707
Both ends pivoted (hinged)	1
One end clamped; other end free	2

As it will be mentioned in the following sections, the springs are supported between two parallel blocks in this study. Therefore, γ=0.5 will be used and $L_f<5.26*D_m$ relation will be examined to check whether buckling may occur or not. Two spring models whose properties are given in Table 3-3 and Table 4-1, are used and according to $L_f<5.26*D_m$ relation, there is no risk of buckling for both springs.

- Spring model-1 → L_f=196 mm, $D_{m=}$46 mm → 196 mm < 242 mm

[Stability condition satisfied]

- Spring model-2 → L_f=354 mm, $D_{m=}$125 mm → 354 mm < 658 mm

[Stability condition satisfied]

3.2. THEORETICAL CALCULATIONS

Theoretical calculations are evaluated according to textbook formulas and the spring properties are given in Table 3-3. In Chapter 3, all springs are modeled according to these spring properties. In the calculations, the maximum shear stress and the deflection are monitored for comparing with the ANSYS results. In theory, the maximum shear stress occurs at the inner side of the coil and may be higher than the theoretical value depending on the spring index and this correction is provided by using the Wahl's stress factor which is given in Eq. (13).

Table 3-3: Spring Properties of Model-A [30]

Wire diameter, d		8.0 mm
Mean diameter of the coil, D		46.0 mm
Number of Active Coils, n		10.0
Number of Total Coils, n'		12.0
Free length of the spring, L_f		195.0 mm
Solid length of the spring, L_s		96.0 mm
Load, W		1640 N
Material (Stainless Steel Wire)	Elastic Modulus, E	E=200 GPa
	Poisson Ratio, ν	ν=0.3
	Shear Modulus, G	G=80 GPa

$$Spring\ index:\ \ C = \frac{D}{d} = \frac{46}{8} = 5.75$$

$$Pitch:\ \ p = \frac{L_F - L_S}{n'} + d = \frac{(195 - 96)}{12} + 8 = 16.25\ mm$$

$$Wahl's\ stress\ factor:\ \ K = \frac{4C - 1}{4C - 4} + \frac{0.615}{C} = \frac{(4 * 5.75 - 1)}{(4 * 5.75 - 4)} + \frac{0.615}{5.75} = 1.265$$

$$Maximum\ Shear\ Stress:\ \ \tau = K \cdot \frac{8W.C}{\pi.d^2} = (1.184) * \frac{(8 * 1640 * 5.75)}{(3.14 * (8 * 10^{-3})^2)} * 10^{-6}$$

$$= \mathbf{474\ MPa}$$

$$Deflection:\ \ \delta = \frac{8W.C^3.n}{G.d} = \frac{(8 * 1640 * 5.75^3 * 10)}{(80 * 10^9 * 8 * 10^{-3})} * 10^3 = \mathbf{39.6\ mm}$$

The maximum shear stress value of 474 MPa and the deflection value of 39.6 mm for the applied load (1640 N) will be investigated in the analysis model and it is expected to obtain similar results in ANSYS.

3.3. ANALYSIS OF CONVENTIONAL HELICAL COIL SPRING

ANSYS 16.0 are used as software for pre and post processing of the static analysis of conventional helical coil springs. Mesh type, mesh size, spring seat types and spring end connection types are all examined in this section. While expecting accurate results, it is also aimed to have an analysis model that can respond faster. Firstly, the spring is meshed with different mesh types and sizes and the convergence of the results is examined. Then, spring seat types are defined and it is decided to use square blocks as spring seat to apply the load easily and accurately. Spring end connection types are examined finally and the analysis model is obtained according to all these considerations.

In the analysis process, the maximum shear stress and the deformation of the coil spring according to applied force are the specified variables that are selected and their convergences are monitored.

During analyses, rigid blocks are designed at the top and the bottom of the spring as spring seats. At the bottom seat, only rotational degree of freedom in z direction is free while only translational degree of freedom in z direction free at the top seat. Therefore, the coil spring is deformed only in z direction when a load is applied at the top seat. The constraints on the coil spring can be seen in Figure 3-6.

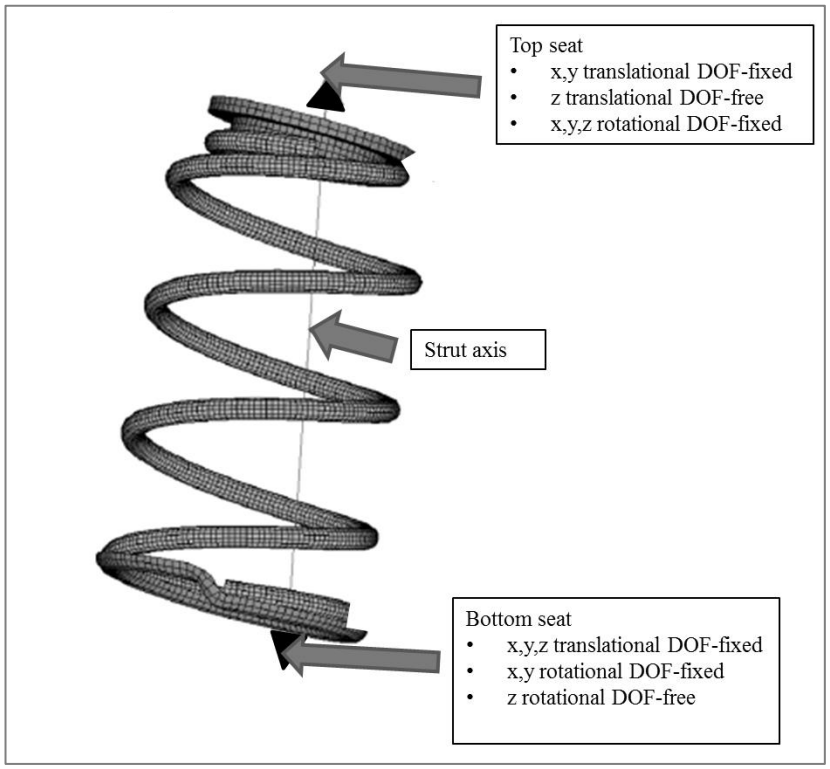

Figure 3-6: Constraints of Coil Spring for Analyses [10]

3.3.1. MESH TYPE

There are mainly two types of meshing method in ANSYS Workbench, tetrahedral and/or hexahedral elements. Unless the mesh features is set, the program generates mesh automatically according to geometry and this generally provides reasonably accurate results. In this part, the effects of meshing type on the results are investigated. Same element sizes are used for both element types, very similar results are obtained in both cases. Hexahedral elements are observed to respond a little faster for this type of geometry. Although the selection of the mesh type does not seem to be significant, tetrahedral elements are more compatible with all geometries. Therefore tetrahedral elements are used for meshing. Mesh visualization and the results of the maximum shear stress and the deflection can be seen from Figure 3-7 to Figure 3-12.

- **Hexahedral Elements**

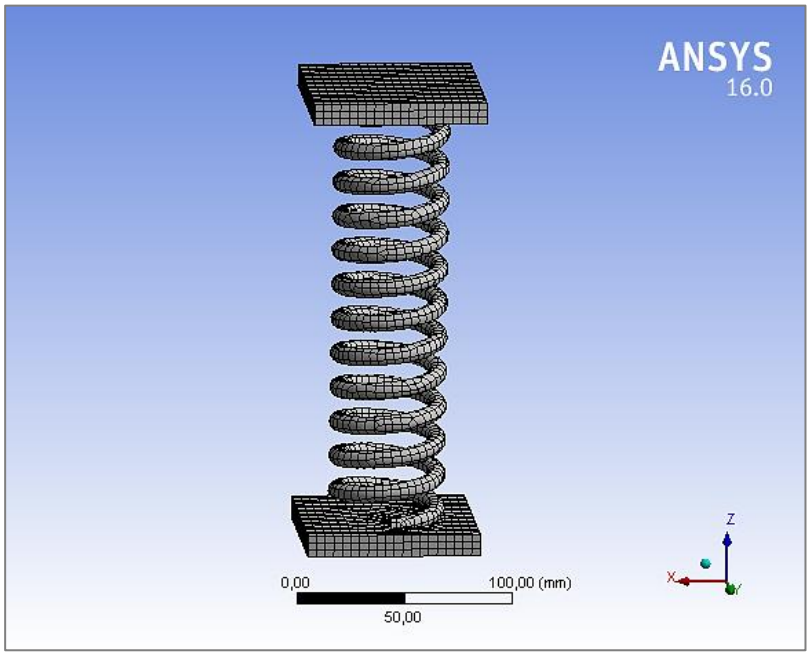

Figure 3-7: Meshing with Hexahedral Elements

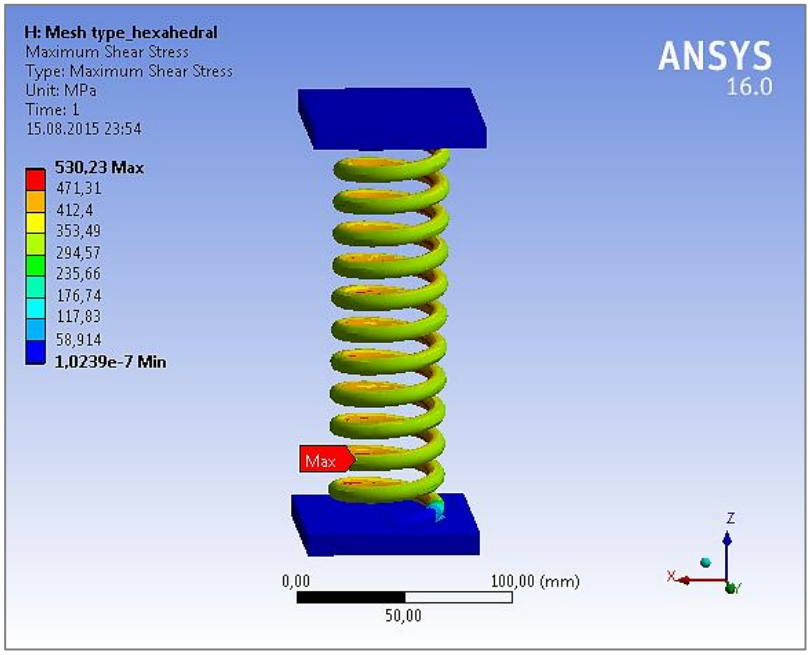

Figure 3-8: Result of Max. Shear Stress Analysis with Hexahedral Elements Mesh

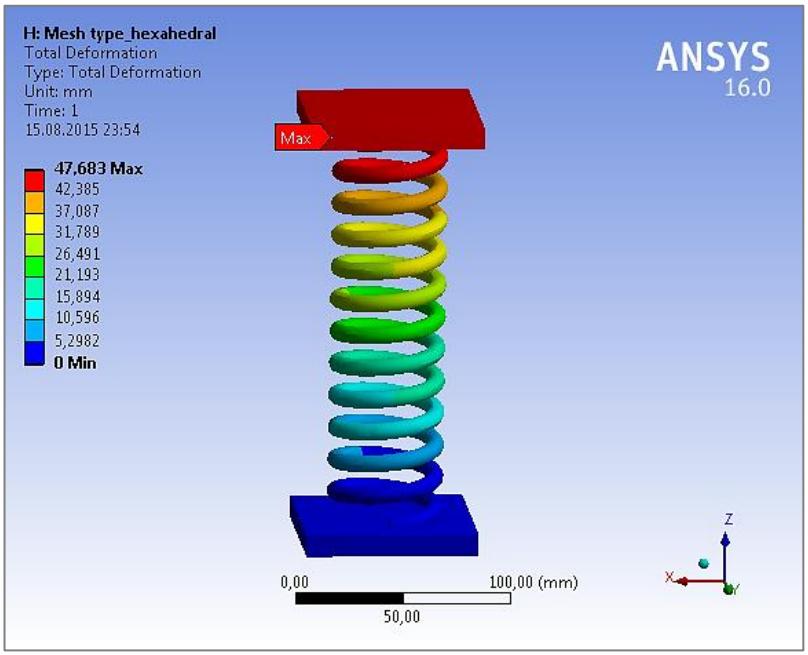

Figure 3-9: Result of Deflection Analysis with Hexahedral Elements Mesh

- **Tetrahedral Elements**

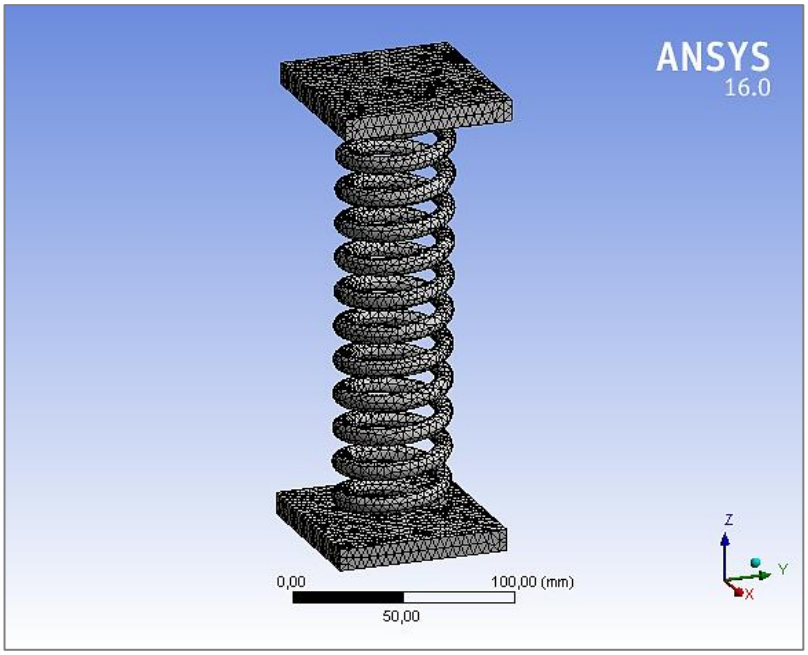

Figure 3-10: Meshing with Tetrahedral Elements

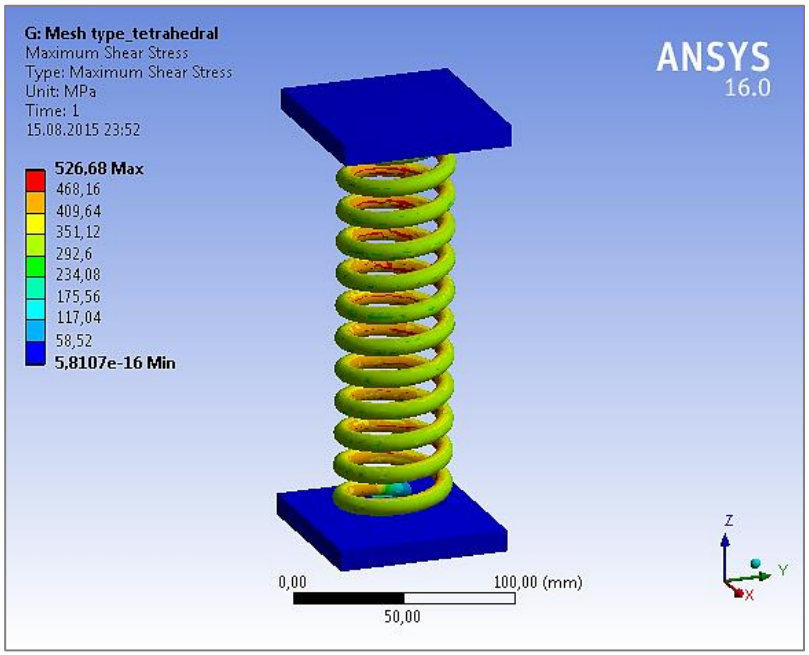

Figure 3-11: Result of Max. Shear Stress Analysis with Tetrahedral Elements Mesh

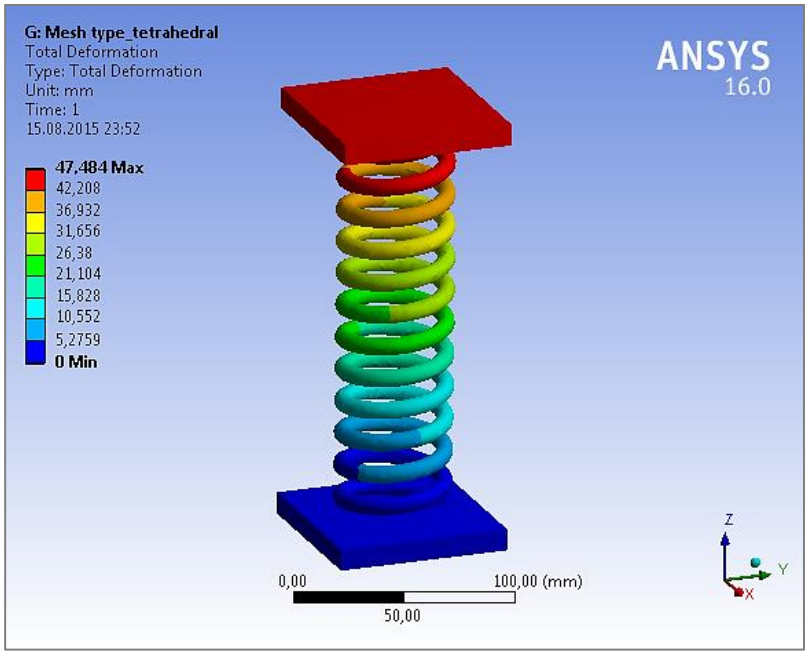

Figure 3-12: Result of Deflection Analysis with Tetrahedral Elements Mesh

3.3.2. MESH SIZE

After the meshing type is specified, analyses are repeated with same element type but with different sizes until the convergence of the results is obtained. Smaller elements make results better till some limiting size with which unexpected results arise around the spring ends and contact regions of the spring end and spring seat. Since the results are justified by investigating the maximum shear stress value which should be at the inside of the coil, the unexpected results at the spring ends and contact regions can be accepted inaccurate results due to the analysis model and are not of concern. On the other hand, very small mesh elements increase the setup time and computational expenses inherently. Table 3-4, Figure 3-13 and Figure 3-14 show how results converge with the change of element size. According the Figure 3-13, mesh size of 2 mm gives the most accurate results and the analysis model is established with 2 mm tetrahedral mesh elements.

Table 3-4: Element Size Effect on the Convergence

Model No	Element Size (mm)	# of elements	# of nodes	Max. Shear stress (MPa)	Max. Deflection (mm)
1	16	2708	6358	568.97	43.062
2	8	5072	10710	539.8	45.292
3	4	28994	50400	526.68	47.484
4	2	239501	363428	497.78	47.587
5	1,5	559833	822671	511.32	47.595
6	1	1856578	2639706	550.88	47.602

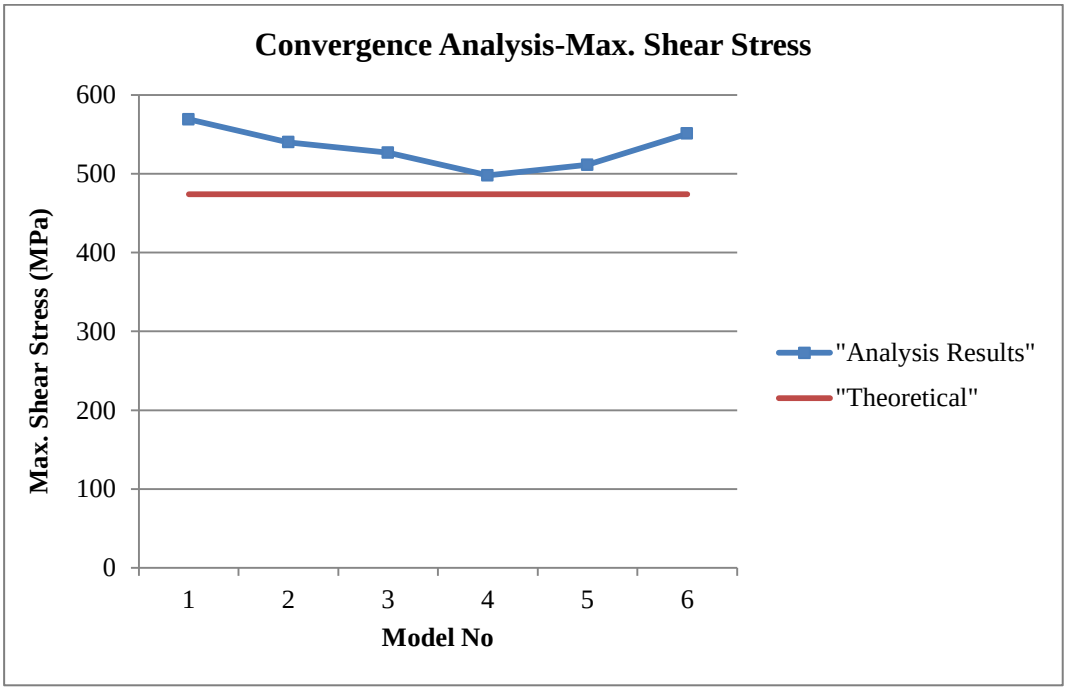

Figure 3-13: Comparison of Max. Shear Stress Analysis Results According to Mesh Size

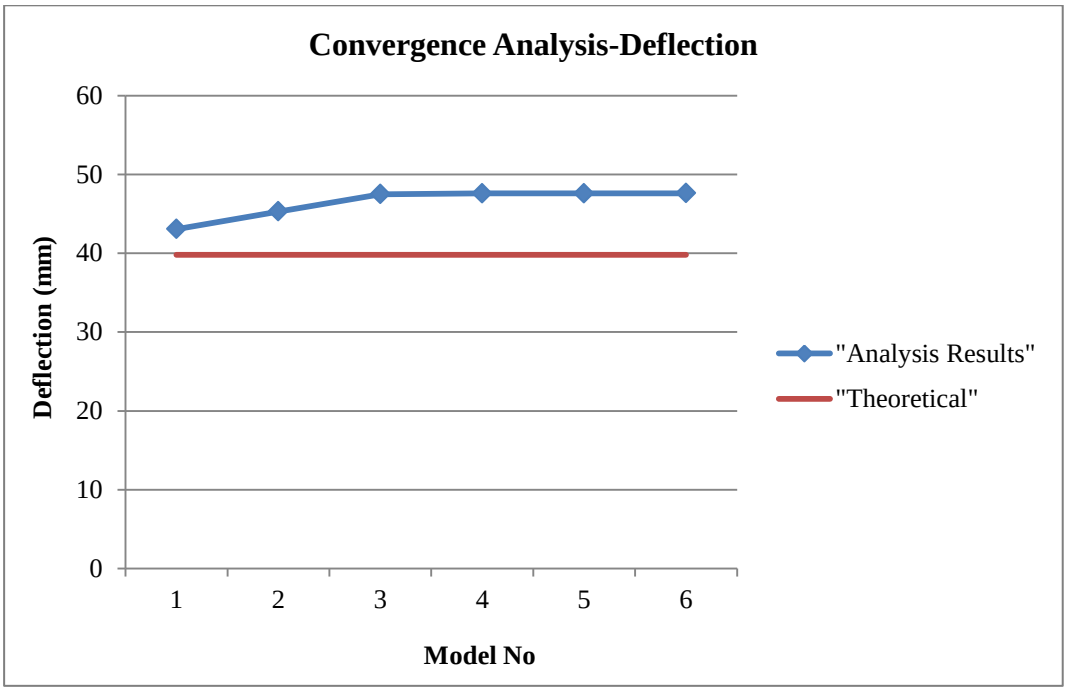

Figure 3-14: Comparison of Deflection Analysis Results According to Mesh Size

3.3.3. SPRING SEAT TYPES

Spring seat design is very important to obtain the proper function of suspension system. In this part, analyses are done with the spring that has no spring seats and it is investigated whether the spring seat affects the results or not. According to the results, there occurs some singular point on coil spring ends due to nonhomogeneous load is applied to the center of the spring. However, by changing the mesh quality in these regions accurate results can be obtained. Nevertheless, it is decided to use blocks as spring seat geometry to be able to apply load more realistic and comparable manner in the analyses of this study. Sizes of the blocks are selected large enough and thick, thus the deformation of the blocks becomes negligible. In other words, blocks those are used as spring seat behave like rigid bodies. Also, the size of the blocks is limited due to increased size of blocks also increases the effort for the analyses.

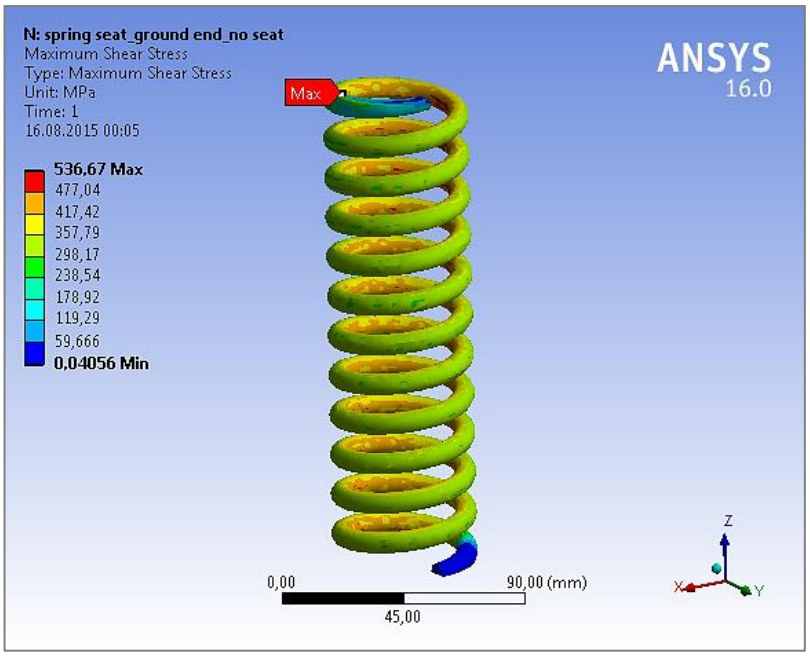

Figure 3-15: Result of Max. Shear Stress Analysis of Coil Spring without Spring Seat

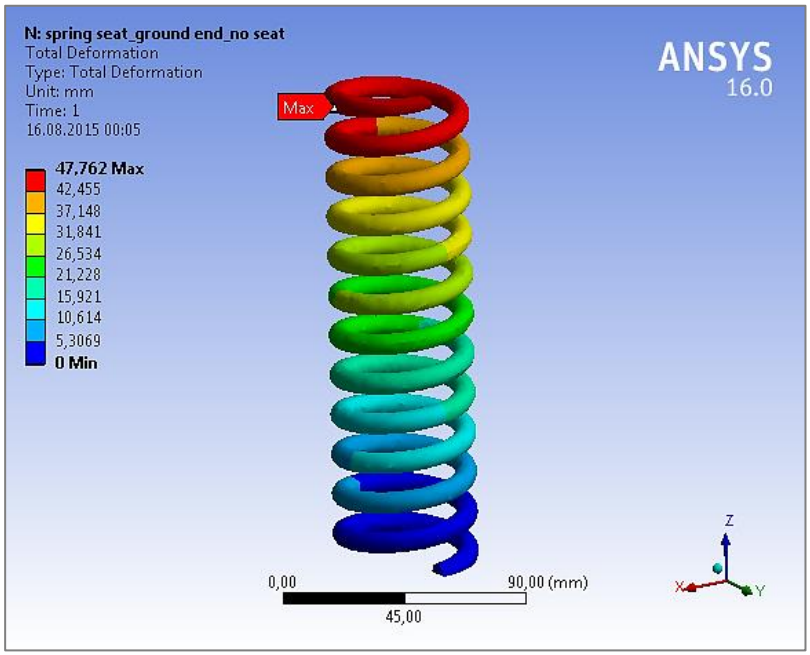

Figure 3-16: Result of Deflection Analysis of Coil Spring without Spring Seat

After analyzing the spring models that do not have spring seat, a few types of spring seats are modeled to enable to apply load to the center of the spring and analyzed for these spring seat models with the same analysis features and compared the results. The analysis results for springs with different spring seats can be seen from Figure 3-17 to Figure 3-24 while the analysis results of spring without spring seat can be seen in Figure 3-15 and Figure 3-16. The comparisons of the results for different spring seat types are presented in Figure 3-25 and Figure 3-26.

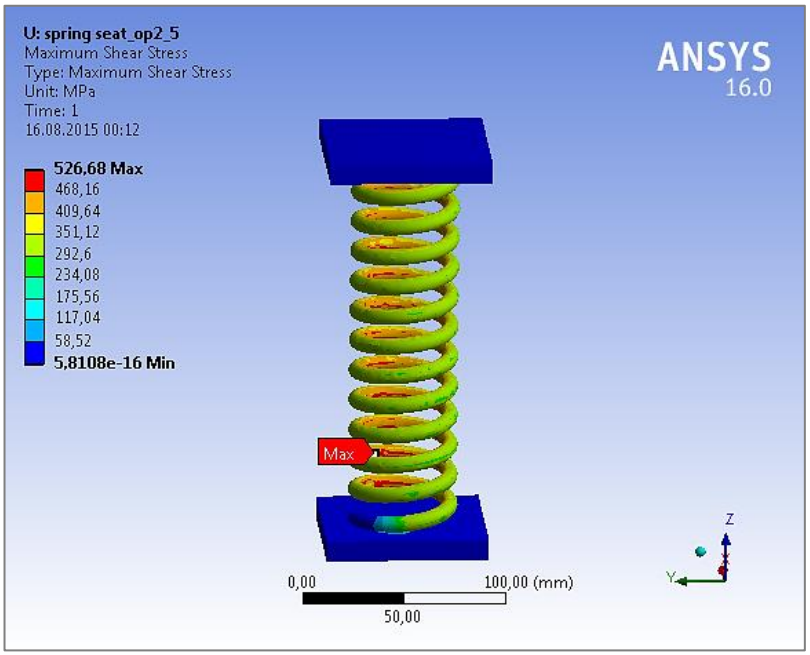

Figure 3-17: Result of Max. Shear Stress Analysis of Coil Spring with Seat Type of Square Blocks

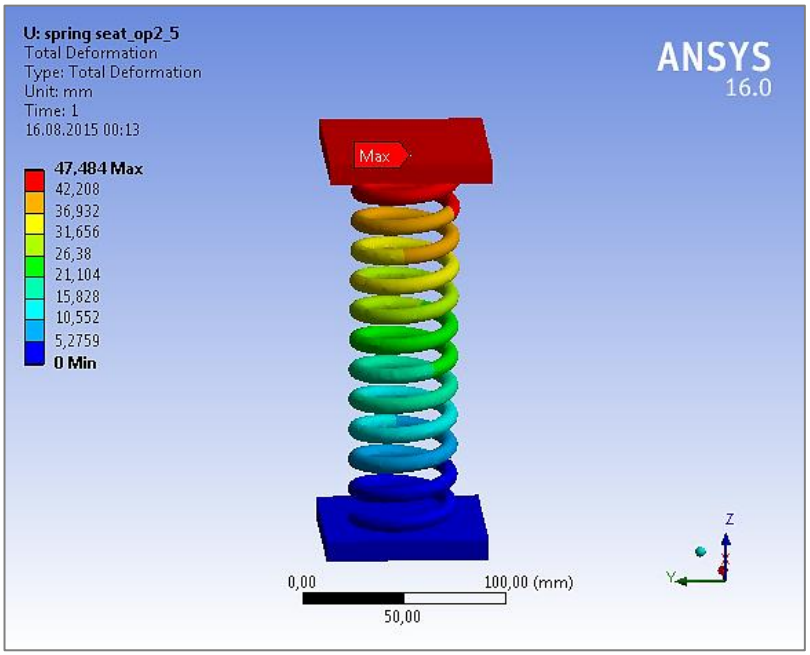

Figure 3-18: Result of Deflection Analysis of Coil Spring with Seat Type of Square Blocks

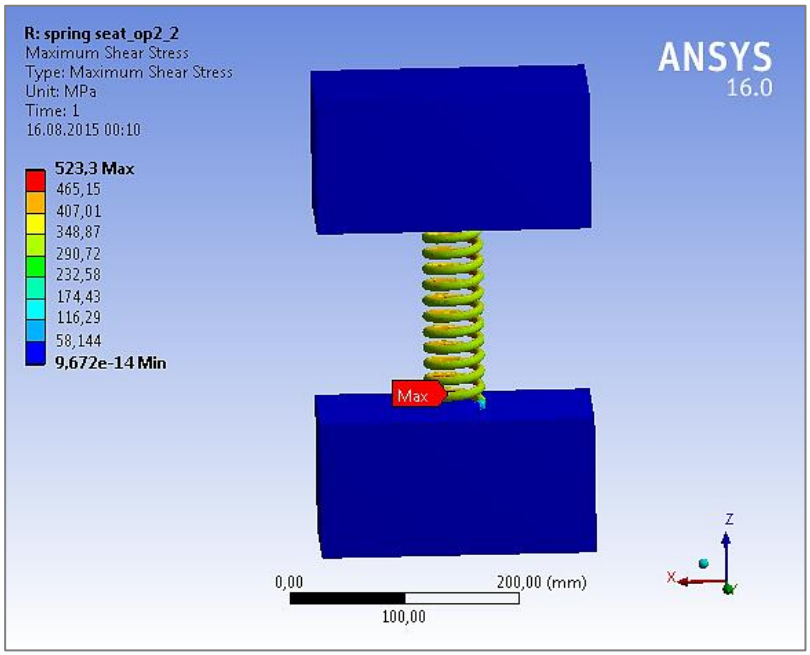

Figure 3-19: Result of Max. Shear Stress Analysis of Coil Spring with Seat Type of Thick Square Blocks

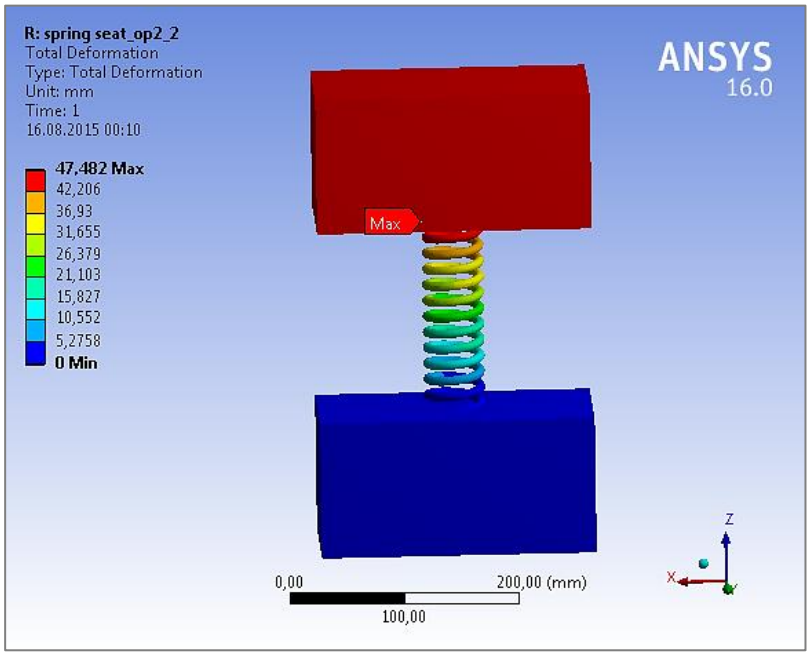

Figure 3-20: Result of Deflection Analysis of Coil Spring with Seat Type of Thick Square Blocks

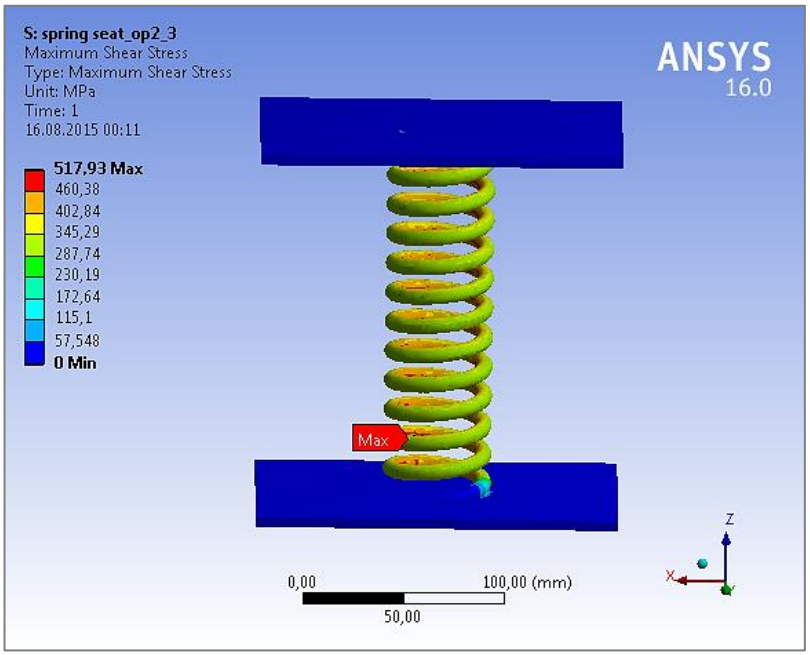

Figure 3-21: Result of Max. Shear Stress Analysis of Coil Spring with Seat Type of Thin Square Blocks

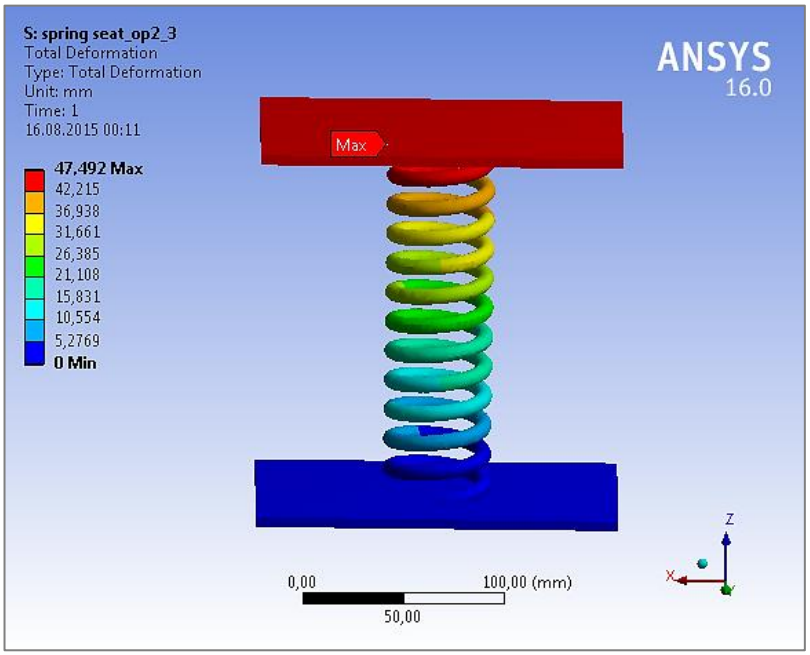

Figure 3-22: Result of Deflection Analysis of Coil Spring with Seat Type of Thin Square Blocks

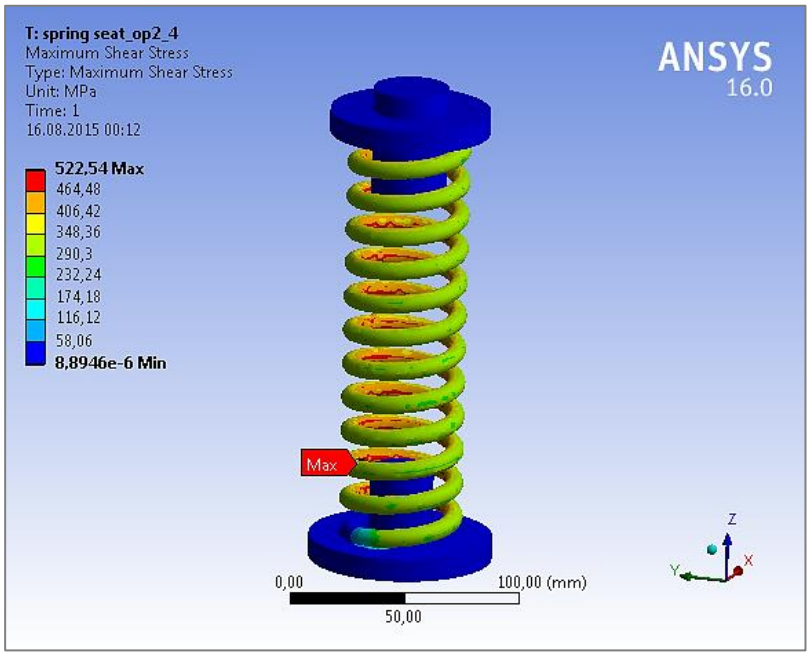

Figure 3-23: Result of Max. Shear Stress Analysis of Coil Spring with Seat Type of Circular Blocks

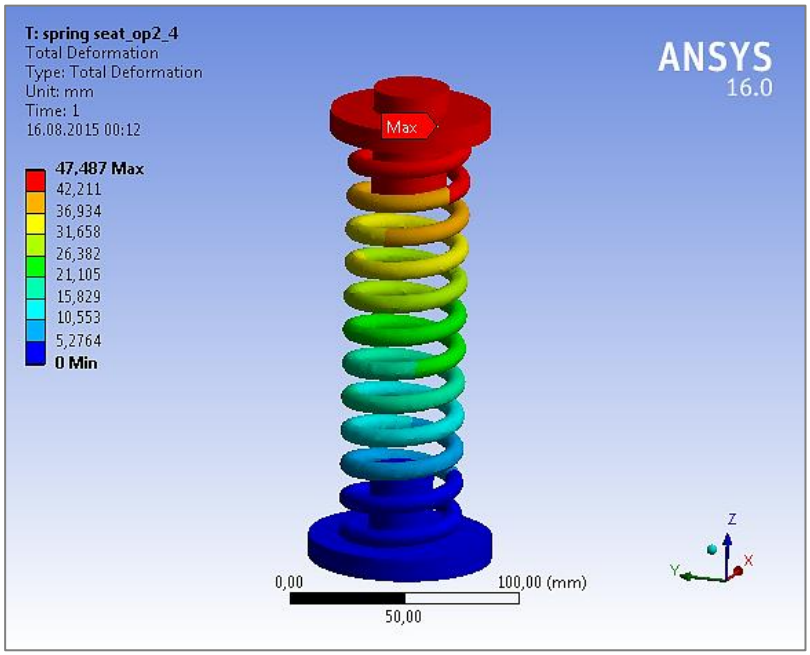

Figure 3-24: Result of Deflection Analysis of Coil Spring with Seat Type of Circular Blocks

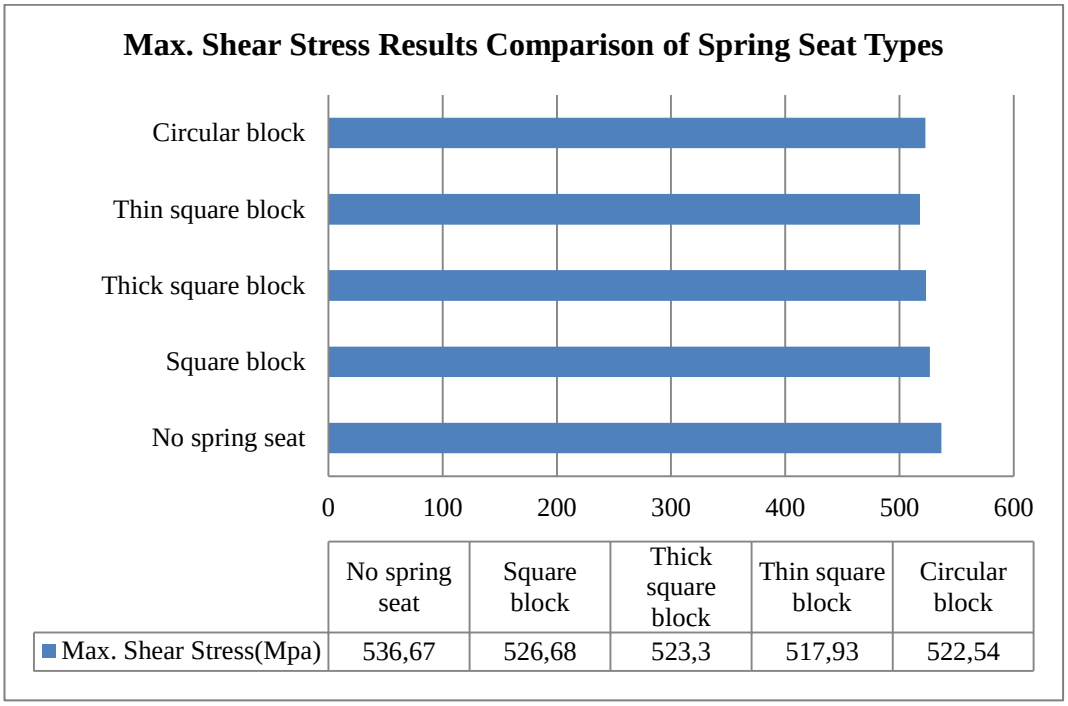

Figure 3-25: Maximum Shear Stress Results Comparison of Spring Seat Types

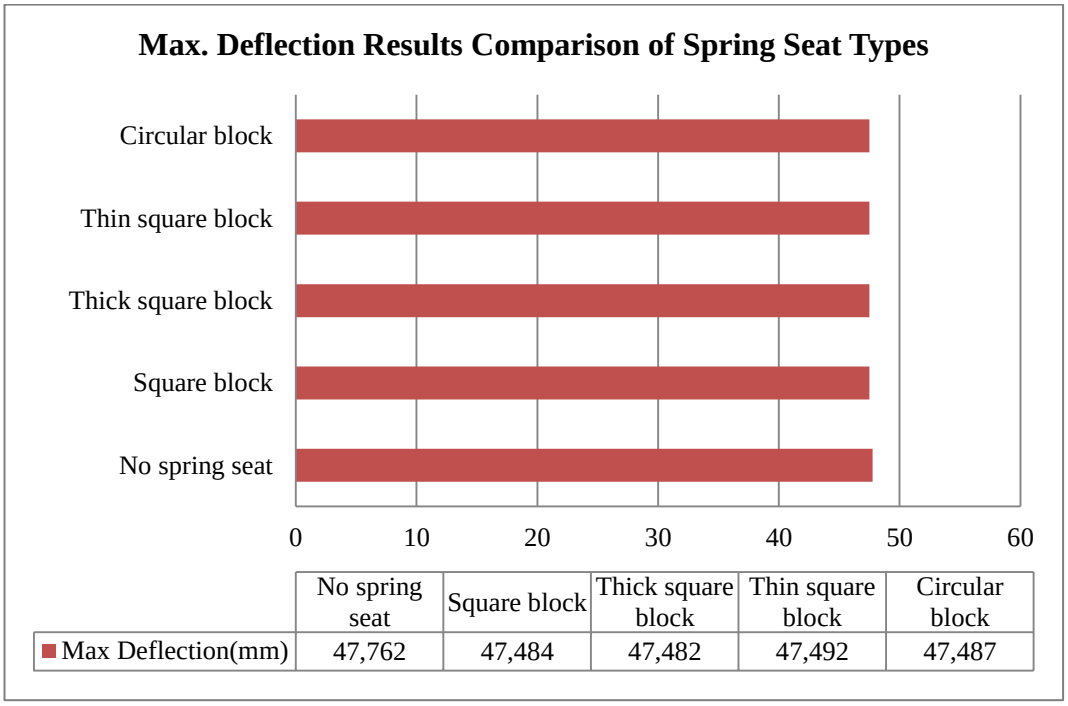

Figure 3-26: Maximum Deflection Results Comparison of Spring Seat Types

3.3.4. SPRING END CONNECTION TYPES

The end connections are suitably formed to apply the load and end connection types are examined in this section. This study is done to see whether having different end connection types affects the analysis results or not. Spring end connection types and the results for each are given in Figure 3-27 to Figure 3-38. The comparisons of the results of the maximum shear stress and the deflection are presented in Figure 3-39 and Figure 3-40 and it can be seen that the spring end connection types has minor effects on the results. As a result, springs can be modeled with any spring end connection types without changing the length of the spring. Commonly used end connections for compression springs are shown in Figure 3-3.

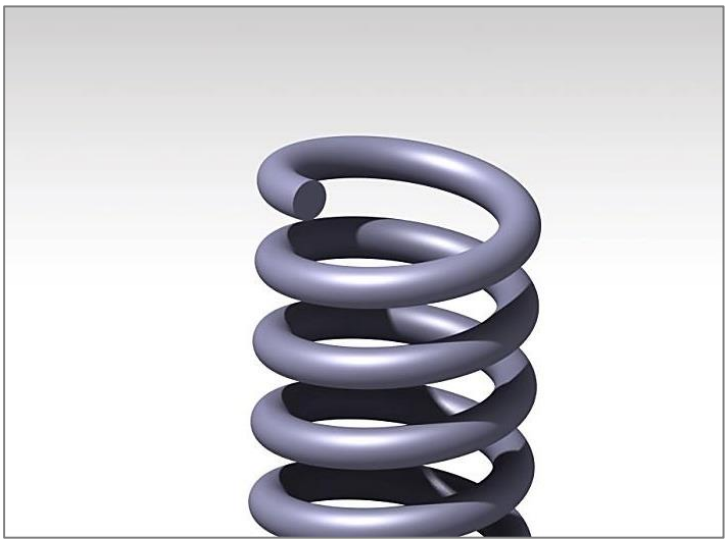

Figure 3-27: Coil Spring with Plain Ends

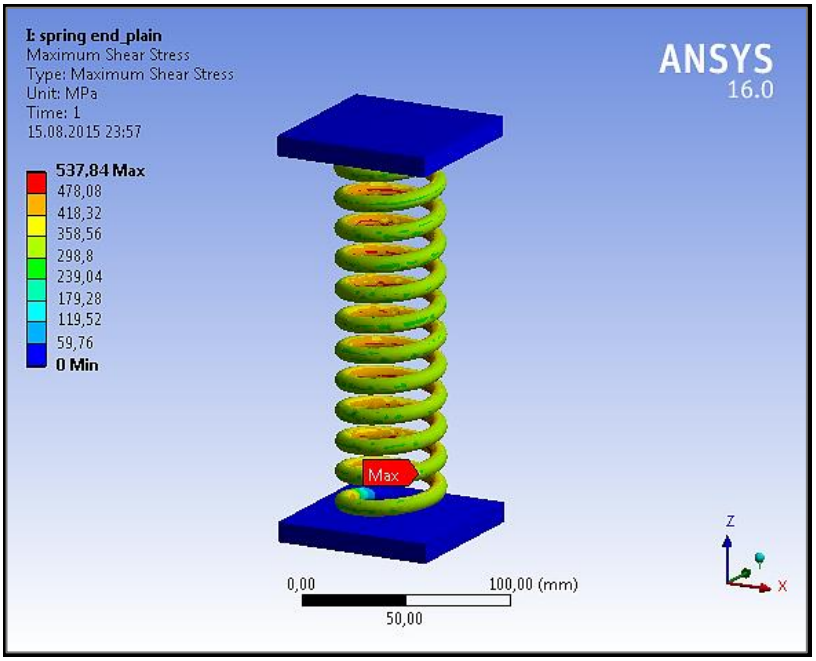

Figure 3-28: Result of Maximum Shear Stress Analysis of Coil Spring with Plain Ends

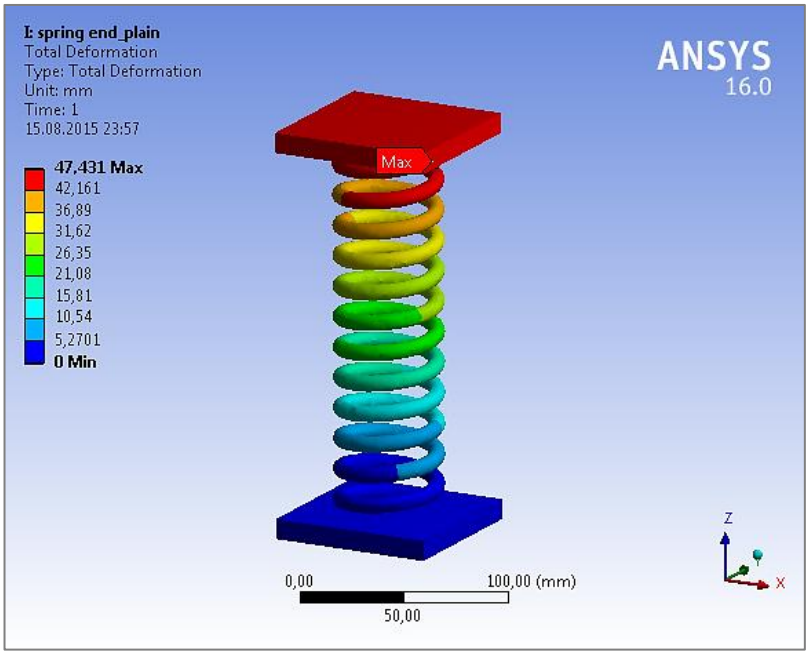

Figure 3-29: Result of Deflection Analysis of Coil Spring with Plain Ends

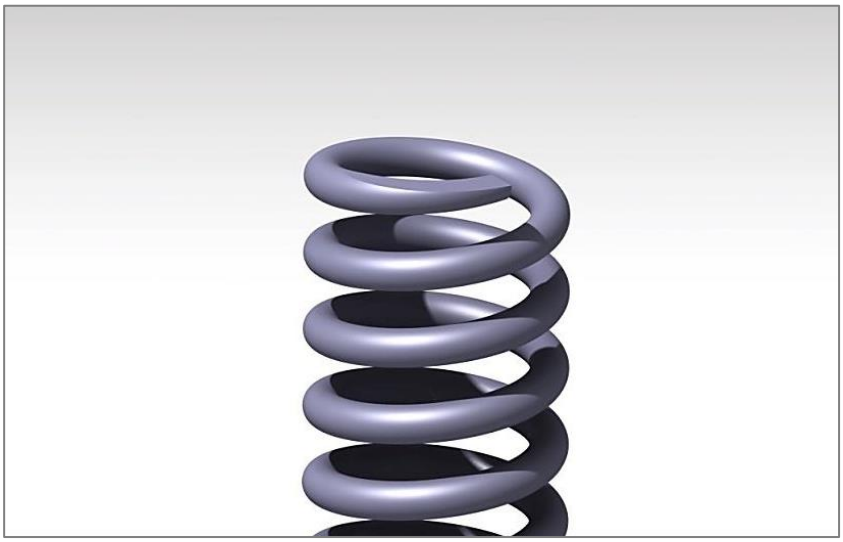

Figure 3-30: Coil Spring with Ground Ends

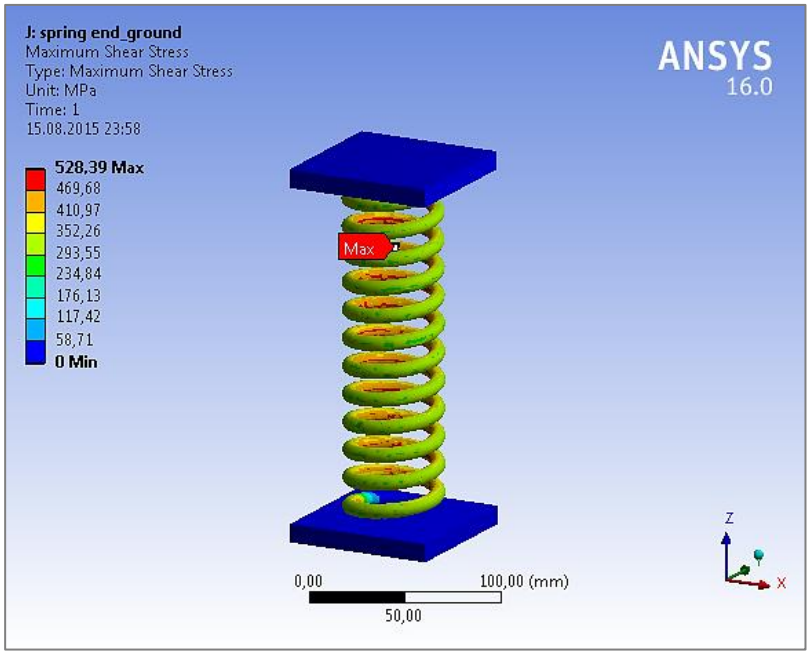

Figure 3-31: Result of Maximum Shear Stress Analysis of Coil Spring with Ground Ends

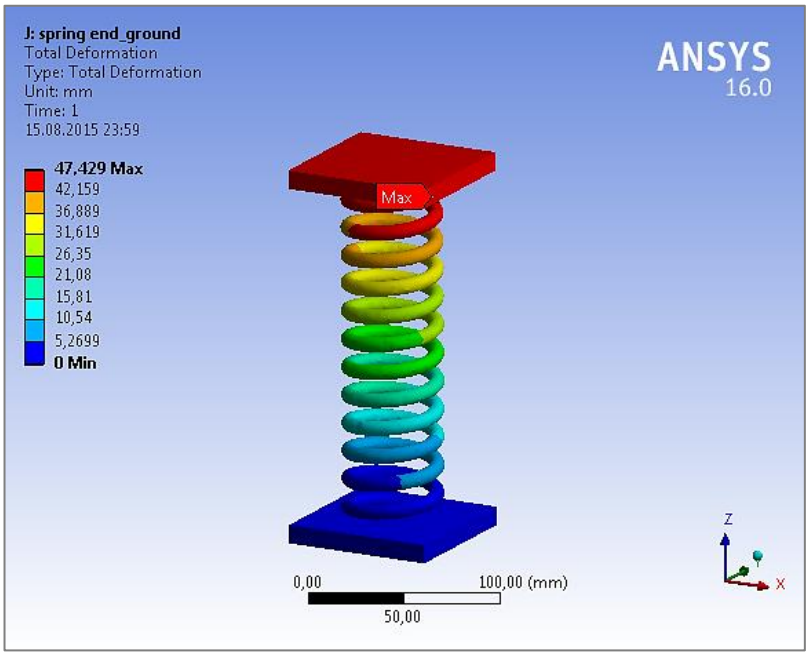

Figure 3-32: Result of Deflection Analysis of Coil Spring with Ground Ends

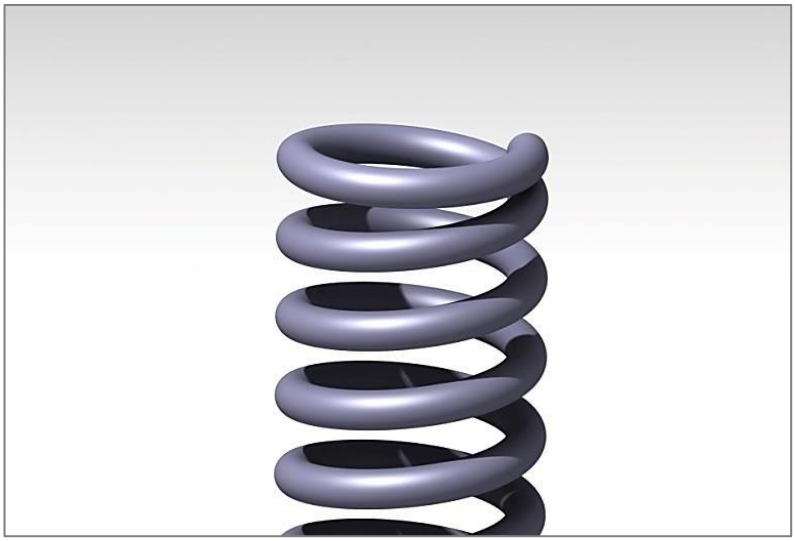

Figure 3-33: Coil Spring with Squared Ends

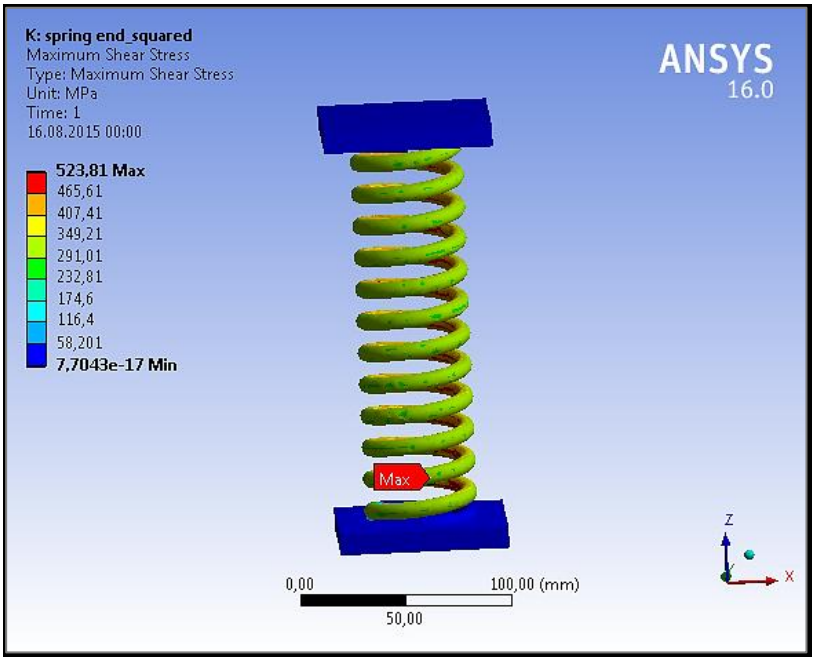

Figure 3-34: Result of Maximum Shear Stress Analysis of Coil Spring with Squared Ends

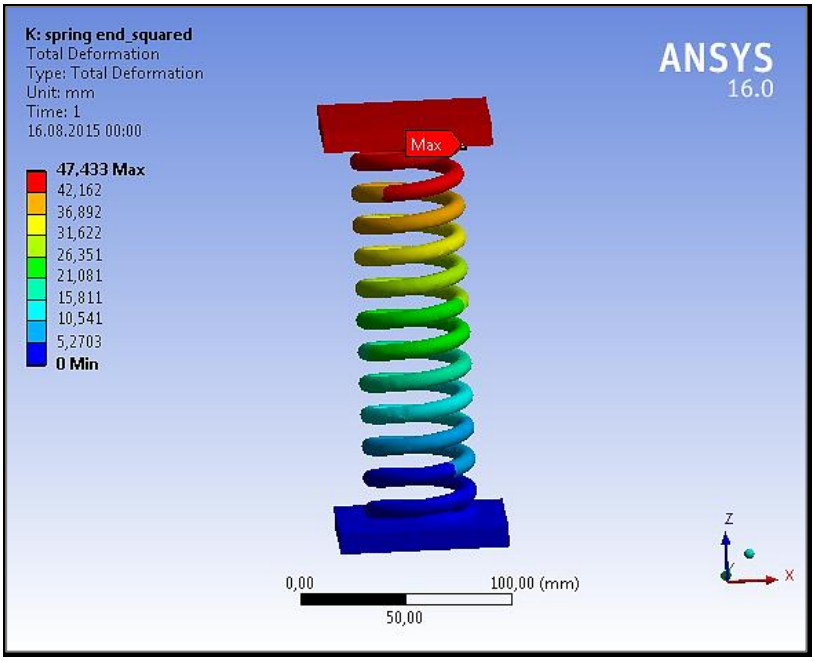

Figure 3-35: Result of Deflection Analysis of Coil Spring with Squared Ends

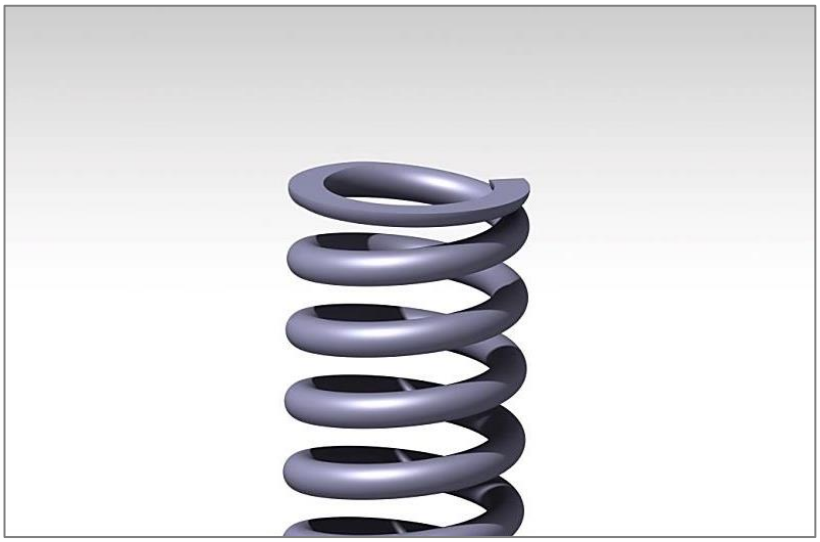

Figure 3-36: Coil Spring with Squared and Ground Ends

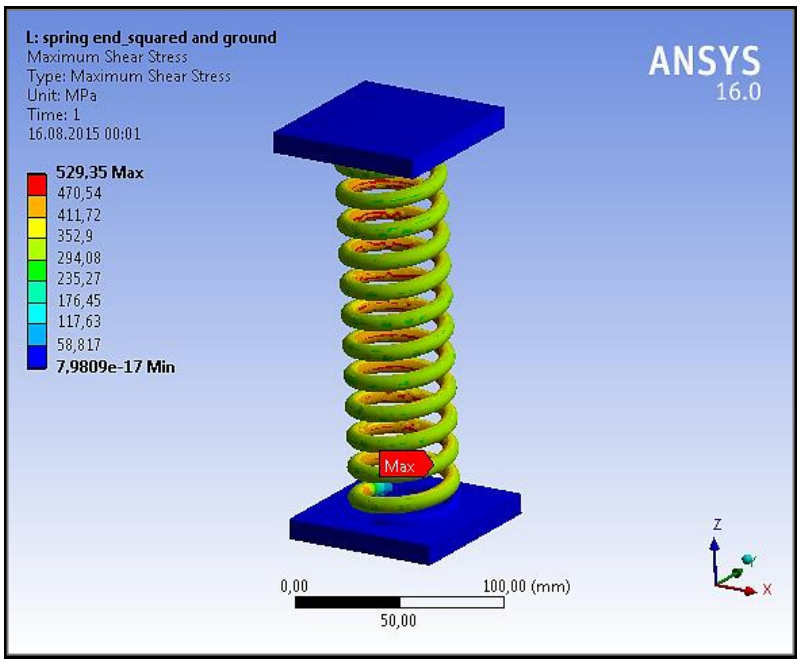

Figure 3-37: Result of Maximum Shear Stress Analysis of Coil Spring with Squared and Ground Ends

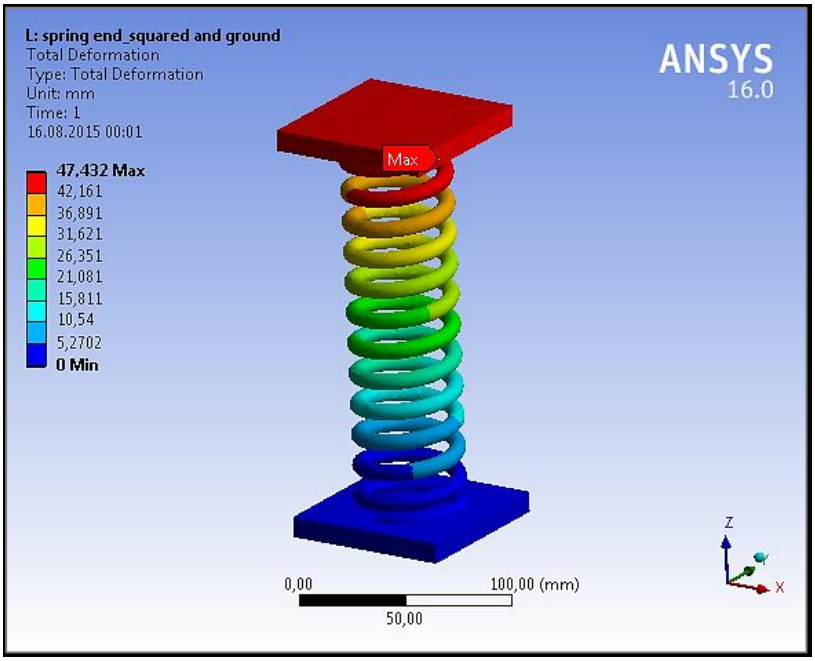

Figure 3-38: Result of Deflection Analysis of Coil Spring with Squared and Ground Ends

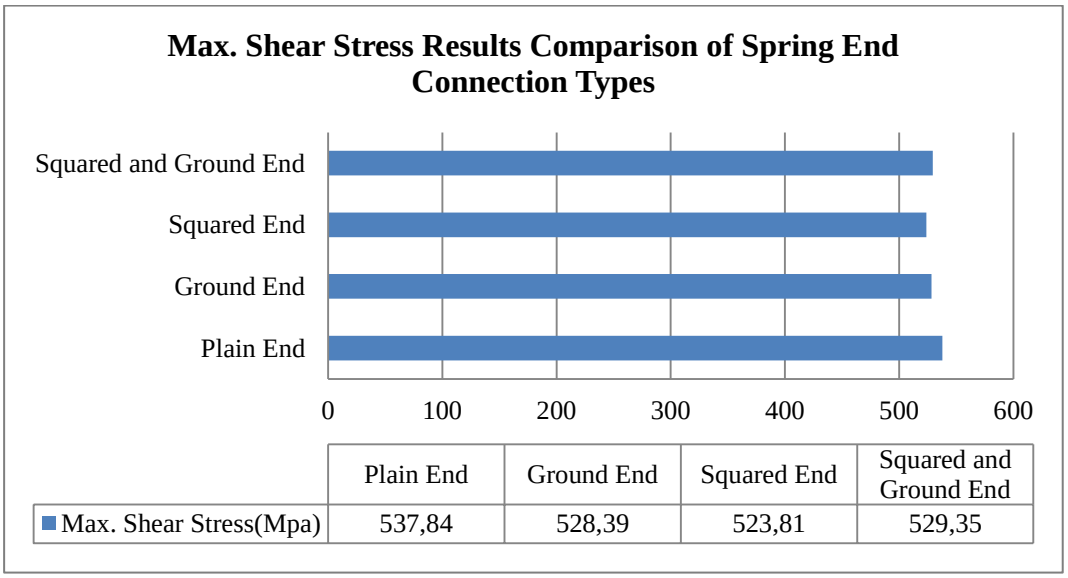

Figure 3-39: Maximum Shear Stress Results Comparison of Spring End Connection Types

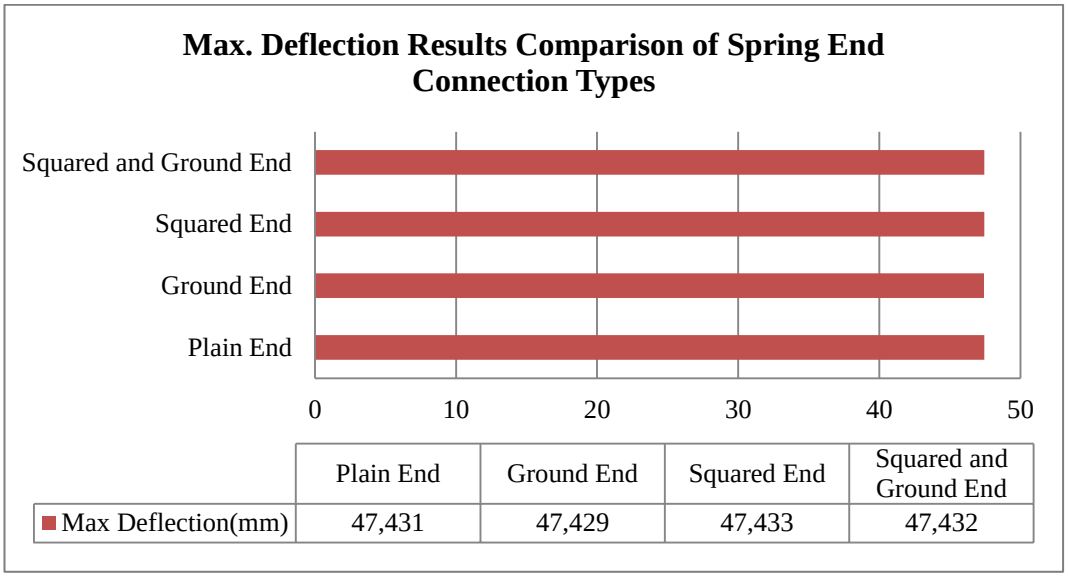

Figure 3-40: Maximum Deflection Results Comparison of Spring End Connection Types

3.4. ANALYSIS OF SIDE LOAD SPRINGS DESIGNED BY VARIOUS METHODS

In this section, some methods are applied to conventional coil springs intuitively to generate side forces without using any mathematical formula. These methods will be explained and results will be compared in this section.

3.4.1. S-SHAPED

Conventional coil springs have a linear center axis line while S-shaped coil springs have a curved centerline. This centerline curvature changes the characteristic of the coil spring and helps to generate side forces. By changing the shape of the curvature, in other words radius of the curvature, magnitude of the generated side force can be changed. In this part of study, curvature is given by offsetting from the center axis and the geometry modification can be seen in Figure 3-41. Since the curvature is given in yz plane, it is expected to obtain side force in y direction when an axial load is applied in z direction. As shown in the following parts, from Figure 3-42 to Figure 3-45, increasing curvature leads increased side force.

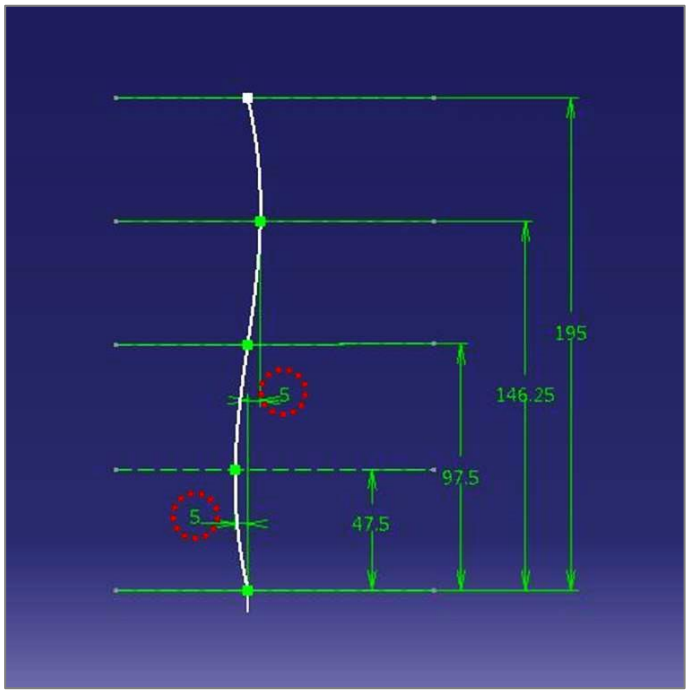

Figure 3-41: Drawing of Centerline Curvature of S-Shaped Coil Spring

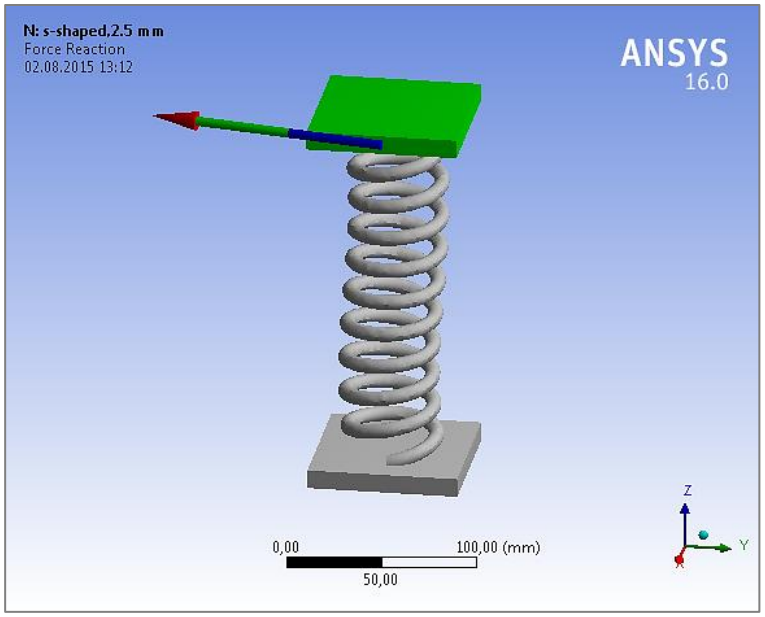

Figure 3-42: Reaction Forces of 2.5 mm Offset S-Shaped Coil Spring

➔ F_x=-1.1739 N, F_y=-6.5942 N, F_z=0 N

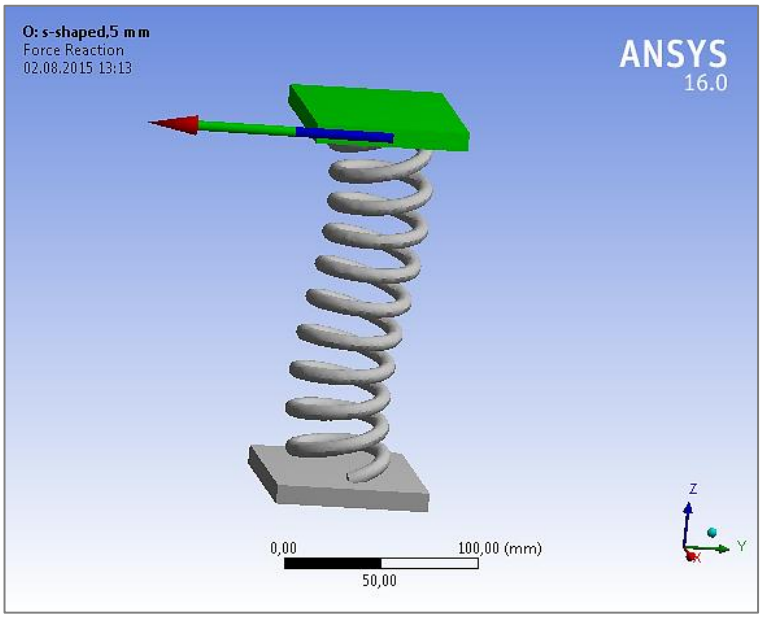

Figure 3-43: Reaction Forces of 5 mm Offset S-Shaped Coil Spring

➔ F_x= -1.1426 N, F_y= -45.678 N, F_z=0 N

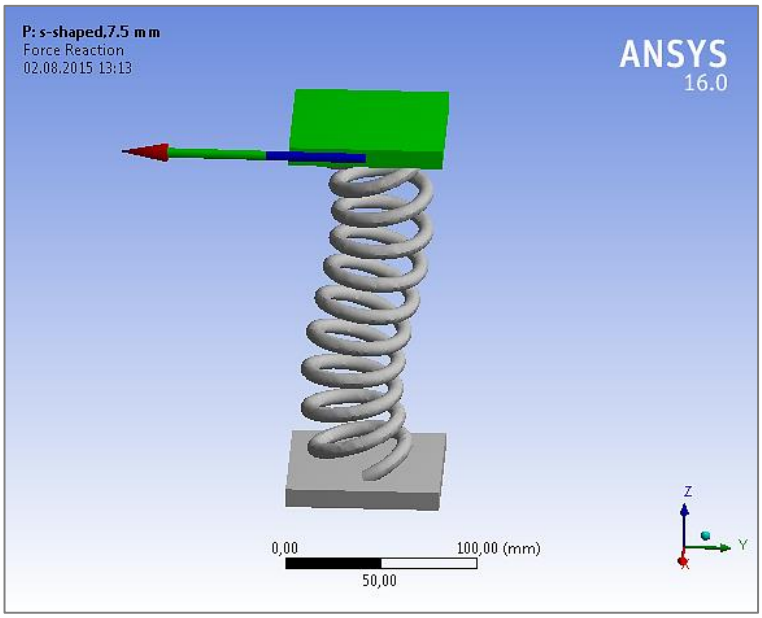

Figure 3-44: Reaction Forces of 7.5 mm Offset S-Shaped Coil Spring

➔ F_x= -1.2248 N, F_y= -86.058 N, F_z=0 N

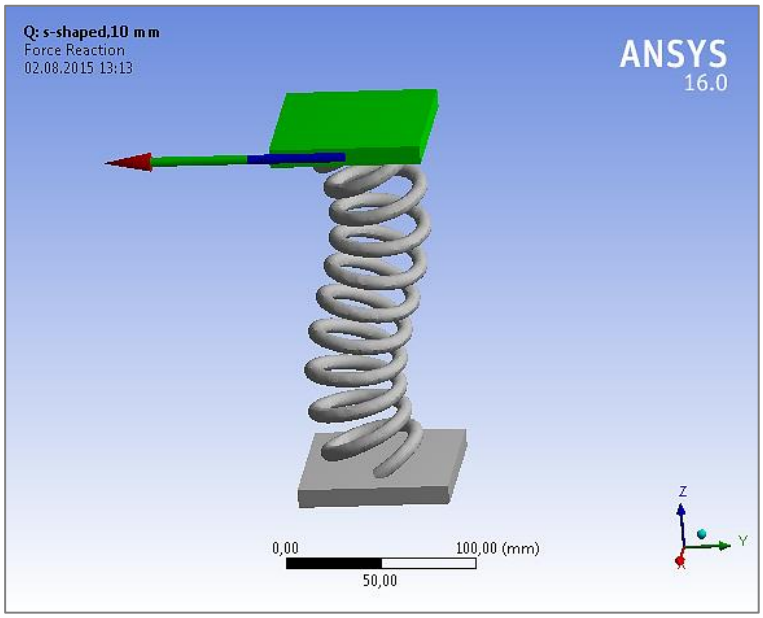

Figure 3-45: Reaction Forces of 10 mm Offset S-Shaped Coil Spring

➔ F_x= -1.2204 N, F_y= -126.31 N, F_z=0 N

When the spring is split into two parts horizontally, having different curvatures on the upper side and the bottom side may affect the magnitude of the generated side force. When compared to the generated side force of equal upper-bottom side curvature S-shaped coil spring, either having greater upper side curvature or having less upper side curvature does not affect the generated side force significantly as seen in Figure 3-46 and Figure 3-47.

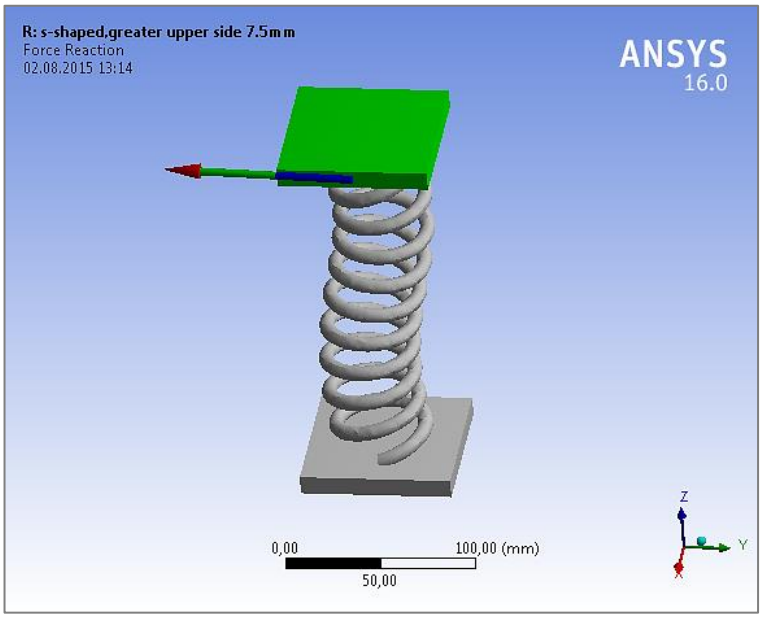

Figure 3-46: Reaction Forces of 7.5 mm Upper-5 mm Bottom Offset S-Shaped Coil Spring

➔ F_x= -3.4292 N, F_y= -66.291 N, F_z=0 N

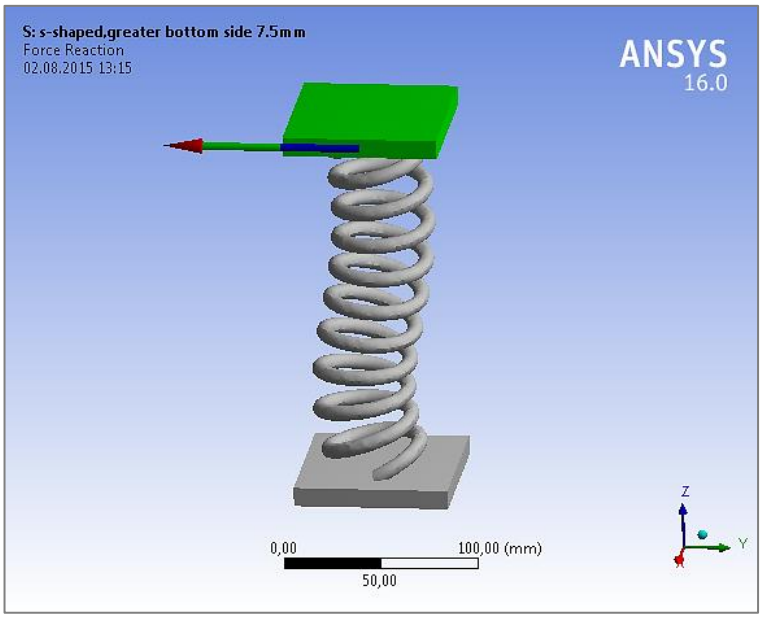

Figure 3-47: Reaction Forces of 5 mm Upper-7.5 mm Bottom Offset S-Shaped Coil Spring

➔ F_x= 0.92115 N, F_y= -65.907 N, F_z=0 N

3.4.2. C-SHAPED

This time, centerline curvature is shaped like C and analyses are repeated with the same way. Amount of curvature is given by offsetting from the spring centerline and the centerline curve can be seen in Figure 3-48. Similarly, the curvature is given in yz plane and a side force in y direction is generated. There is a weakly increasing tendency of generated side force according to increased curvature. As shown from Figure 3-49 to Figure 3-51, increasing curvature leads increased side force; however it does not make a significant change.

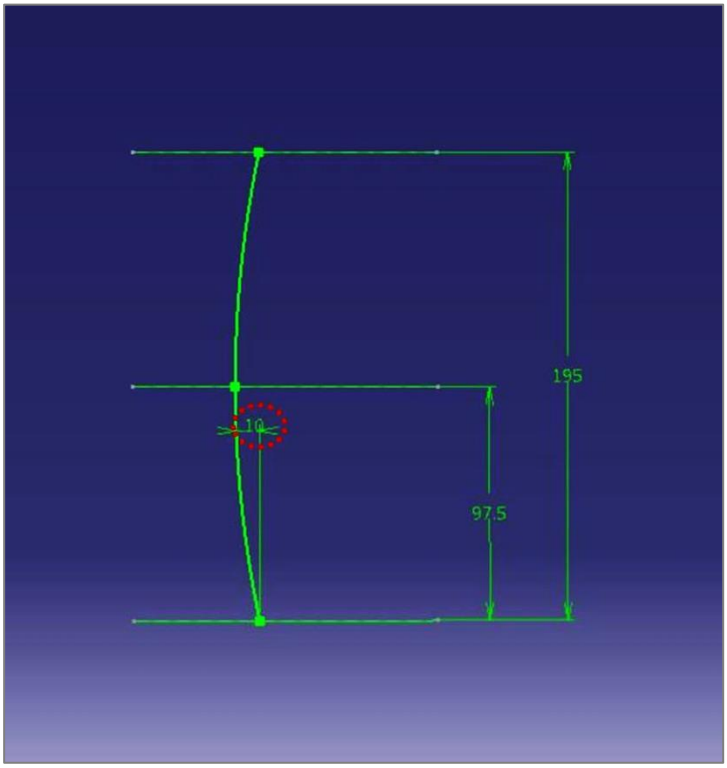

Figure 3-48: Drawing of Centerline Curvature of C-Shaped Coil Spring

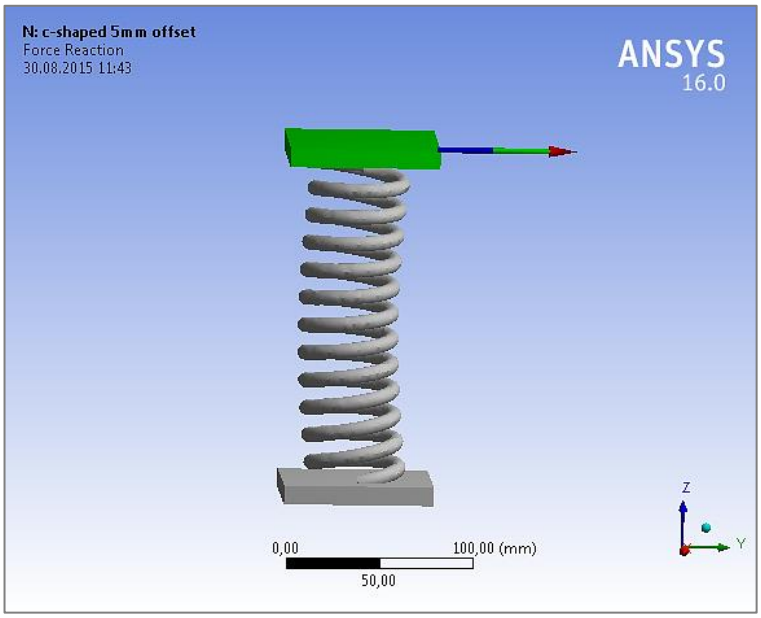

Figure 3-49: Reaction Forces of 5 mm Offset C-Shaped Coil Spring

➔ F_x=5.3478 N, F_y=11.479 N, F_z=0 N

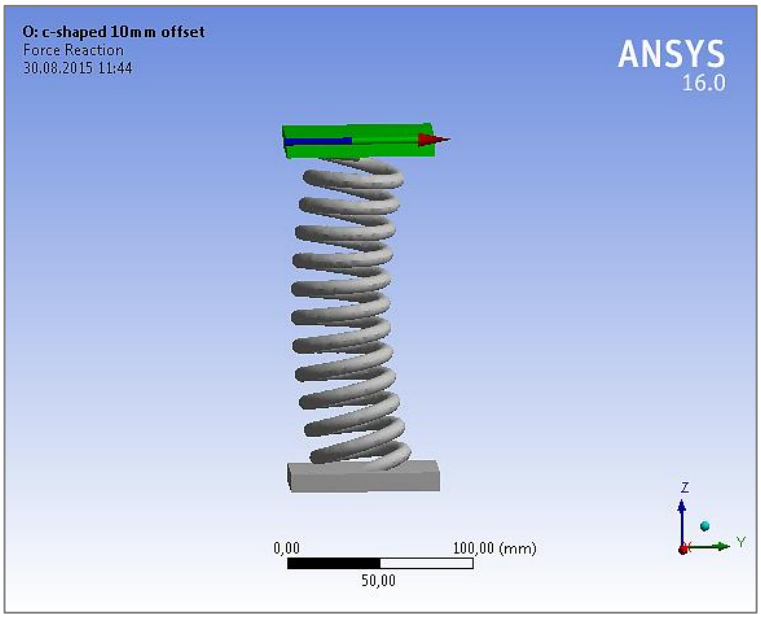

Figure 3-50: Reaction Forces of 10 mm Offset C-Shaped Coil Spring

➔ F_x=4.9033 N, F_y=12.916 N, F_z=0 N

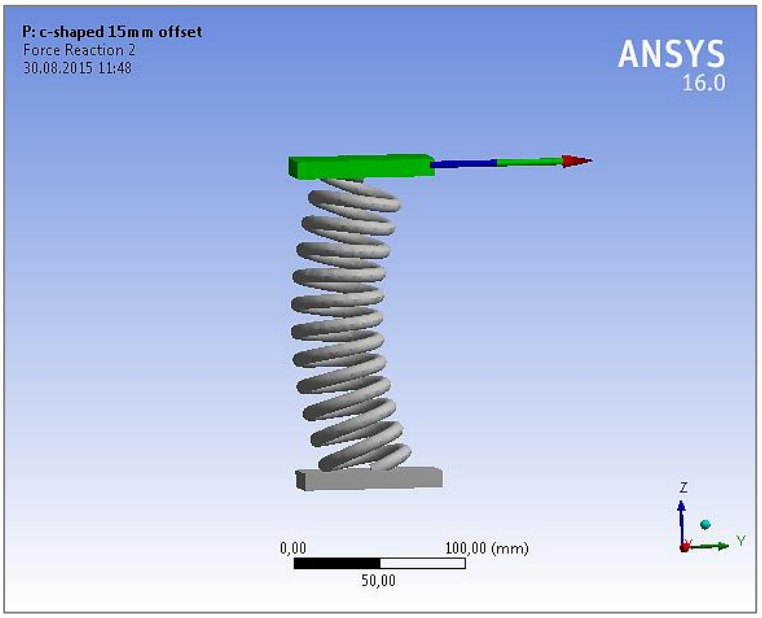

Figure 3-51: Reaction Forces of 15 mm Offset C-Shaped Coil Spring

➔ F_x=3.1054 N, F_y=16.211 N, F_z=0 N

3.4.3. L-SHAPED

In 2001, reducing side force by using L-shaped coil spring was studied by Hamano and Nakamura [6]. Actually, L-shaped coil spring is a solution similar to mounting spring inclined to the strut axis to reduce side force. L-shaped spring is designed by inclining the conventional coil spring to a certain direction with a certain inclined angle. When the angle increases, generated side force increases too. Amount of inclination is given by tilting the centerline axis and can be seen in Figure 3-52. Also, the results of generated side forces can be seen in Figure 3-53 and Figure 3-54.

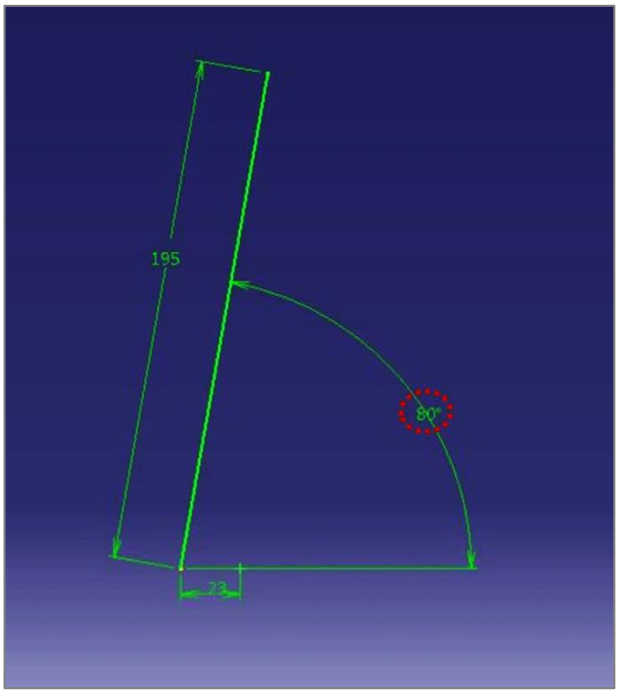

Figure 3-52: Drawing of Centerline Curvature of L-Shaped Coil Spring

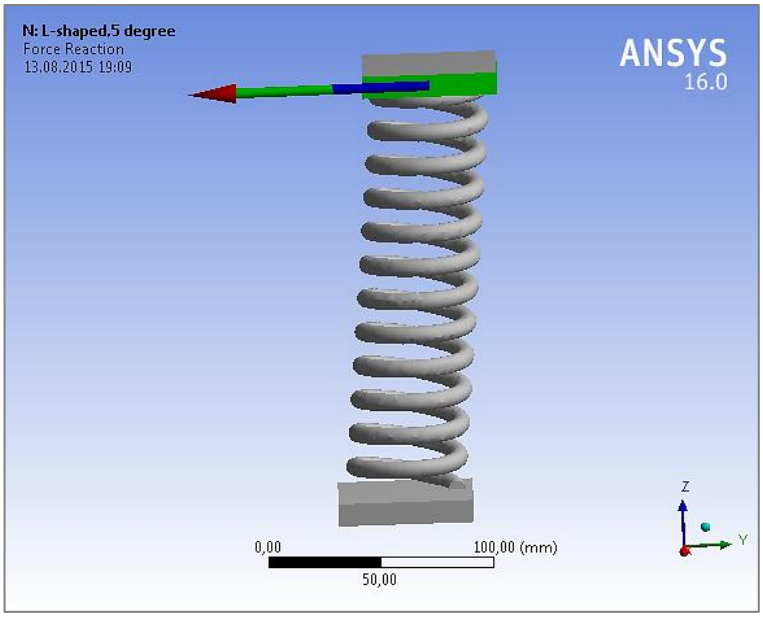

Figure 3-53: Reaction Forces of 5 Degrees L-Shaped Coil Spring

➔ F_x=4.6034 N, F_y=-121.79 N, F_z=0 N

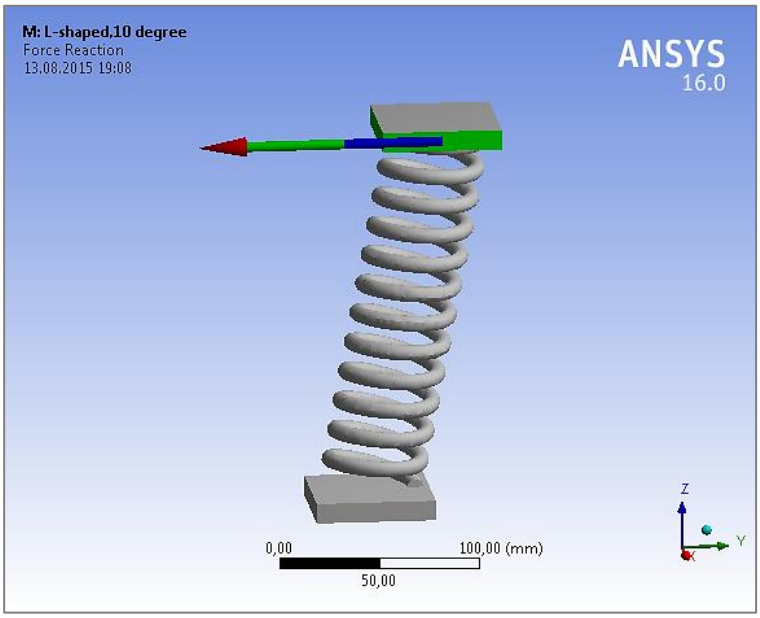

Figure 3-54: Reaction Forces of 10 Degrees L-Shaped Coil Spring

➔ F_x=0.7583 N, F_y=-254.72 N, F_z=0 N

3.4.4. VARYING WIRE DIAMETER

A coil spring with different wire diameters on the different sections may also generate lateral forces. However, there is no study covering in detail this type of coil springs that are used as side load springs in the literature. Moreover, the magnitude and the direction of generated lateral force cannot be controlled in this manner and manufacturing process may be expensive and challenging. When a conventional coil spring is split into three parts that have different wire diameters, this coil spring generates more lateral forces compared to conventional coil spring. Several options of varying wire diameter and generated side forces of these springs can be seen from Figure 3-55 to Figure 3-58.

Figure 3-55: 3D Model of Varying Wire Diameter Coil Spring

Option-1: Bottom part→d=8 mm, middle part→d=6 mm, upper part→d=10 mm

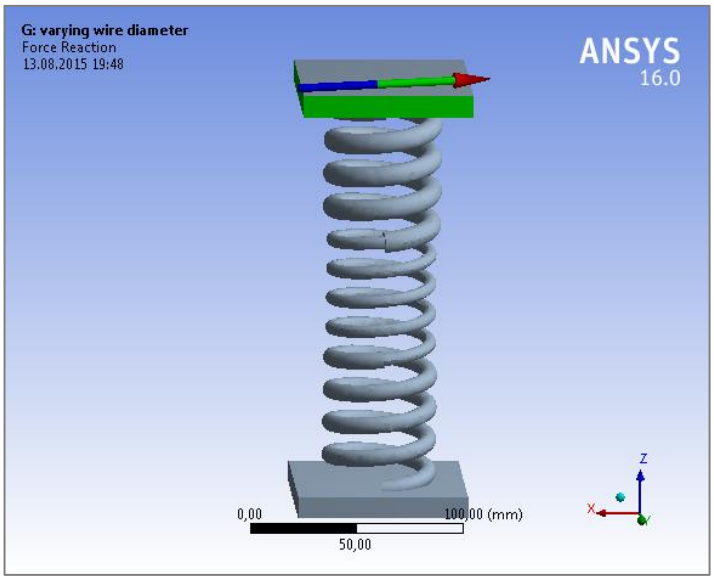

Figure 3-56: Reaction Forces of Varying Wire Diameter Coil Spring, Option-1

➔ F_x=-44.734 N, F_y=-9.0359 N, F_z=0 N

Option-2: Bottom part→d=8 mm, middle part→d=10 mm, upper part→d=6 mm

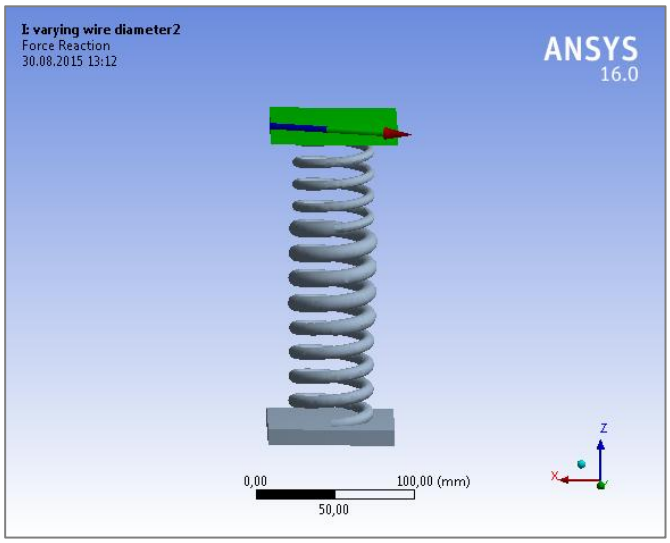

Figure 3-57: Reaction Forces of Varying Wire Diameter Coil Spring, Option-2

➔ F_x=-16.375 N, F_y=5.4561 N, F_z=0 N

Option-3: Bottom part→d=6 mm, middle part→d=8 mm, upper part→d=10 mm

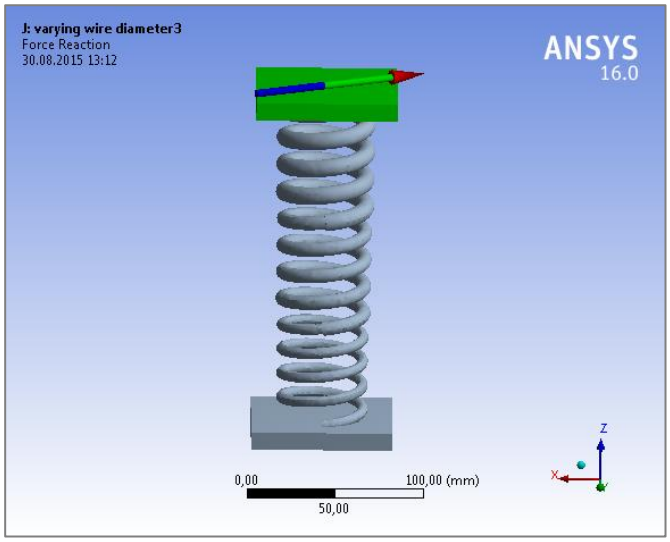

Figure 3-58: Reaction Forces of Varying Wire Diameter Coil Spring, Option-3

➔ F_x=-30.731 N, F_y=-15.76 N, F_z=0 N

3.4.5. PIGTAIL

Most side load springs have pigtail coil at the ends, the pigtails generally have different diameters and the last coils have different helix angles. This geometry provides absorbing lateral forces on the shock absorber. Other advantages of pigtail coil springs are reduced overall height and related to the reduced weight. Coils engage each other and do not contact in operation and this prevents the impact noise of coils. The pigtail coil spring design is mentioned in some studies, and design steps will be given in the next section. A typical pigtail coil spring can be seen in Figure 3-59.

Figure 3-59: Pigtail Coil Spring [31]

- **Pigtail Design**

In order to remove side load on the damper of the MacPherson strut suspension, another design method is the coil springs with pigtail ends on the both ends. In 2010, Choi [11] introduced a study including the pigtail design formulation and design method of that study will be summarized in this part.

As shown in Figure 3-60, the pigtails at the top and bottom begin at points A and B, respectively, at which the radius is D/2. The radii decreased to R_p at the points C and D. Beyond these points, a circular arc with constant radius R_p is continued with the center points E and F up to the end points G and H, respectively. While the arc angle of the pigtail end at the bottom is fixed at 90 degrees, the arc angle at the top is variable with the magnitude θ_p. The design variables are the radius of the pigtail end R_p, central angle θ_p of the pigtail at the top, and the length h that controls the variable pitch length of each coil according to relations given in Figure 3-60. The rest of the parameters, coil diameter D, wire diameter d, and angle of line of force α are constants.

There are spring seats at the top and bottom that the spring is in contact with. At the upper seat, all of the degrees of freedom are fixed, while displacement in the z direction is free at the bottom seat. The spring is subjected to compressive displacement and the reaction forces are obtained at the top seat. The anti-side load vector is obtained in the x and y direction and the resultant force on the spring can be obtained by the difference of the original and anti-side load vectors. This relation can be seen in Figure 3-61. In the future work of this thesis study, side load spring design may be combined with pigtail spring design and a new side load spring design method may be proposed.

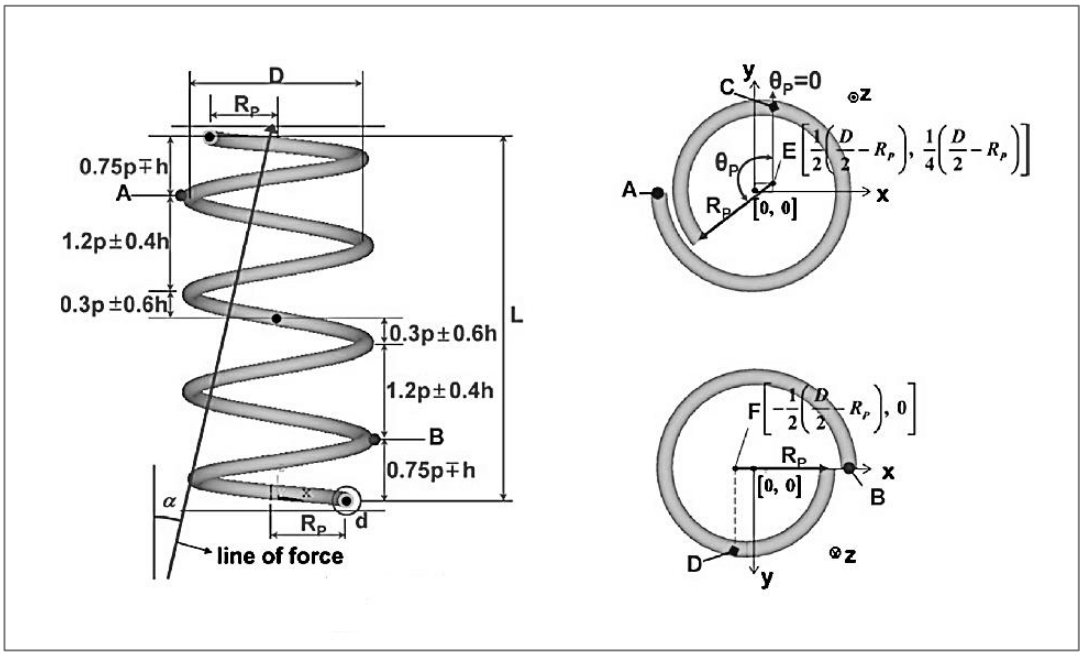

Figure 3-60: Variables of Pigtail Spring Design [11]

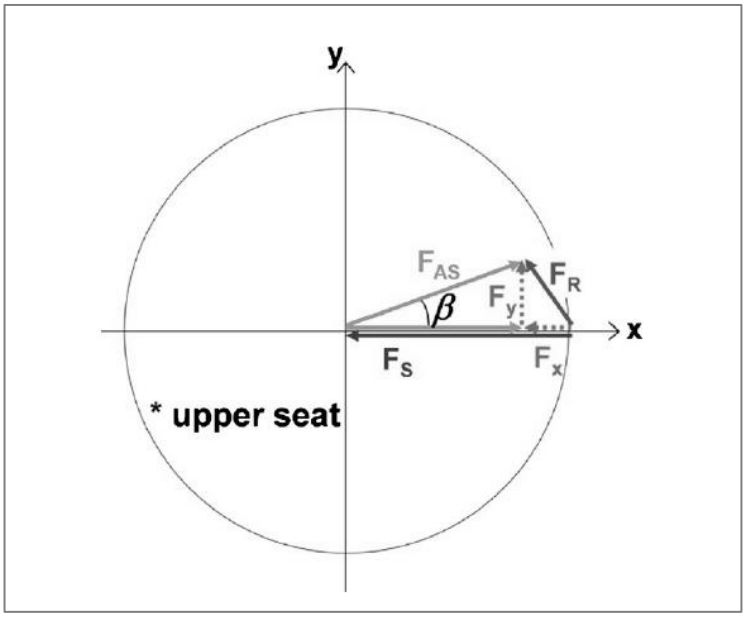

Figure 3-61: Force Diagram of the Side Loads of Pigtail Spring [11]

3.4.6. OTHER DESIGN METHODS

There are several other modifications that can be applied to coil springs, some of them may generate side forces while some of them may not. These modifications may be applied for side load springs to obtain different amount of side loads while some of them may generate side force as their own characteristic. These methods will be briefly mentioned here.

- **Inclined End Coils**

Inclining the geometry of the end coils can also generate side forces, however instead of giving inclination to the end coils as seen in Figure 3-62, usually angled spring pans are used. In 2000, Tao and Bishop investigated the effect of spring seat orientation; the results show that increase of inclination angle of spring seats helps to reduce side load [32].

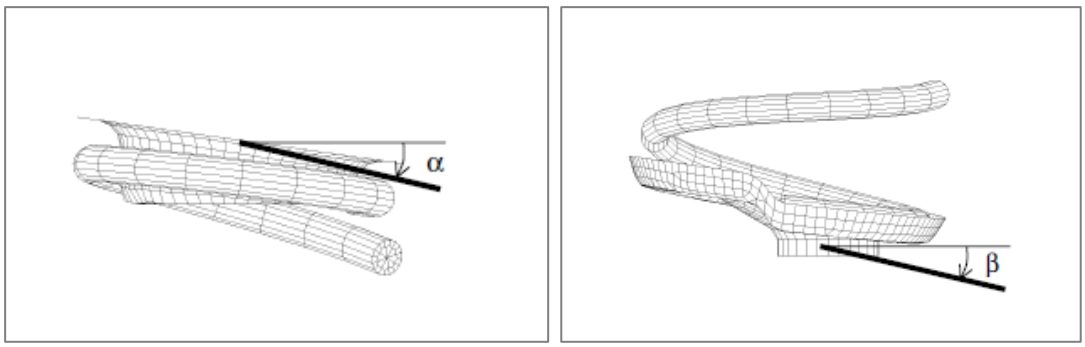

Figure 3-62: Spring Seats Inclination [33]

- **V-Shaped**

V-shaped and conical shape springs offer varying spring rate instead of a constant spring rate. These types of springs do not generate extra side force and are not used while designing side load springs. However, these methods may help to generate different side forces for different deflections of side load springs and may be investigated. A few types of conical and V-shaped coil springs can be seen in Figure 3-63.

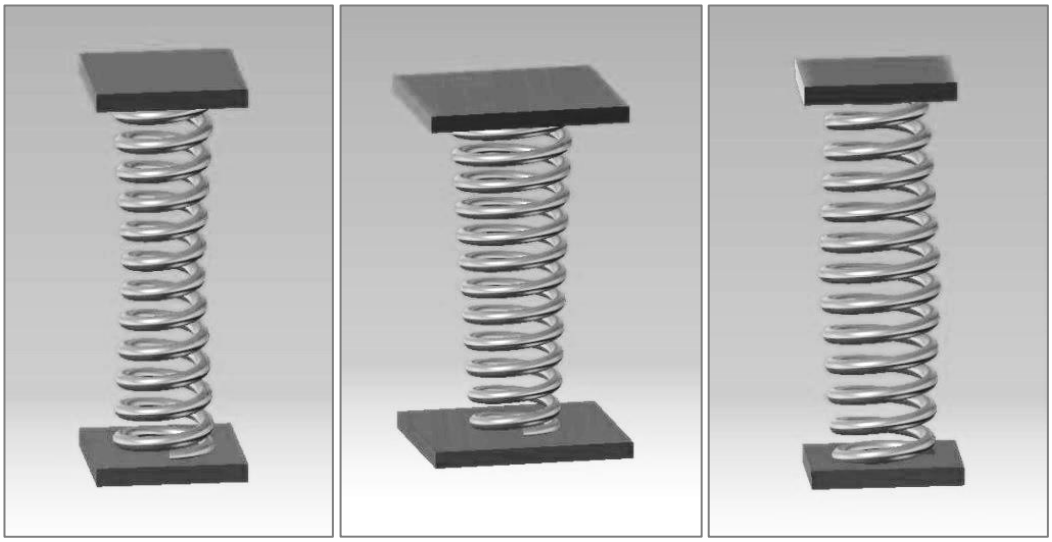

Figure 3-63: Conical Forms of Coil Spring

- **Offset on the End Coils**

By giving offset to the end coils as in Figure 3-64, side force can be generated. This method is mentioned by Gillet and Ouakka in 2006, and details can be seen in [34].

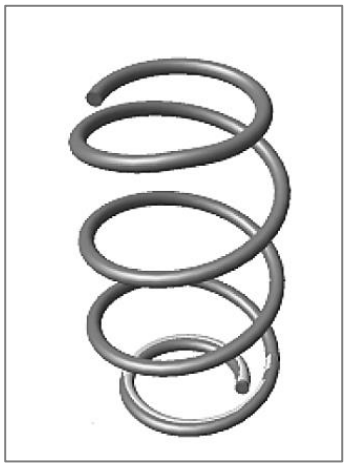

Figure 3-64: Coil Spring with Offsetting End Coils [34]

- **Varying Pitch**

Varying pitch that can be seen in Figure 3-65, affects the spring characteristic but not in such way that it generates side force. It only changes the stiffness features of the coil spring and enables the coil spring progressive rate stiffness. However, coil springs with pigtail ends generally use varying pitch, especially at the end coils.

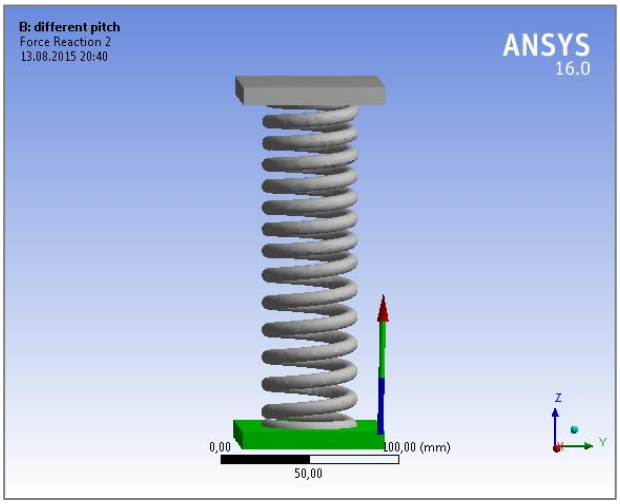

Figure 3-65: Varying Pitch Coil Spring

CHAPTER 4

DESIGN AND ANALYSIS OF SIDE LOAD SPRINGS

4.1. SIDE FORCE PROBLEM OF MACPHERSON STRUT SUSPENSION

In this section, side force problem of the MacPherson strut suspension is examined and mathematical model for spring centerline curvature is developed. As shown in Figure 4-1, there exists a side force F_Q acting on the top of the damper rod and creates a bending moment on the damper. This side load increases the inner friction between the damper parts and results in reduced ride comfort and increased wear of the damper parts. In addition to that, vertical vibrations may be transferred to the vehicle body of vehicles with MacPherson strut suspension due to the fact that light road excitation may not be able to overcome the inner friction and this can cause to failure of operation of the suspension. In order to eliminate this side force, coil spring may be mounted at an inclination to the centerline of the strut. This approach, however, may not generally be possible because of space limitations. Therefore, side load springs have been used to generate lateral forces to counter side forces.

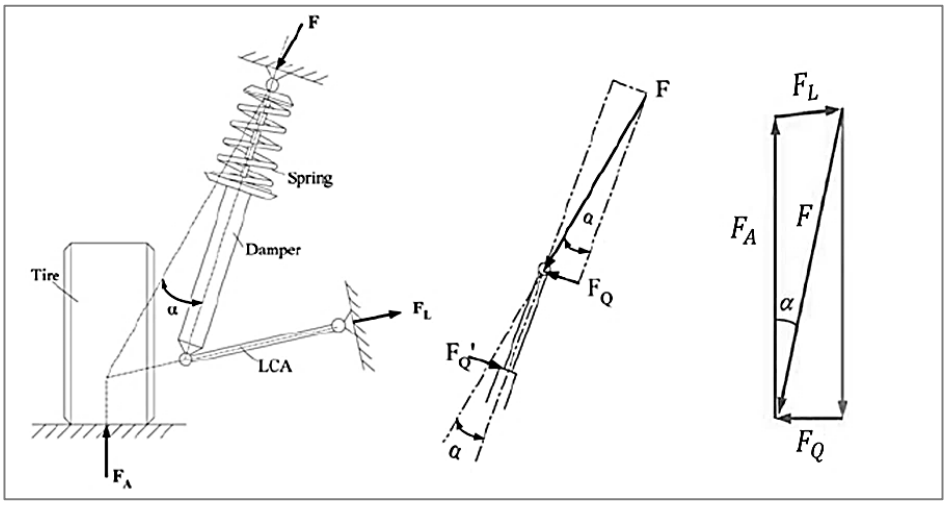

Figure 4-1: Vector of Forces Acting on the MacPherson Strut Suspension [9]

In this study, a mathematical formulation is developed for the spring centerline curvature and side load springs are modeled according to this formula. The modeled side load springs are analyzed and the generated side forces are obtained, and the analyses are carried on until the side force is minimized. The design flow chart can be seen in Figure 4-2.

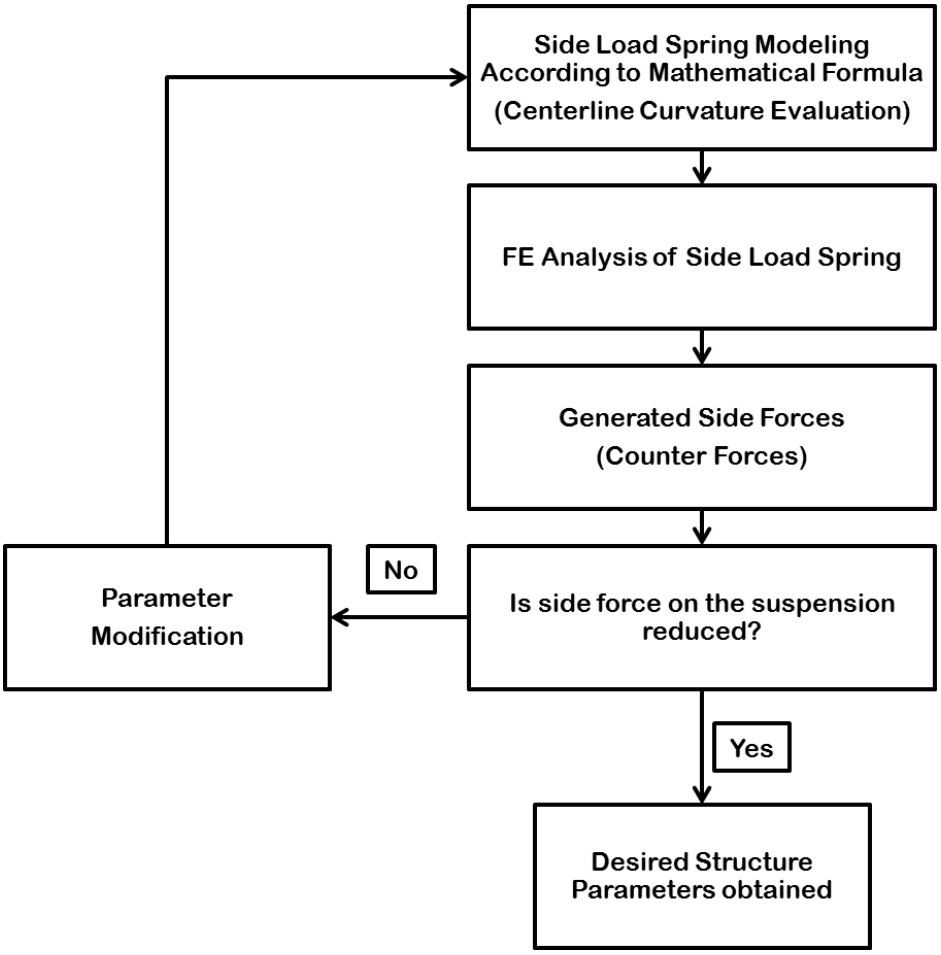

Figure 4-2: Design Procedure Chart

4.2. MATHEMATICAL MODEL

4.2.1. CENTERLINE CURVATURE DESIGN

Assuming the curvature of spring centerline (ρ) is very small, the lateral displacement of coil spring during compression and extension can be neglected. Also, it can be accepted that the corresponding curve length (A_1) is equal to the vertical length of a line (H_1) connecting the arc start and finish points vertically, as can be seen in Figure 4-3. In other words, the length of l_1 can be assumed zero for a very small curvature.

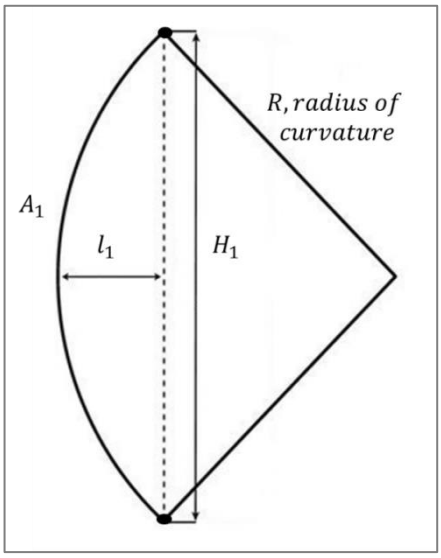

Figure 4-3: Radius of Curvature Illustration

The 2D drawing of side load coil spring can be seen in Figure 4-4; it is drawn exaggeratedly to show the curvature; however when the coil spring is compressed to working length (L_w), its shape looks almost like a conventional coil spring.

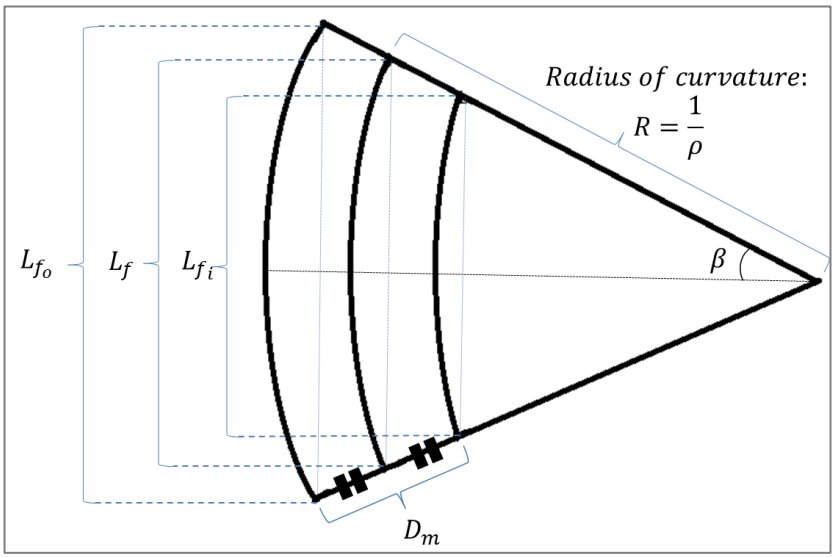

Figure 4-4: Lengths of Coil Spring with Curved Centerline

- **Constant Curvature Design**

In 2008, paper presented by Liu, Zhuang, Yu, and Lou explains the initial curvature calculation to derive mathematical formulation [9]. In 2012, a similar study was performed by Joshi and Chhabra [12]. For a coil spring with constant curvature, spring geometry has a shape during free and working lengths like in Figure 4-5 and some parameters which will be used in calculations are shown. The main assumptions for the calculations are given in Eqs. (21), (22) and (23). When spring is compressed from its free length (L_f) to working length (L_w), vertical decrements on the outer and inner side of the spring are given in Eqs. (26) and (27). Since the vertical decrements are different on the outer and inner side, there exists a difference of vertical spring force on the outer and inner side of coil spring. Therefore, spring force action line shifts a certain displacement according to these forces and this displacement is designated as c whose calculation is given in Eq. (31) and value is given in Eq. (32).

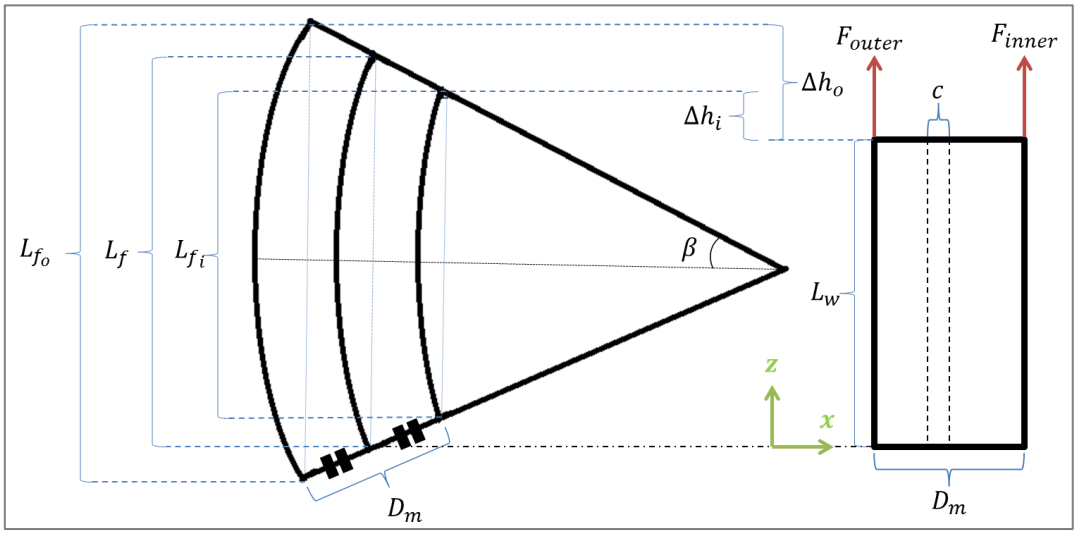

Figure 4-5: Coil Spring with Centerline of Constant Curvature and Compressed State

Main assumptions for the calculations;

$$\rho \cong 0 \text{ or } R \cong \infty \tag{21}$$

$$\arcsin \beta \cong \frac{L_f}{2} \tag{22}$$

$$\sin \beta \cong \tan \beta = \frac{(L_f/2)}{(1/\rho)} = \frac{L_f * \rho}{2} \tag{23}$$

Free length of the inner and outer side;

$$\begin{aligned} L_{f_i} &= 2 * sin\beta * \left(\frac{1}{\rho} - \frac{D_m}{2}\right) = 2 * \left(L_f * \frac{\rho}{2}\right) * \left(\frac{1}{\rho} - \frac{D_m}{2}\right) \\ &= \left(L_f * \frac{\rho}{2}\right) * \left(\frac{2}{\rho} - D_m\right) \end{aligned} \tag{24}$$

$$\begin{aligned} L_{f_o} &= 2 * sin\beta * \left(\frac{1}{\rho} + \frac{D_m}{2}\right) = 2 * \left(L_f * \frac{\rho}{2}\right) * \left(\frac{1}{\rho} + \frac{D_m}{2}\right) \\ &= \left(L_f * \frac{\rho}{2}\right) * \left(\frac{2}{\rho} + D_m\right) \end{aligned} \tag{25}$$

Vertical decrements of the inner and outer side when spring compressed to working length of L_w;

$$\begin{aligned} \Delta h_i &= L_{f_i} - L_w = \frac{L_f * \rho}{2} * \left(\frac{2}{\rho} - D_m\right) - L_w \\ &= L_f - L_w - \frac{L_f * \rho * D_m}{2} \end{aligned} \tag{26}$$

$$\begin{aligned} \Delta h_o &= L_{f_o} - L_w = \frac{L_f * \rho}{2} * \left(\frac{2}{\rho} + D_m\right) - L_w \\ &= L_f - L_w + \frac{L_f * \rho * D_m}{2} \end{aligned} \tag{27}$$

Magnitude of the vertical forces on the inner and outer side can be written as;

$$F_{inner} = k * \Delta h_i = k * \left(L_f - L_w - \frac{L_f * \rho * D_m}{2} \right) \quad \textbf{(28)}$$

$$F_{outer} = k * \Delta h_o = k * \left(L_f - L_w + \frac{L_f * \rho * D_m}{2} \right) \quad \textbf{(29)}$$

Magnitude of the total vertical force can be written as;

$$F_v = \frac{1}{2} * k * (\Delta h_i + \Delta h_o) = k * (L_f - L_w) \quad \textbf{(30)}$$

Calculation of displacement of the spring force action line;

$$F_{outer} * \left(\frac{D_m}{2} - c \right) = F_{inner} * (\frac{D_m}{2} + c)$$

$$k * \left(L_f - L_w + \frac{L_f * \rho * D_m}{2} \right) * \left(\frac{D_m}{2} - c \right) = k * \left(L_f - L_w - \frac{L_f * \rho * D_m}{2} \right) * (\frac{D_m}{2} + c) \quad \textbf{(31)}$$

Displacement of the spring force action line becomes;

$$c = \frac{\rho * D_m^2 * L_f}{4 * (L_f - L_w)} \rightarrow \rho = 4 * c * \frac{(L_f - L_w)}{D_m^2 * L_f} \quad \textbf{(32)}$$

Eq. (32) only provides an initial value for the curvature and finite element analysis and simulation has to be employed to this equation to obtain more actual centerline curvature.

By using the assumptions defined in Eqs. (21) and (22), it can be said that x' is very small. Since x'<<1, then $(x')^2$ can be neglected and Eq. (33) takes the form of Eq. (34).

$$\rho = \frac{x''}{[(1 + (x')^2]^{\frac{3}{2}}} \tag{33}$$

$$\rho \approx \frac{d^2x}{dz^2} = x'' \tag{34}$$

Adapting Eq. (33) to the case of this study, formula for the actual curvature can be obtained. Double integration of Eq. (32) with respect to z will give the expression for the profile of center curvature of the coil spring.

$$x = \iint \frac{d^2x}{dz^2} \rightarrow x = \iint \rho dz^2 \tag{35}$$

$$\begin{aligned} x = \iint \rho dz^2 &= \iint \frac{4 * c * \left(L_f - L_w\right)}{D_m^2 * L_f} \, dz^2 \\ &= \int \frac{4 * c * \left(L_f - L_w\right)}{D_m^2 * L_f} * z + U_1 \\ &= \frac{2 * c * \left(L_f - L_w\right)}{D_m^2 * L_f} * z^2 + U_1 * z + U_2 \end{aligned} \tag{36}$$

Assuming that U_1=0 and U_2=0, then Eq. (36) becomes;

$$x = \frac{2 * c * \left(L_f - L_w\right)}{D_m^2 * L_f} * z^2 \tag{37}$$

The second order equation (37) will give the profile of center curve. After this, the spring whose properties are given in Table 4-1 will be used in this study. For specific values of c, center curve of coil spring can be seen in Figure 4-6. Since changing curvature design, which will be studied in the following section, also covers constant curvature design, no more details are pursued in here.

Table 4-1: Spring Properties of Model-B [9]

Wire diameter, d		12 mm
Mean diameter of the coil, D		125 mm
Number of Active Coils, n		4.9
Number of Total Coils, n’		6.5
Free length of the spring, L_f		354.0 mm
Solid length of the spring, L_s		78.0 mm
Material (Stainless Steel Wire)	Elastic Modulus, E Poisson Ratio, ν Shear Modulus, G	E=200 GPa ν=0.3 G=80 GPa

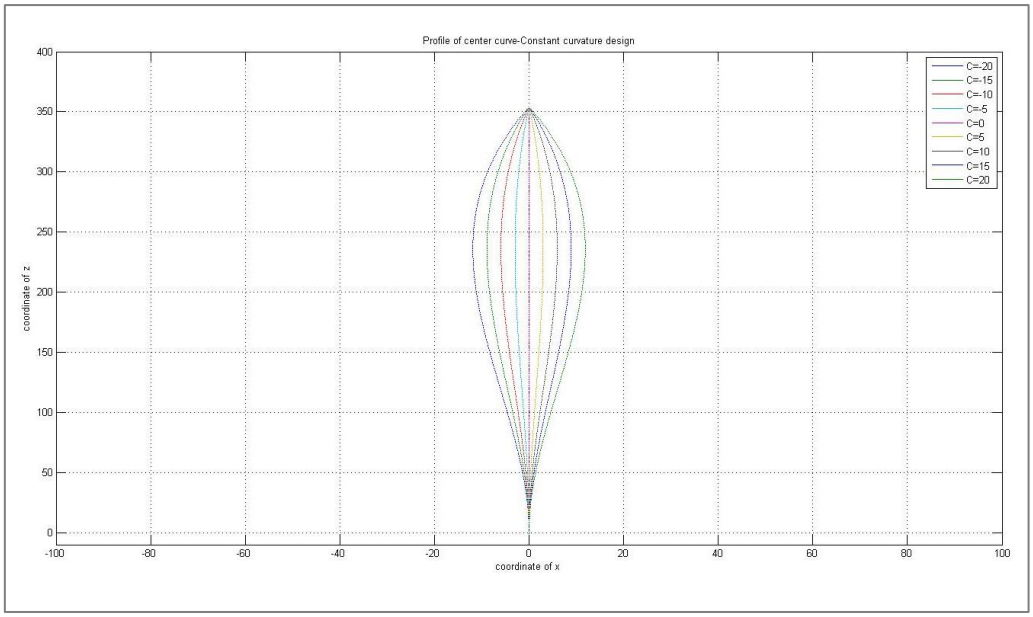

Figure 4-6: Center Curve Profiles for Different Offsets-Constant Curvature Design

- **Changing Curvature Design**

For a coil spring with varying curvature, spring force action line has an angle (α) and may have an offset at the top seat as shown in Figure 4-7. The Eq. (32) can be applied for this case.

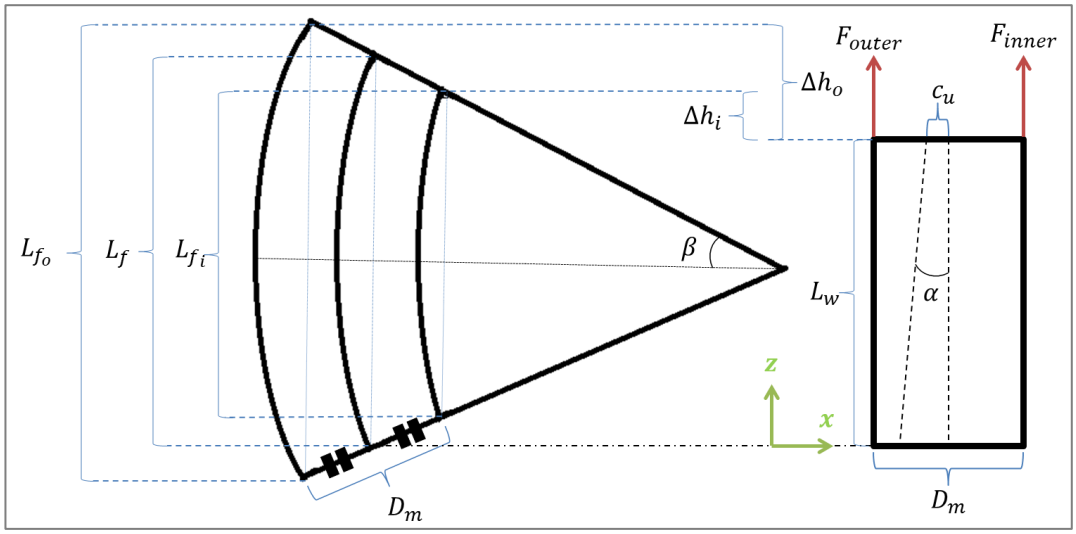

Figure 4-7: Coil Spring with Centerline of Changing Curvature and Compressed State

Displacement of the spring force action line can be expressed as;

$$c(z) = c_u + \left(L_f - z\right) * tan\alpha \tag{38}$$

Then, Eq. (32) can be written in the form of below;

$$\begin{aligned} \rho(z) &= \frac{4 * \left(L_f - L_w\right)}{D_m^2 * L_f} * c(z) \\ &= \frac{4 * \left(L_f - L_w\right)}{D_m^2 * L_f} * \left[c_u + \left(L_f - z\right) * tan\alpha\right], z \in [0, L_f] \end{aligned} \tag{39}$$

Eq. (39) only provides an initial value for the curvature and finite element analysis and simulation has to be employed to obtain more actual centerline curvature.

Similar to constant curvature side load spring design, same operations will be repeated here. Using Eq. (39), formulation for the actual curvature can be obtained. Double integration of Eq. (39) with respect to z will give the formula for the profile of center curvature of the coil spring.

$$x = \iint \rho(z)dz^2 = \iint \frac{4 * \left(L_f - L_w\right)}{D_m^2 * L_f} * \left[c_u + \left(L_f - z\right) * tan\alpha\right]dz^2 \qquad z \in [0, L_f] \tag{40}$$

$$x = \iint \frac{4 * \left(L_f - L_w\right)}{D_m^2 * L_f} * \left[c_u + \left(L_f - z\right) * tan\alpha\right]dz^2$$

$$= \int \left\{\frac{4 * \left(L_f - L_w\right)}{D_m^2 * L_f} * \left[c_u * z + \left(L_f * z - \frac{z^2}{2}\right) * tan\alpha\right] + U_1\right\}dz \tag{41}$$

$$= \frac{4 * \left(L_f - L_w\right)}{D_m^2 * L_f} * \left[-\frac{tan\alpha}{6} * z^3 + \frac{\left(L_f * tan\alpha + c_u\right)}{2} * z^2\right] + U_3 * z + U_4$$

$$z \in [0, L_f]$$

Assuming that U_3=0 and U_4=0, then Eq. (41) becomes;

$$x = \frac{4 * \left(L_f - L_w\right)}{D_m^2 * L_f} * \left[-\frac{tan\alpha}{6} * z^3 + \frac{\left(L_f * tan\alpha + c_u\right)}{2} * z^2\right], \qquad z \in [0, L_f] \tag{42}$$

The cubic equation (42) will give the profile of center curve for changing curvature design. For a specific value of α, center curve of coil spring can be seen in Figure 4-8 for different c_u values.

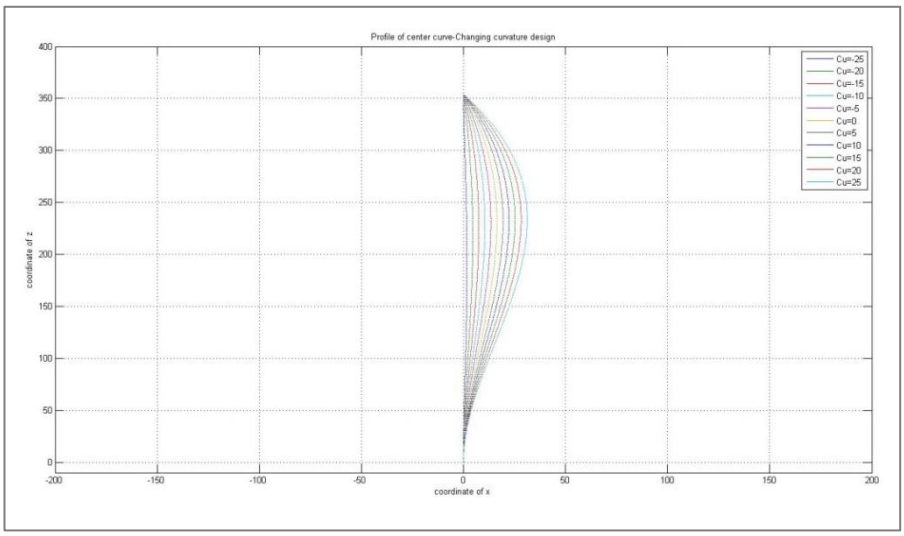

Figure 4-8: Center Curve Profiles for Different Offsets-Changing Curvature Design

Similarly, for a specific value of c_u, center curve of coil spring can be seen in Figure 4-9 for different α values.

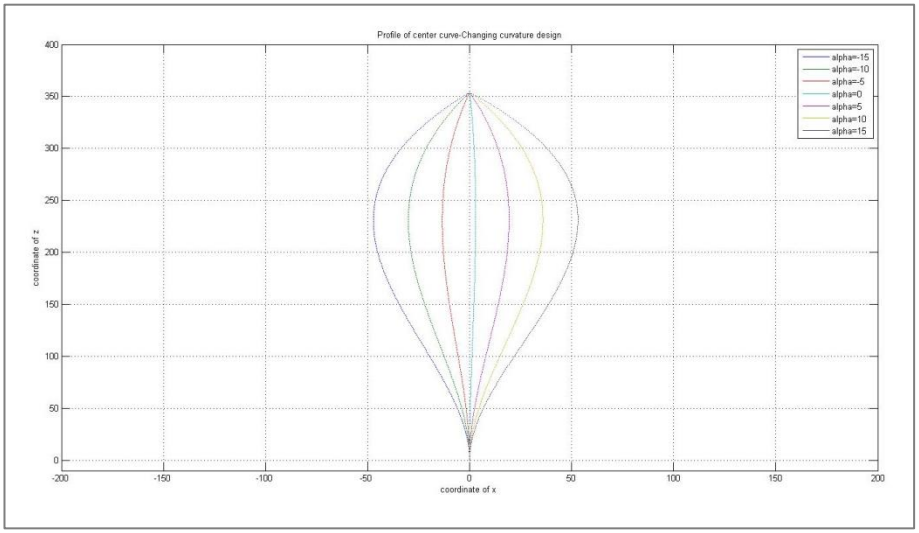

Figure 4-9: Center Curve Profiles for Different Angles-Changing Curvature Design

Lastly, for specific values of α and c_u, the center curve of coil spring can be seen in Figure 4-10. 3D plots that visualize the side load spring for specific values of α and c_u, can be seen in Figure 4-11, Figure 4-13 and Figure 4-15, while 2D plots of the center curve is given in Figure 4-12, Figure 4-14 and Figure 4-16.

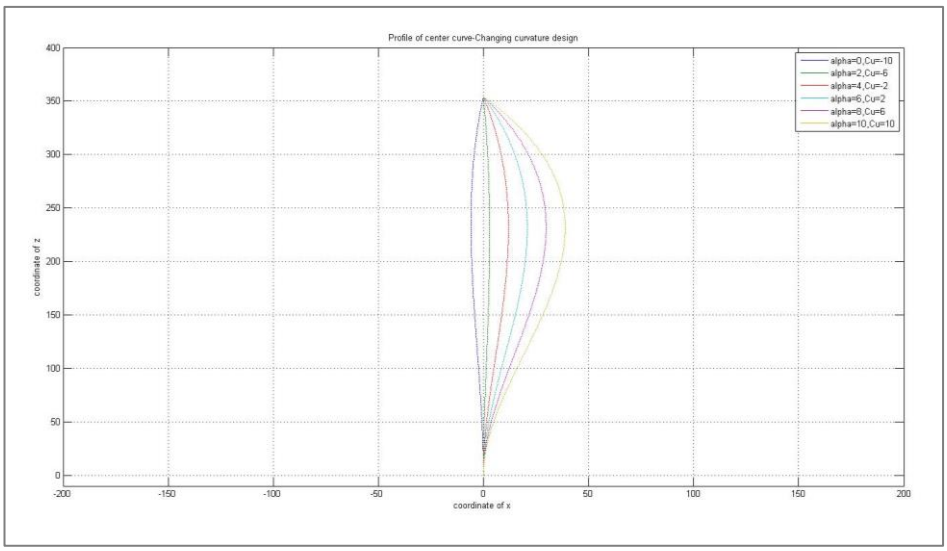

Figure 4-10: Center Curve Profiles for Specific Offsets and Angles-Changing Curvature Design

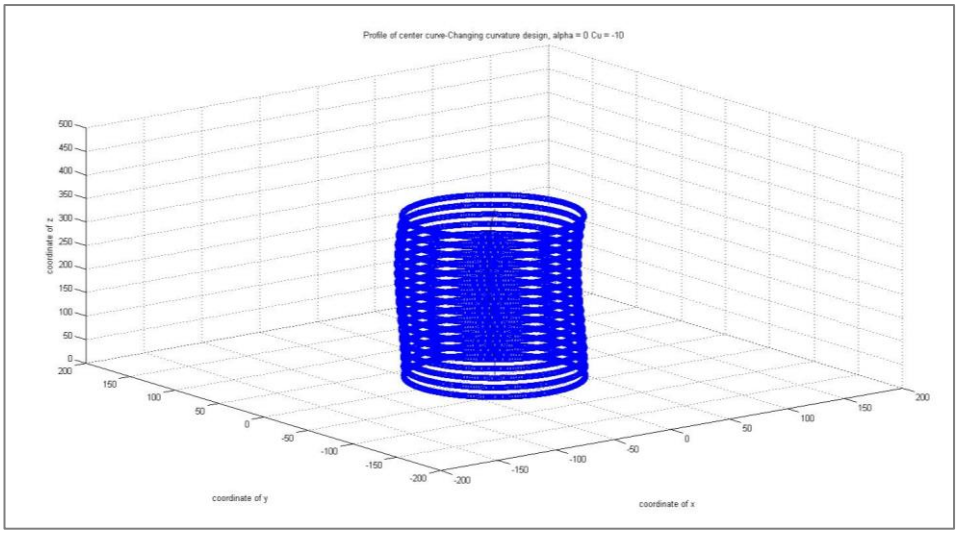

Figure 4-11: 3D Center Curve Profile for α=0°, c_u=-10 mm-Constant Curvature Design

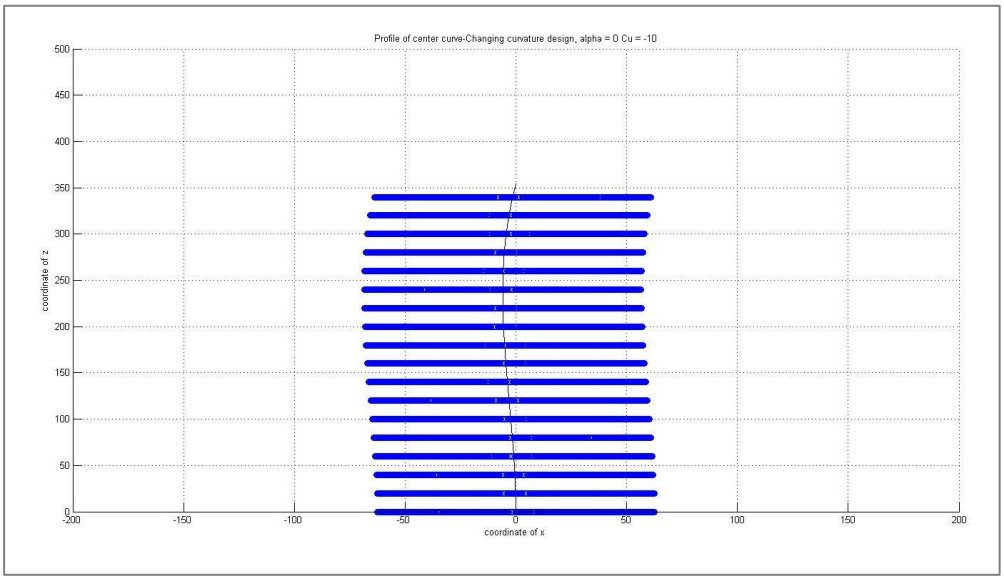

Figure 4-12: 2D Center Curve Profile-XZ Plane View for α=0°, c_u=-10 mm-Constant Curvature Design

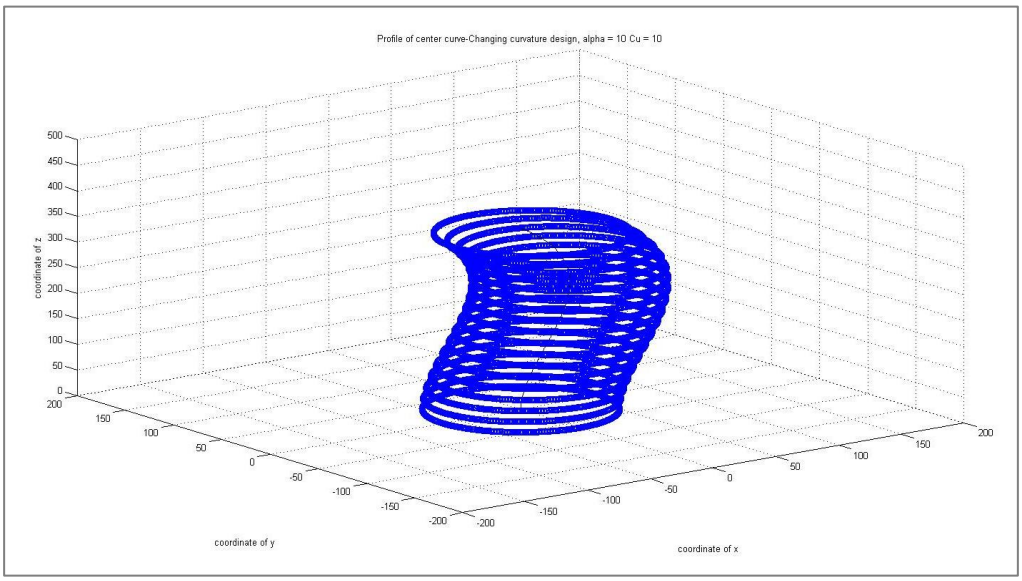

Figure 4-13: 3D Center Curve Profile for α=10°, c_u=10 mm-Changing Curvature Design

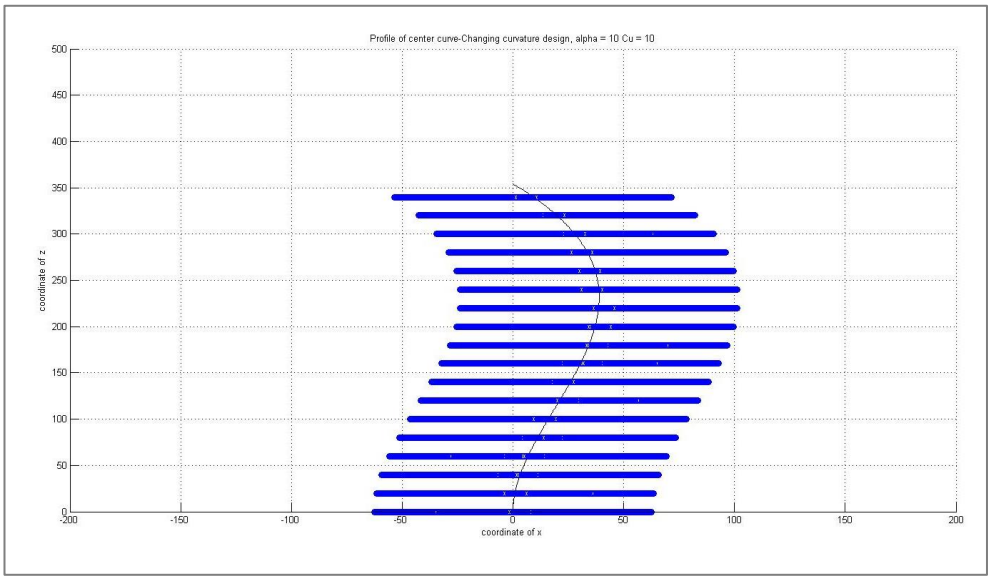

Figure 4-14: 2D Center Curve Profile-XZ Plane View for α=10°, c_u=10 mm-Changing Curvature Design

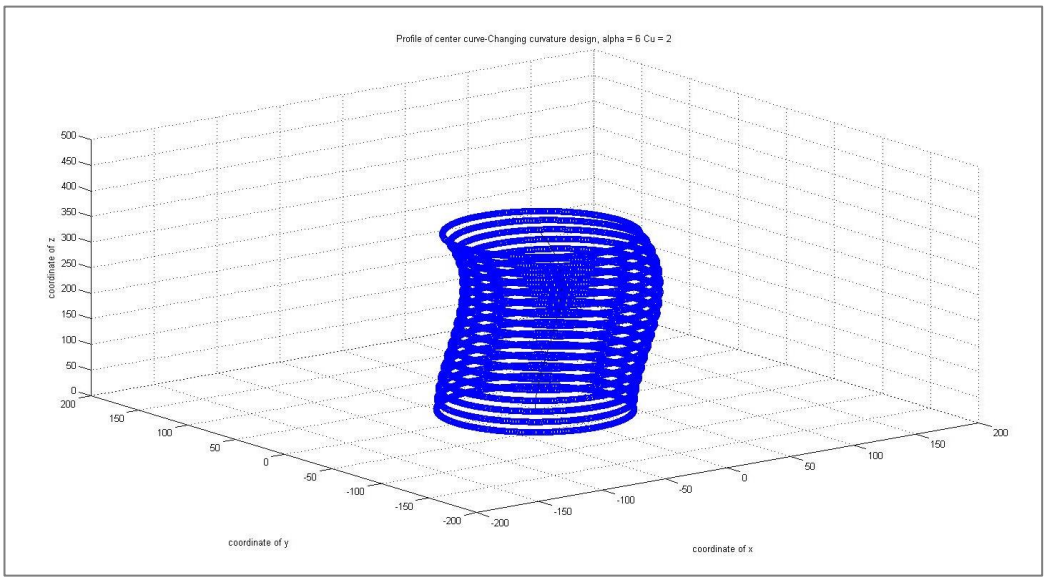

Figure 4-15: 3D Center Curve Profile for α=6°, c_u=2 mm-Changing Curvature Design

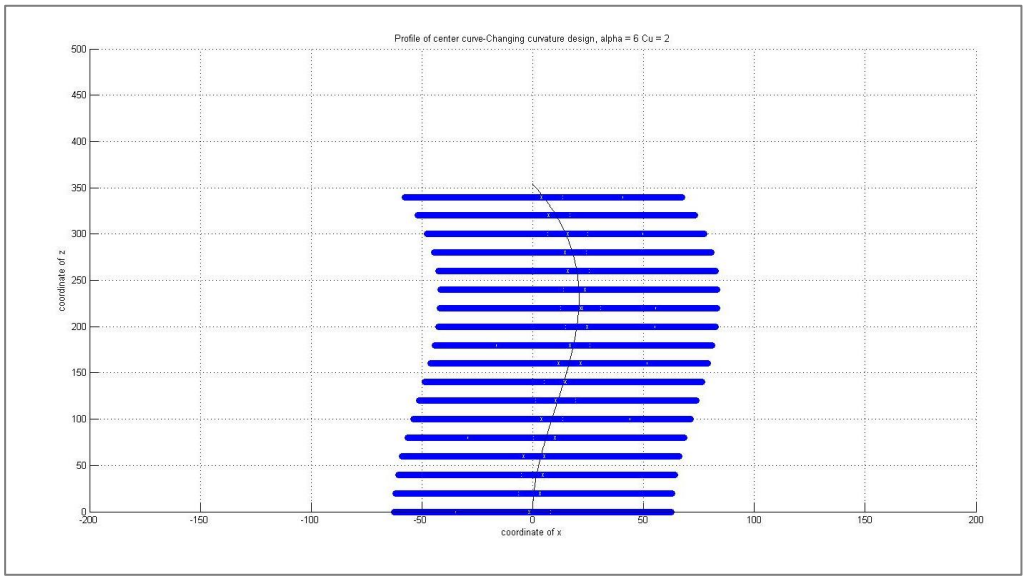

Figure 4-16: 2D Center Curve Profile-XZ Plane View for α=6°, c_u=2 mm-Changing Curvature Design

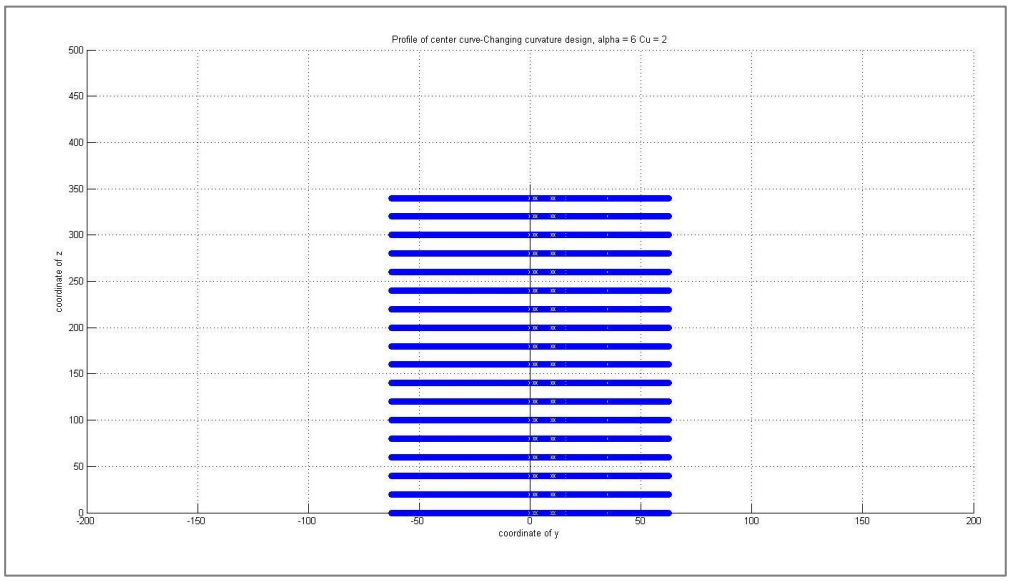

Figure 4-17: 2D Center Curve Profile-YZ Plane View for α=6°, c_u=2 mm-Changing Curvature Design

Figure 4-17 is same for all configurations; spring centerline from yz plane view is still a straight line while it is curved when viewed from the other plane, xz plane.

Those spring models are generated in MATLAB script file, and then center curve profile is exported as to Excel file and this file is imported to the CATIA, and finally side load springs are modeled for analysis as will be explained in section 4.3.

- **Changing Curvature Design-Modified**

For a coil spring with varying curvature, spring force action line has an angle (α) and may have an offset at the top seat as shown in Figure 4-7. The Eq. (42) is derived for evaluating the profile of center curve for changing curvature design.

If it is assumed that the stiffness of the designed side load spring is equal the stiffness of the conventional coil spring, Eq. (42) can be changed slightly and the stiffness of the spring can be included to this equation as a design parameter.

Then, the spring force action line angle (α) is derived from the input parameters; the deflection (δ) and the desired lateral force (F_{LD}) corresponding to that deflection. Eq. (42) can be modified to Eq. (47) by using the equations from Eq. (43) to Eq. (46). Eq. (48) is another centerline curvature formulation which contains the stiffness parameters of the spring.

$$F_v = \delta * k \tag{43}$$

Recall the stiffness of the spring;

$$k = \frac{G.d}{8C^3.n} \tag{44}$$

Total force on the suspension is;

$$F = (F_{LD}^2 + F_v^2)^{\frac{1}{2}} \tag{45}$$

The spring force action line angle (α) becomes;

$$\alpha = \arctan\left(\frac{F_{LD}}{Fv}\right) = \arctan\left(\frac{F_{LD}}{\delta * k}\right) = \arctan\left(\frac{8 * F_{LD} * C^3 * n}{\delta * G * d}\right) \quad \textbf{(46)}$$

Centerline curvature equation becomes;

$$x = \frac{4 * \left(L_f - L_w\right)}{D_m^2 * L_f} * \left[-\frac{F_{LD}}{6 * \delta * k} * z^3 + \frac{\left(L_f * \left(\frac{F_{LD}}{\delta * k}\right) + c_u\right)}{2} * z^2 \right], \quad \textbf{(47)}$$

$$z \in [0, L_f]$$

Eq. (47) can also be expressed as;

$$x = \frac{16 * \left(L_f - L_w\right)}{D_m^2 * L_f} * \left[-\frac{F_{LD} * C^3 * n}{3 * \delta * G * d} * z^3 + \left(\frac{L_f * F_{LD} * C^3 * n}{\delta * G * d} + 0.125 * c_u\right) * z^2 \right], \quad \textbf{(48)}$$

$$z \in [0, L_f]$$

Since the trigonometric functions take negative values for specific intervals, Eqs. (47) and (48) should be used carefully.

4.3. MODELING AND ANALYSIS OF SIDE LOAD SPRINGS

In this section, analyses of side load springs modeled according to mathematical model which are obtained in Eqs. (37) and (42) will be examined. Before the analysis of side load spring models, analysis results of conventional coil springs will be given firstly.

$$Spring\ index: \ C = \frac{D}{d} = \frac{125}{12} = 10.4$$

$$Pitch:\ \ p = \frac{L_F - L_S}{n'} + d = \frac{(354 - 22.4)}{6.5} + 12 = 63\ mm$$

$$Wahl's\ stress\ factor:\ \ K = \frac{4C - 1}{4C - 4} + \frac{0.615}{C} = \frac{(4 * 10.4 - 1)}{(4 * 10.4 - 4)} + \frac{0.615}{10.4} = 1.14$$

$$Maximum\ Shear\ Stress:\ \ \tau = K \cdot \frac{8W.C}{\pi.d^2} = (1.14) * \frac{(8 * 2000 * 10.4)}{(3.14 * (12 * 10^{-3})^2)} * 10^{-6}$$

$$= \mathbf{420\ MPa}$$

$$Deflection:\ \ \delta = \frac{8W.C^3.n}{G.d} = \frac{(8 * 1640 * 5.75^3 * 10)}{(80 * 10^9 * 8 * 10^{-3})} * 10^3 = \mathbf{96\ mm}$$

According to the theoretical results, the maximum shear stress is about 420 MPa while the deflection is 96 mm for the applied load of 2000 N. If the applied load is increased to 5000 N, the maximum shear stress will be 1050 MPa, the deflection of the coil spring will be 240 mm and the generated side forces are very low for both cases. The results can be seen from Figure 4-18 to Figure 4-23.

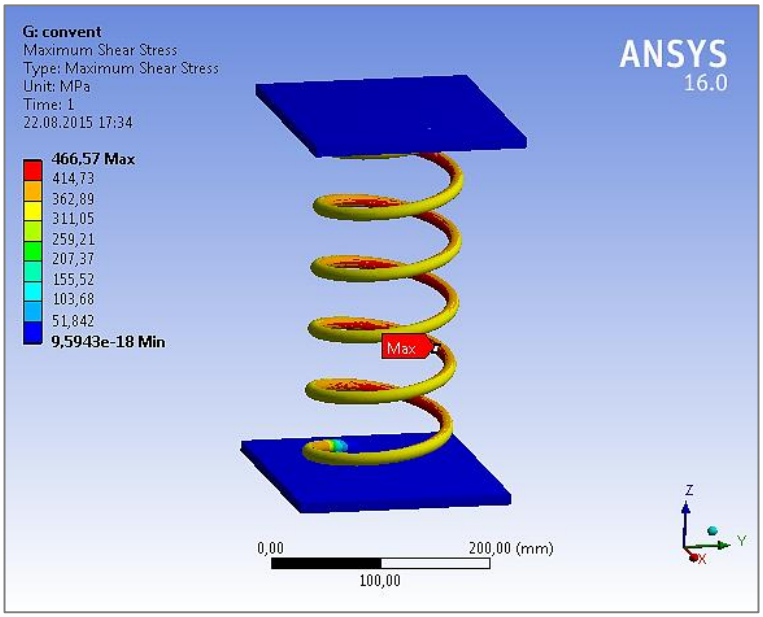

Figure 4-18: Result of Max. Shear Stress Analysis for the Applied Force of 2000 N, Spring Model-B (conventional)

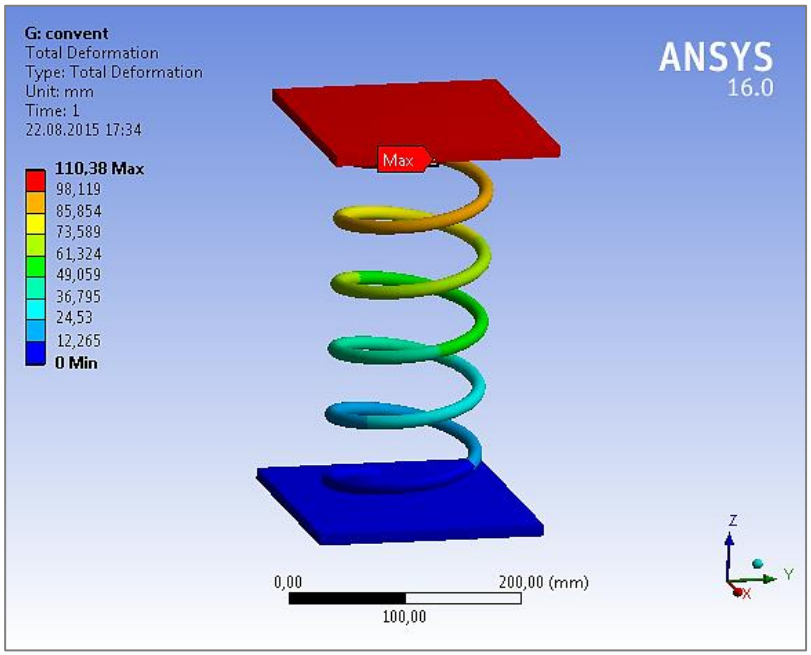

Figure 4-19: Result of Deflection Analysis for the Applied Force of 2000 N, Spring Model-B (conventional)

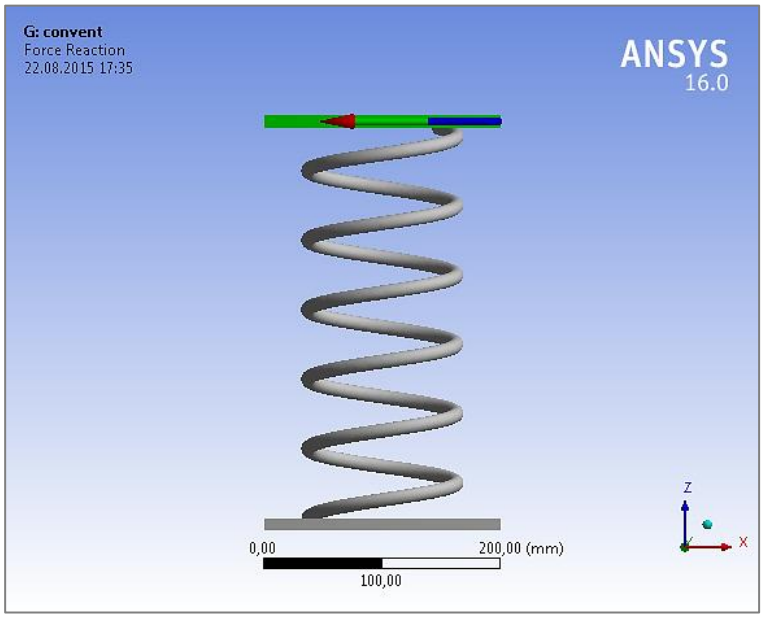

Figure 4-20: Side Force Analysis for the Applied Force of 2000 N, Spring Model-B (conventional)

➔ F_x= -1.2485 N, F_y= -0.2888 N, F_z= 0 N

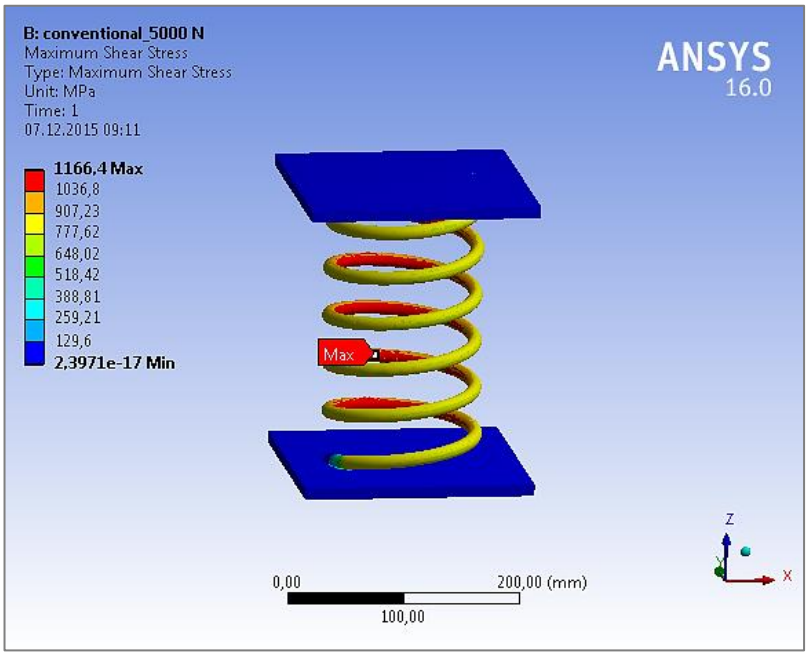

Figure 4-21: Result of Max. Shear Stress Analysis for the Applied Force of 5000 N, Spring Model-B (conventional)

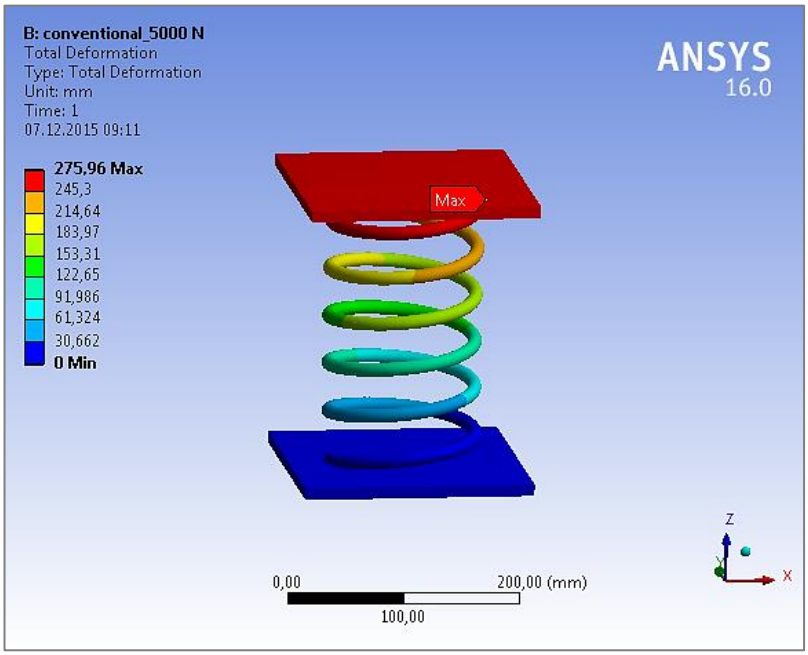

Figure 4-22: Result of Deflection Analysis for the Applied Force of 5000 N, Spring Model-B (conventional)

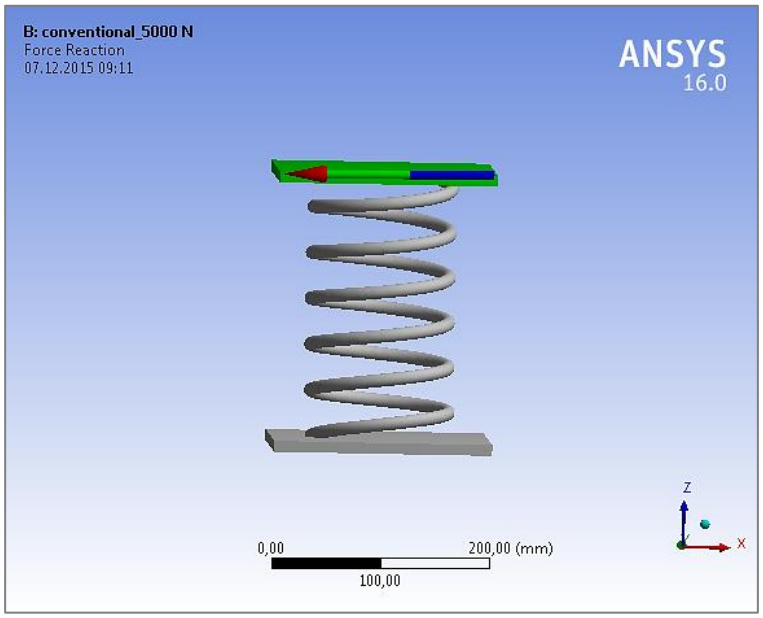

Figure 4-23: Side Force Analysis for the Applied Force of 5000 N, Spring Model-B (conventional)

➔ F_x= -3.1211 N, F_y= -0.7222 N, F_z= 0 N

According to the analyses results, conventional springs generate negligible side forces. Therefore, side load springs are modeled and analyses for different models of side load springs are performed. Maximum shear stress and the deflection values are nearly the same as those of the conventional design, however lateral forces change significantly.

In this section of the study, the curvature of the coil spring is given in xz plane and it is expected to obtain side force in x direction when an axial load is applied in z direction. Therefore, side force generation investigation will be done only in x direction.

For the model of side load springs with c_u=2 mm, α=6° and c_u=10 mm, α=10° generated side forces according to axial force of 2000 N can be seen Figure 4-24 and Figure 4-25.

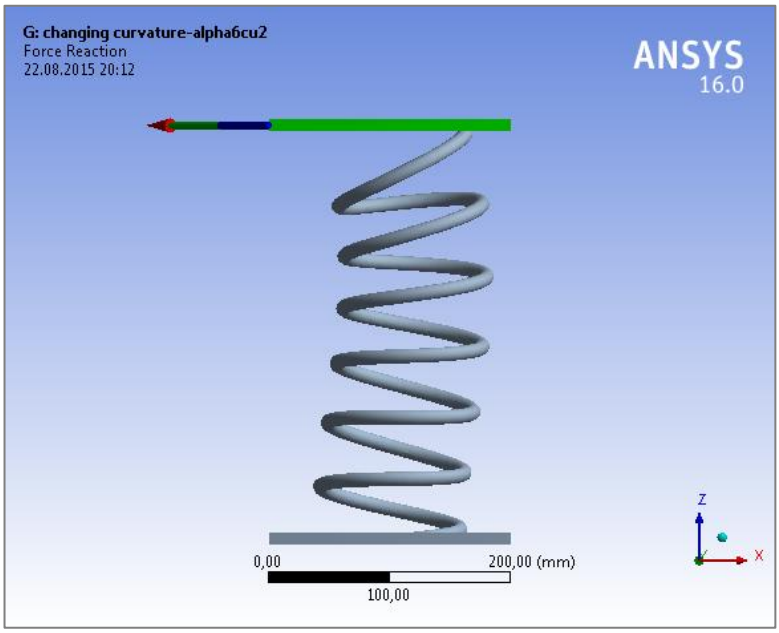

Figure 4-24: Side Force Analysis for Spring Model-B, c_u=2 mm and α=6°

➔ F_x= -98.539 N (For the applied force of 2000 N)

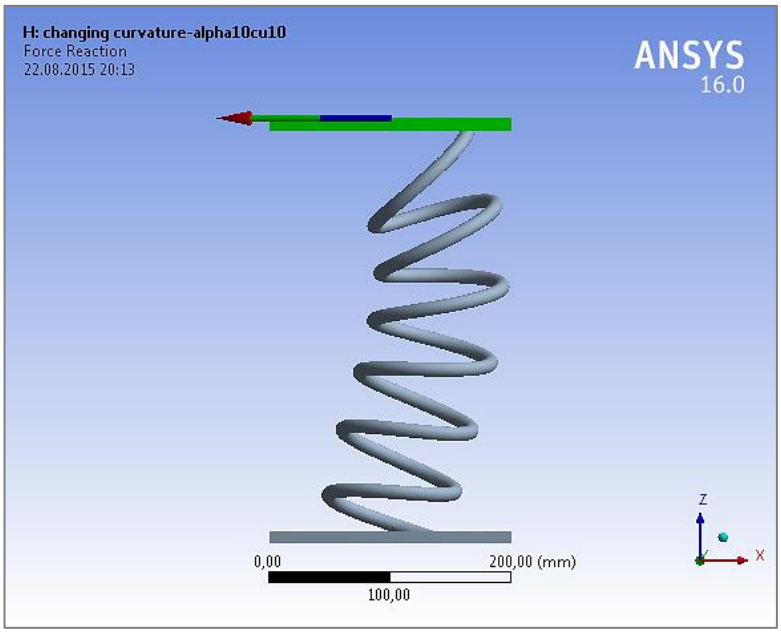

Figure 4-25: Side Force Analysis for Spring Model-B, c_u=10 mm and α=10°

➔ F_x= -271.14 N (For the applied force of 2000 N)

For the model of side load spring with c_u=2 mm, α=6° side force generation change according to applied force and the deformation is given in Figure 4-26 and Figure 4-27, respectively.

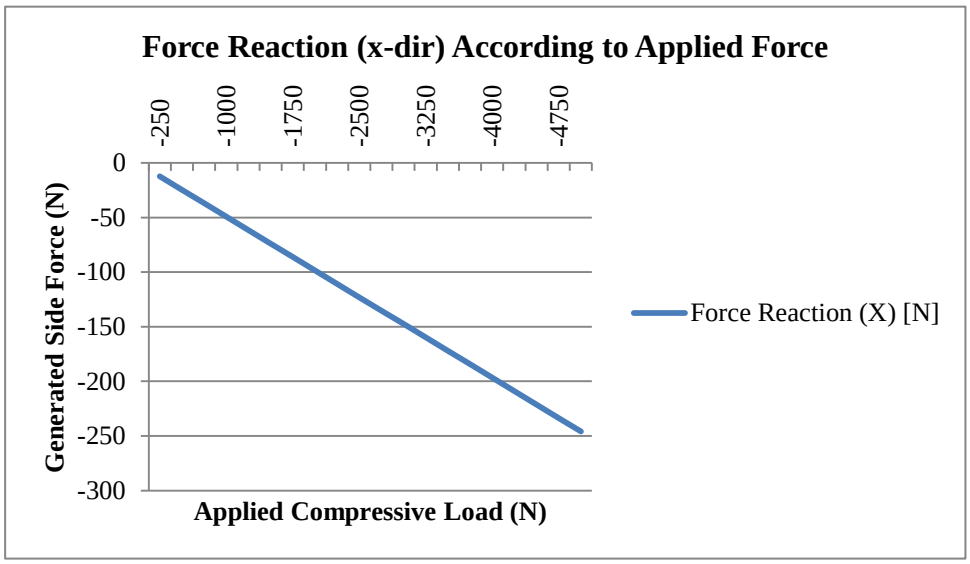

Figure 4-26: Generated Side Force According to Applied Load (c_u=2 mm and α=6°)

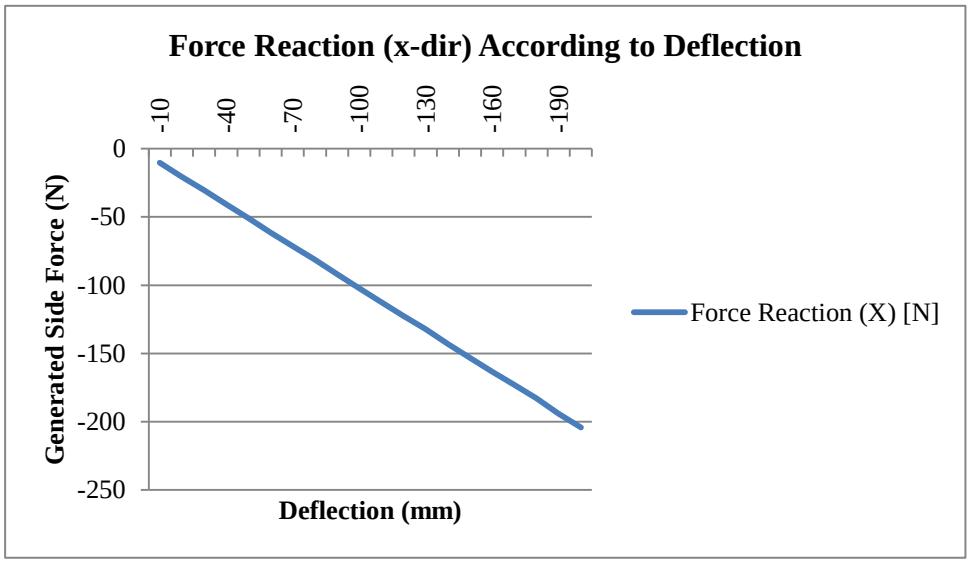

Figure 4-27: Generated Side Force According to Given Deflection (c_u=2 mm and α=6°)

As shown in Figure 4-26 and Figure 4-27, generated side force according to deflection or force shows a linear characteristic which seems unrealistic. It is thought that this is caused by analysis model and these results are investigated furthermore. These studies will be explained in the next section.

4.3.1. NONLINEARITY INVESTIGATION OF ANALYSES

During analyses of the side load spring, it is seen that side load spring still has a linear characteristic when a force or a displacement is applied, despite is the expectation of a nonlinear behavior. Thus, an examination for nonlinearity is needed and studies with the analysis model are performed. In this section, side load spring model with $\alpha=6°$, $c_u=2$ mm is used for all analyses.

As the first step, the number of increments of applied force is examined and it is seen that changing number of steps of applied force has minor effect to the results. In Figure 4-28 and Figure 4-29 , it can be seen that the results are still linear.

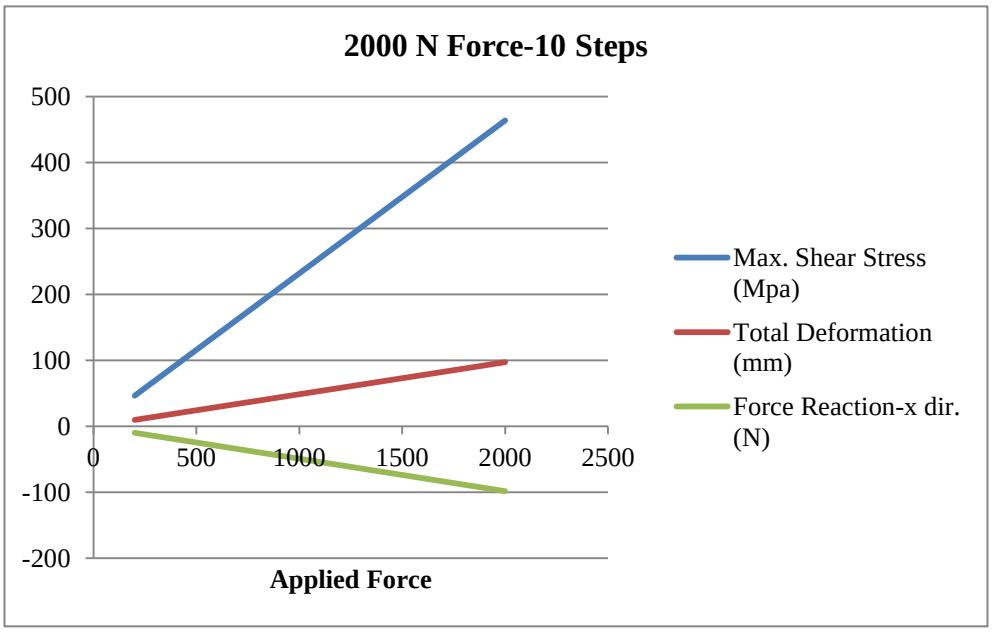

Figure 4-28: Analysis Results for Applied Force of 2000 N-10 Steps

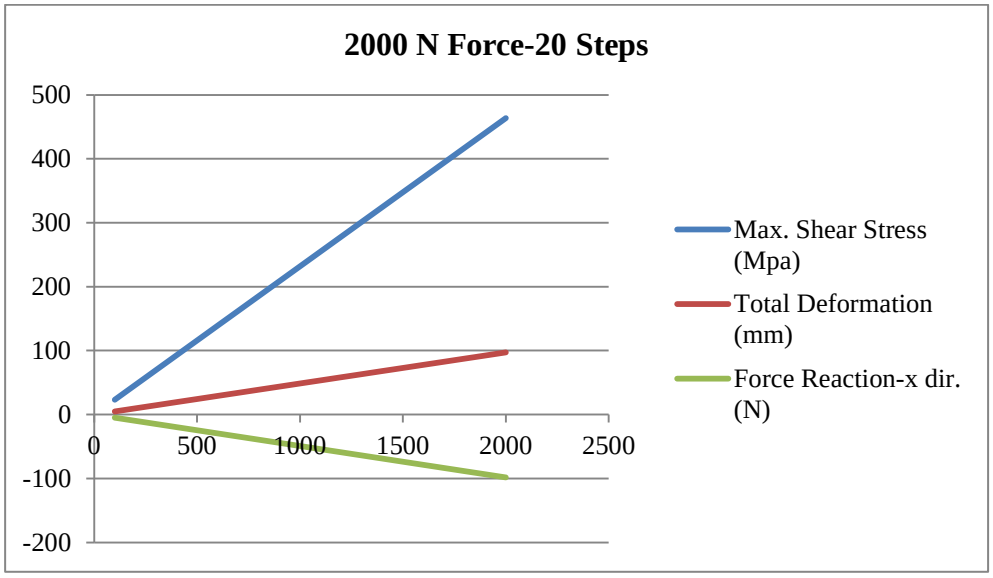

Figure 4-29: Analysis Results for Applied Force of 2000 N-20 Steps

Then, number of substeps is changed and it is seen that this helps to obtain the more realistic results. Results of analysis with all substeps can be seen from Figure 4-30 to Figure 4-37.

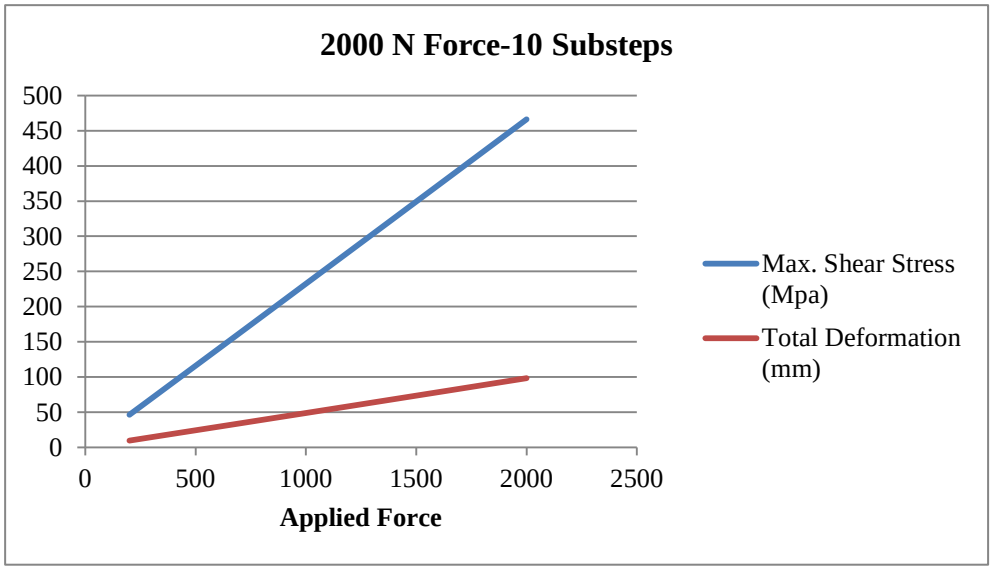

Figure 4-30: Analysis Results for Applied Force of 2000 N-10 Substeps

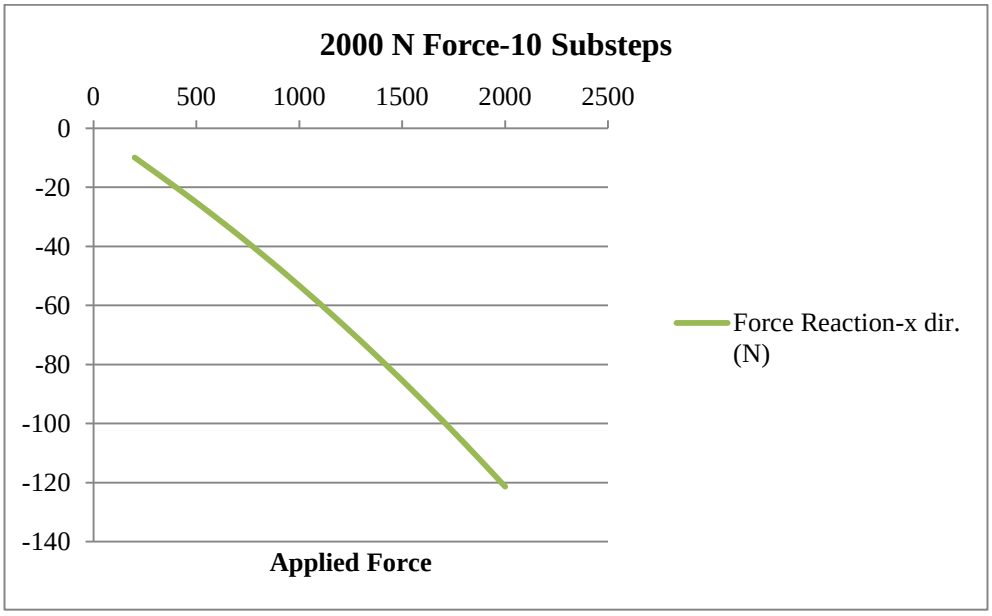

Figure 4-31: Force Reaction Result for Applied Force of 2000 N-10 Substeps

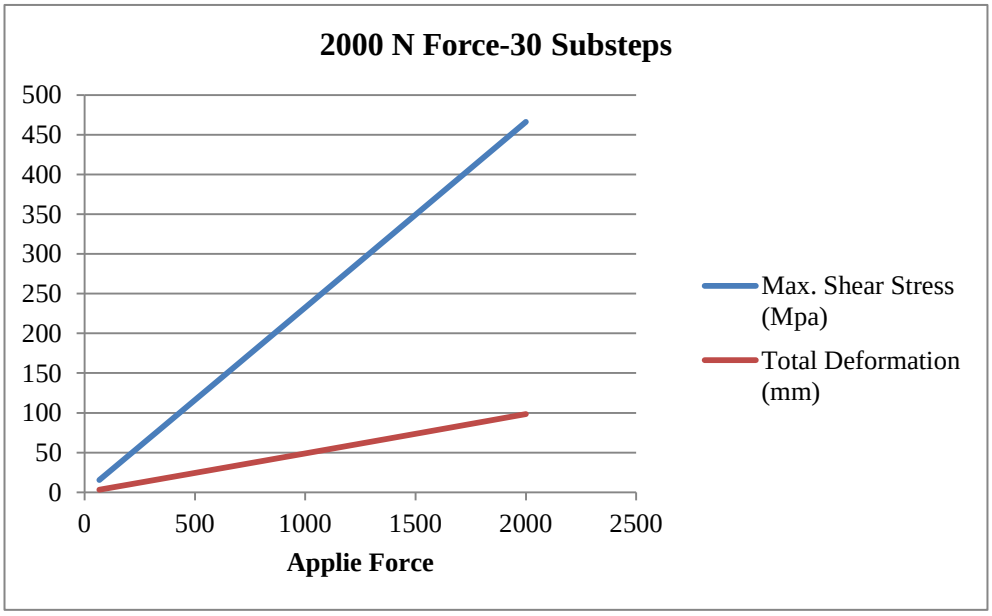

Figure 4-32: Analysis Results for Applied Force of 2000 N-30 Substeps

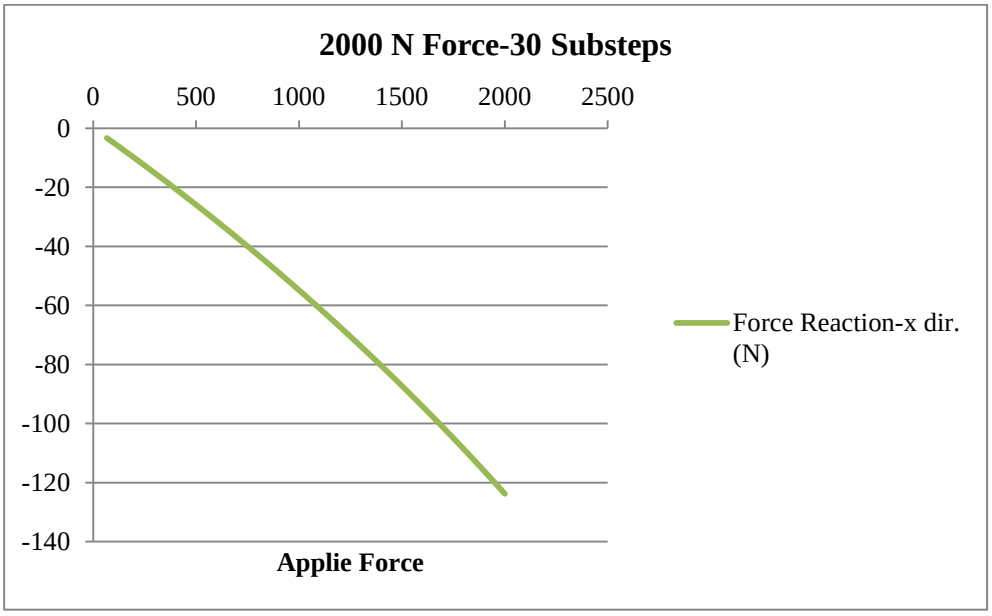

Figure 4-33: Force Reaction Result for Applied Force of 2000 N-30 Substeps

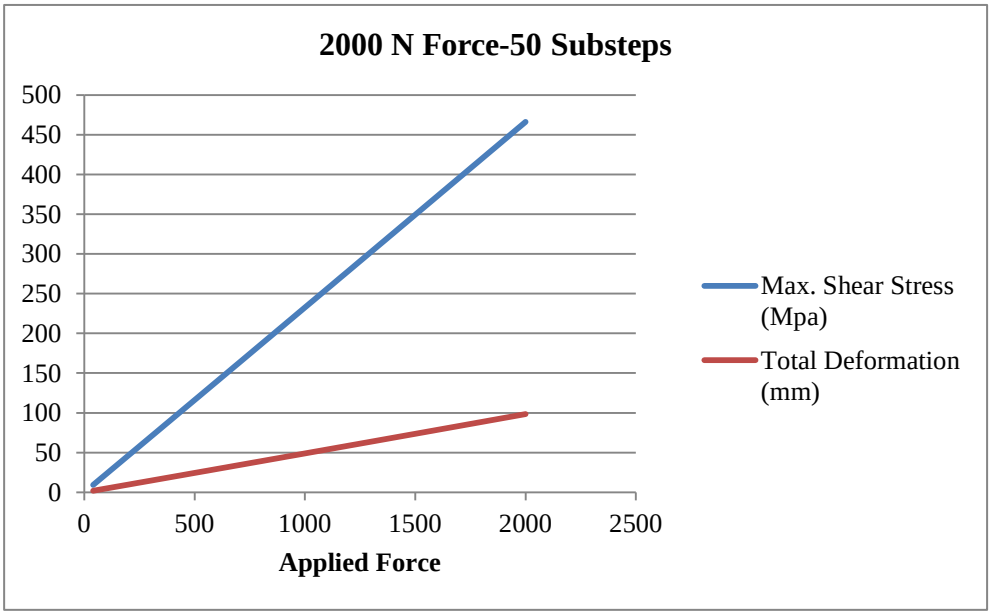

Figure 4-34: Analysis Results for Applied Force of 2000 N-50 Substeps

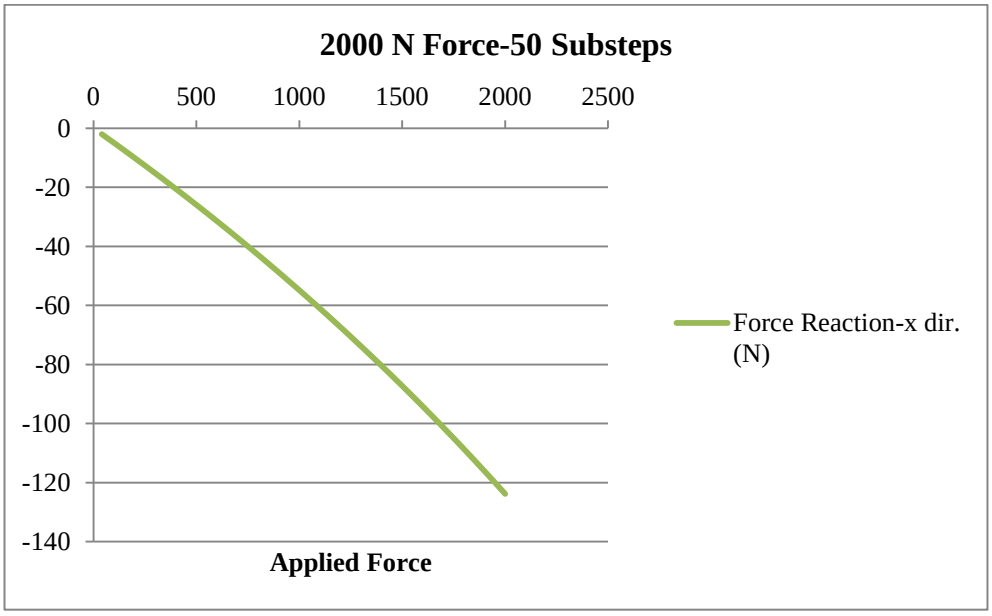

Figure 4-35: Force Reaction Result for Applied Force of 2000 N-50 Substeps

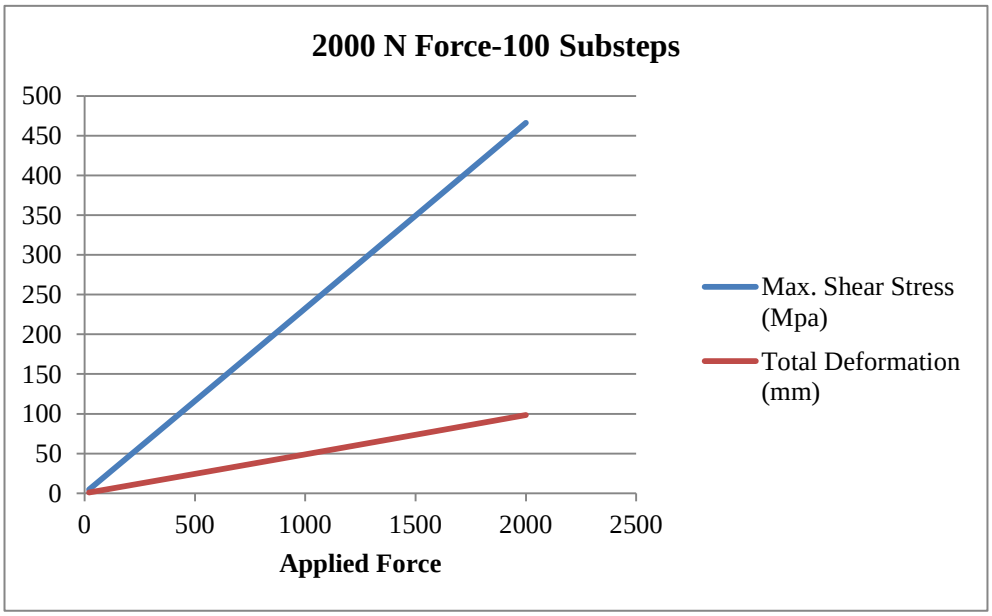

Figure 4-36: Analysis Results for Applied Force of 2000 N-100 Substeps

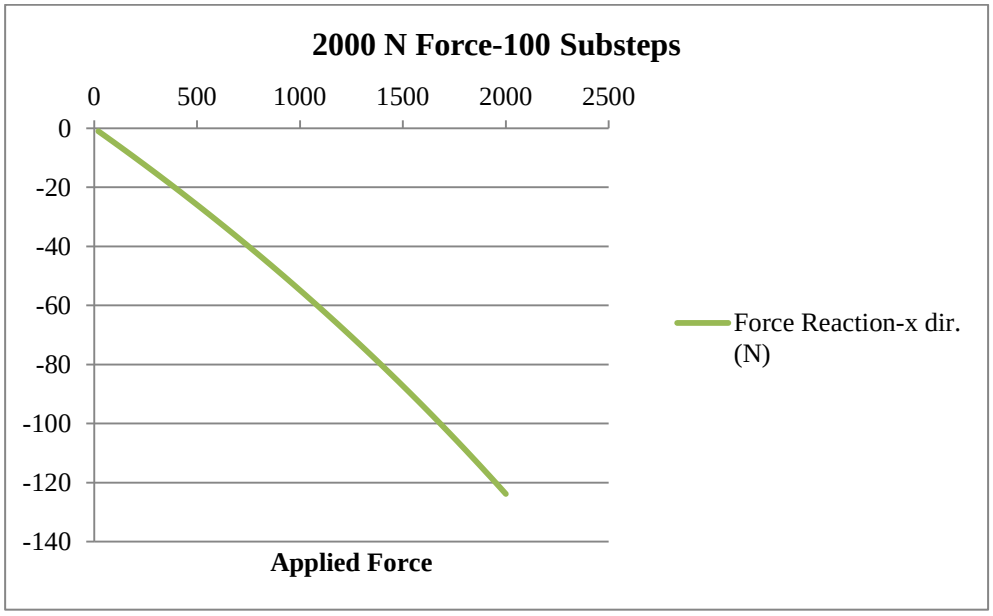

Figure 4-37: Force Reaction Result for Applied Force of 2000 N-100 Substeps

For the applied force of 2000 N coil spring maintains linear behavior and analysis results are also nearly linear. When the applied force is increased to 5000 N, the results of the force reaction become nonlinear which is more realistic and expected. The maximum shear stress and the total deformation results are almost linear for all analyses and do not change according to analysis settings and the applied force. Analysis results for different number of substeps according to the applied force of 5000 N can be seen from Figure 4-38 to Figure 4-43. Increasing the number of substeps helps to obtain more realistic results, but also increases the analysis time and effort. Therefore, it is decided to use 30 substeps in analyses.

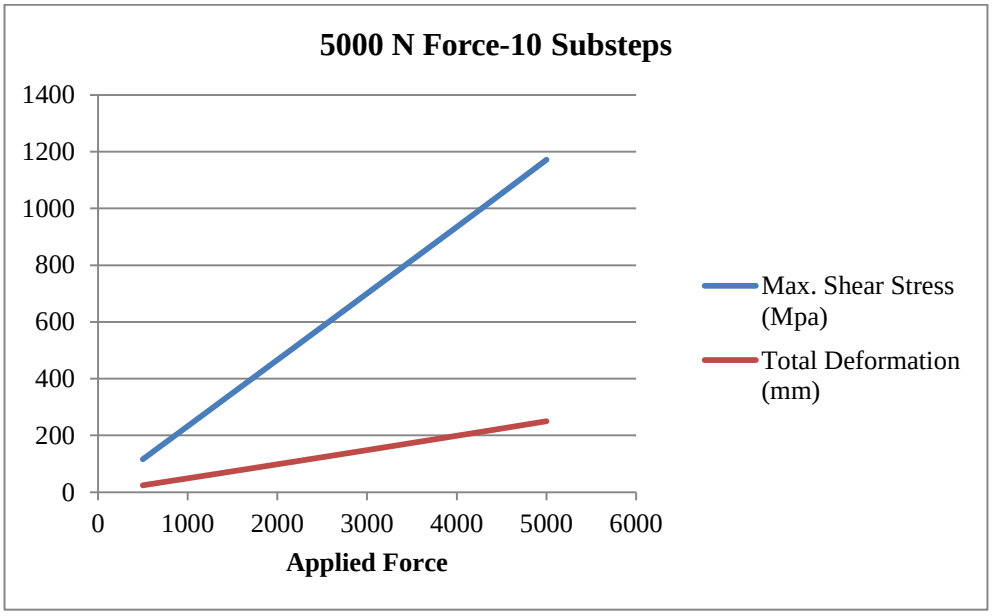

Figure 4-38: Analysis Results for Applied Force of 5000 N-10 Substeps

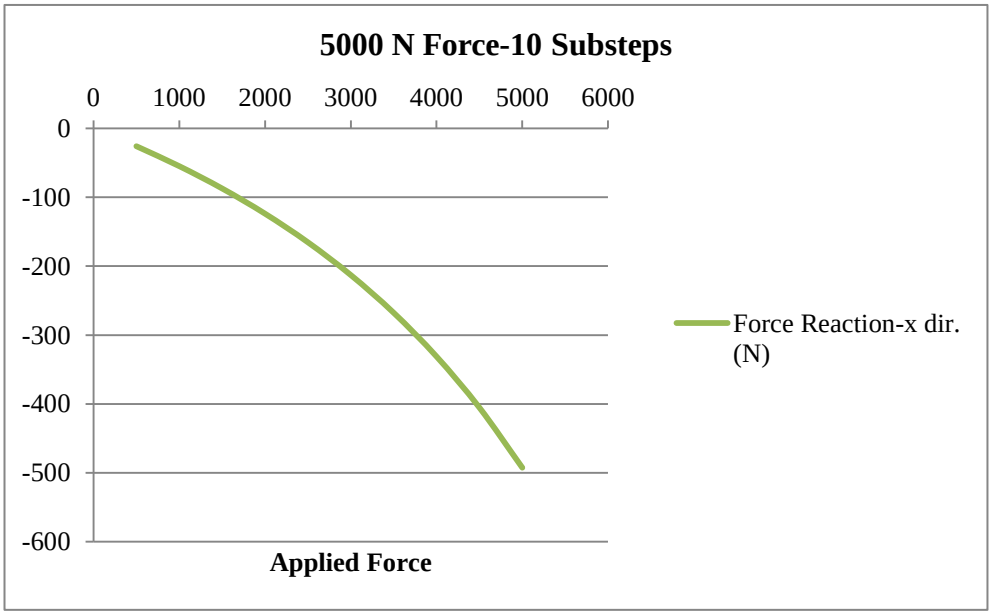

Figure 4-39: Force Reaction Result for Applied Force of 5000 N-10 Substeps

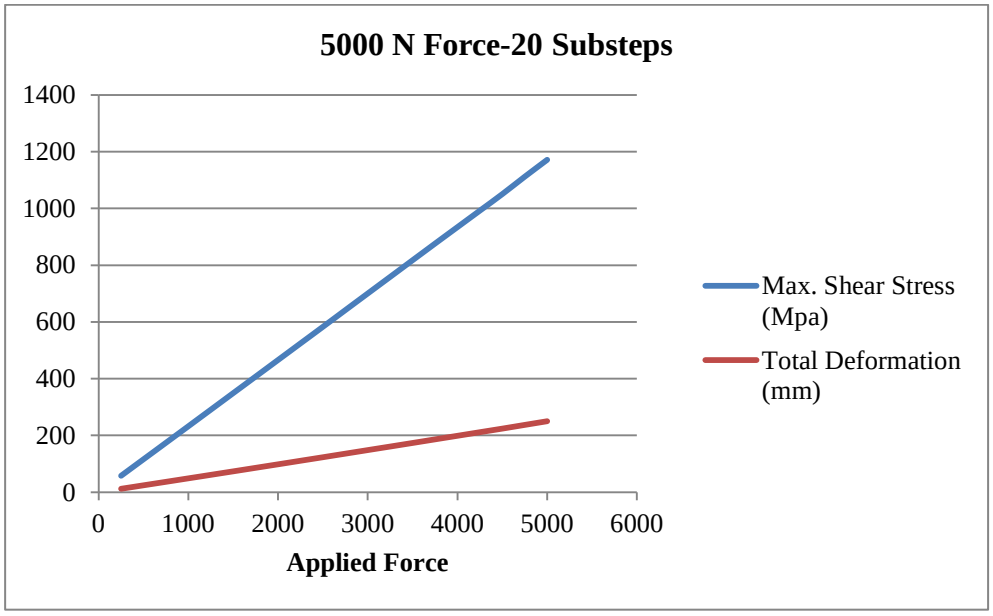

Figure 4-40: Analysis Results for Applied Force of 5000 N-20 Substeps

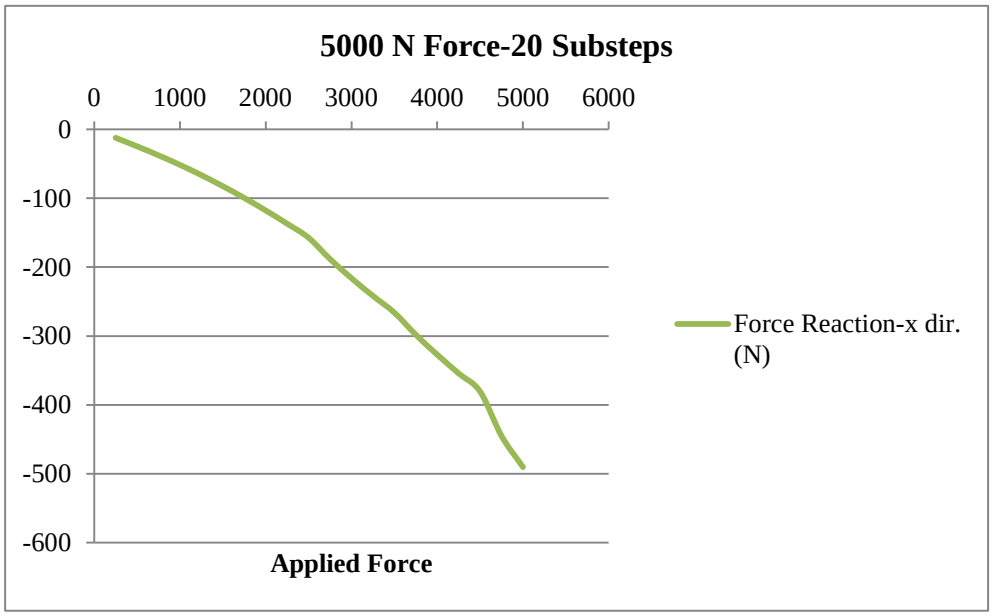

Figure 4-41: Force Reaction Result for Applied Force of 5000 N-20 Substeps

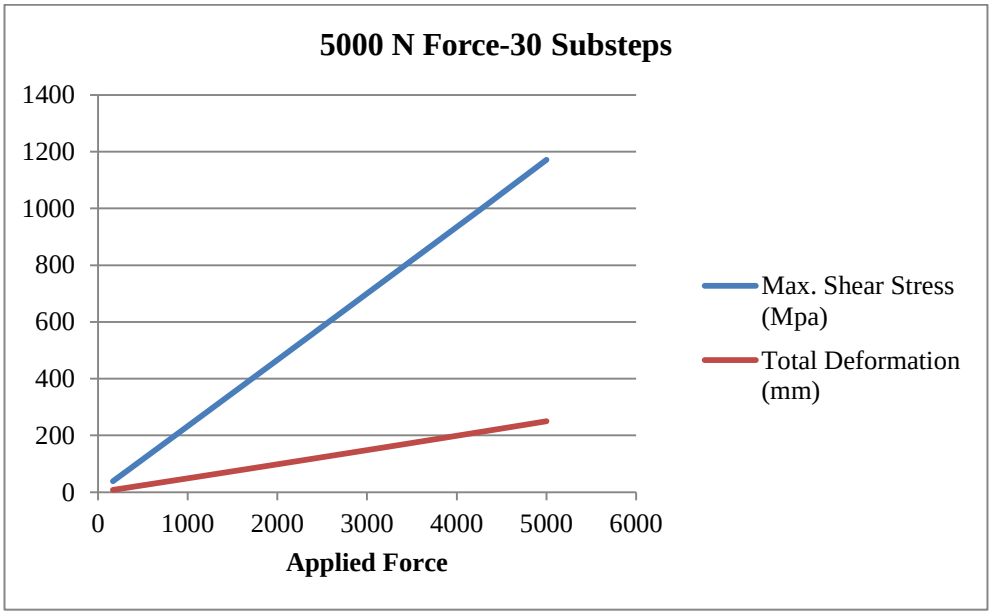

Figure 4-42: Analysis Results for Applied Force of 5000 N-30 Substeps

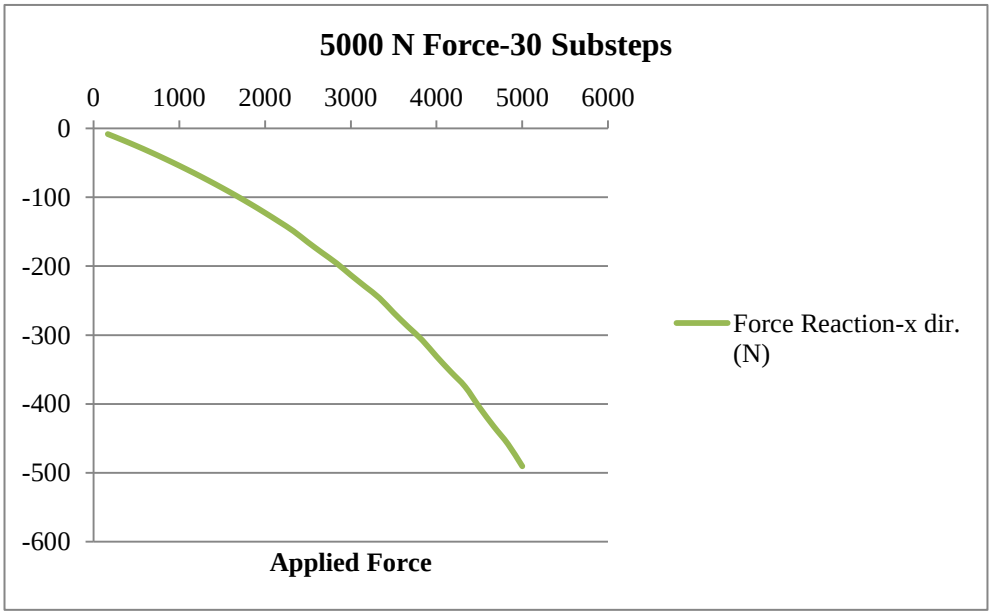

Figure 4-43: Force Reaction Result for Applied Force of 5000 N-30 Substeps

4.3.2. SIDE FORCE REDUCTION ANALYSIS

After nonlinearity investigation of analyses is completed, side force reduction of different side load spring models are examined. Results show that, side load springs modeled with offered mathematical model in section 4.2, reduce lateral force significantly by generating anti side forces. These results can be seen from Figure 4-44 to Figure 4-48.

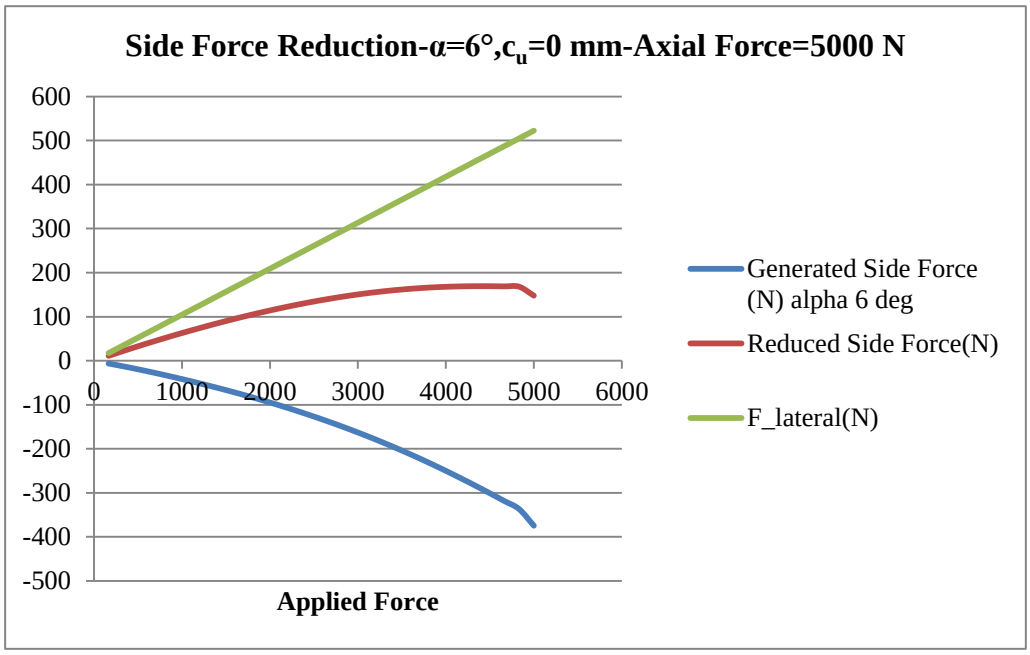

Figure 4-44: Side Force Reduction for Side Load Spring with α=6°, c_u=0 mm

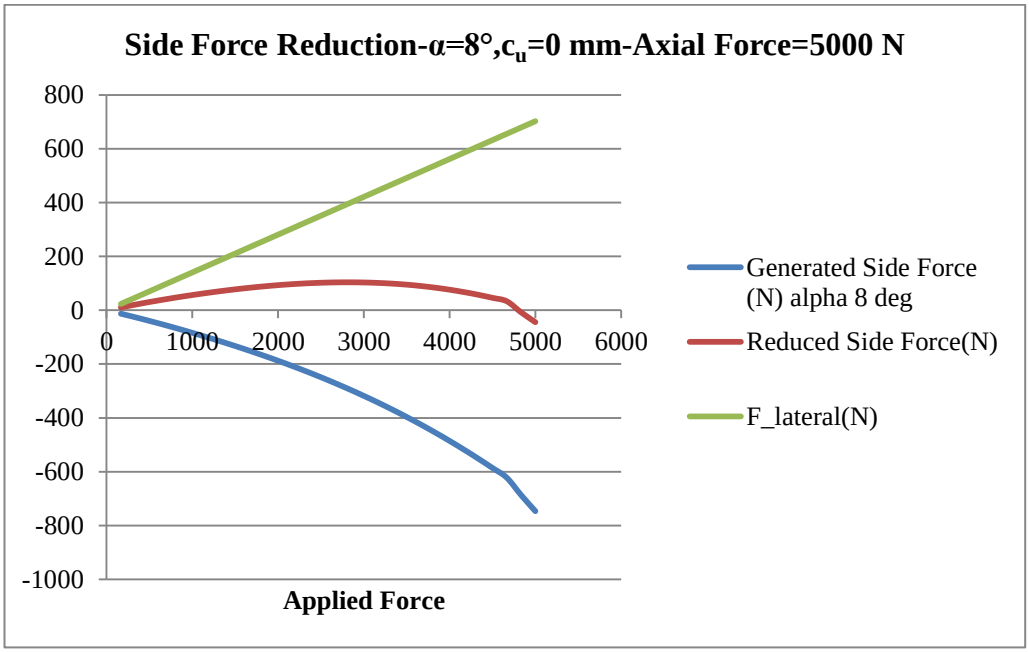

Figure 4-45: Side Force Reduction for Side Load Spring with α=8°, c_u=0 mm

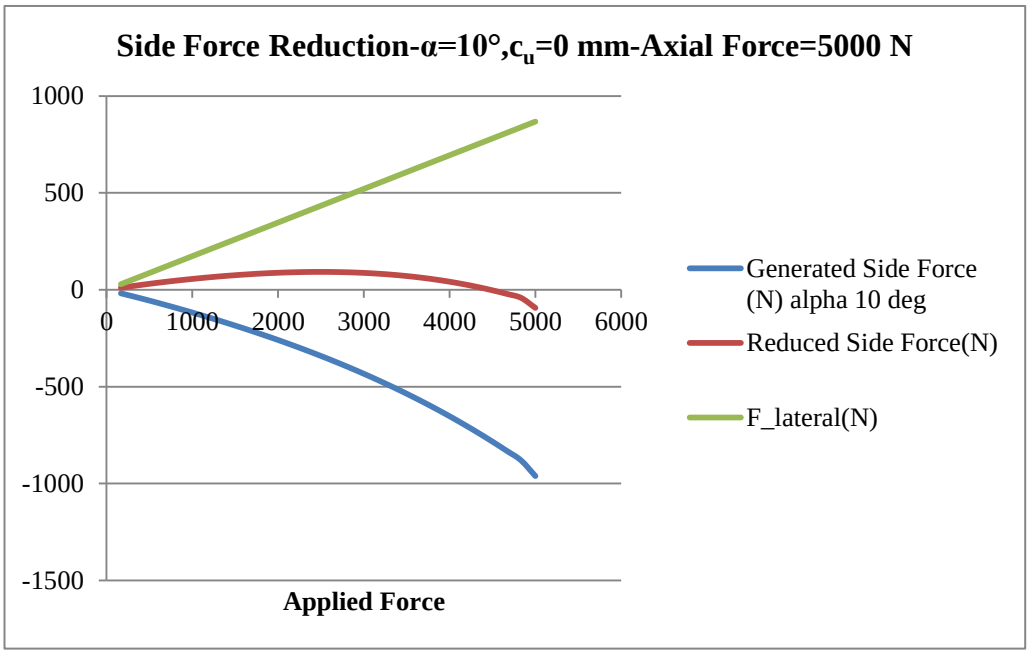

Figure 4-46: Side Force Reduction for Side Load Spring with α=10°, c_u=0 mm

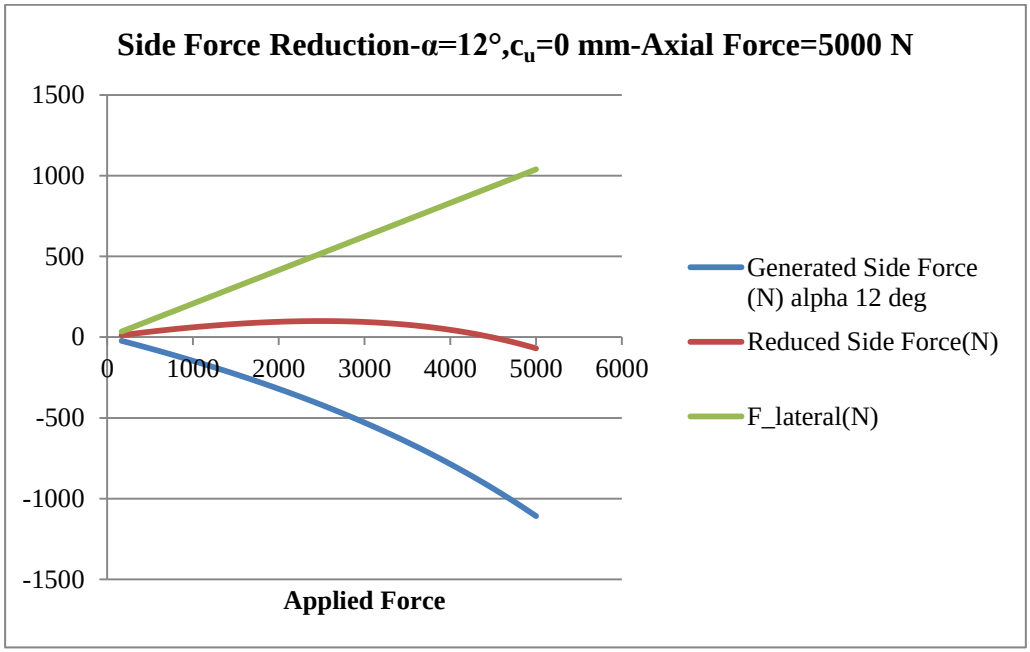

Figure 4-47: Side Force Reduction for Side Load Spring with α=12°, c_u=0 mm

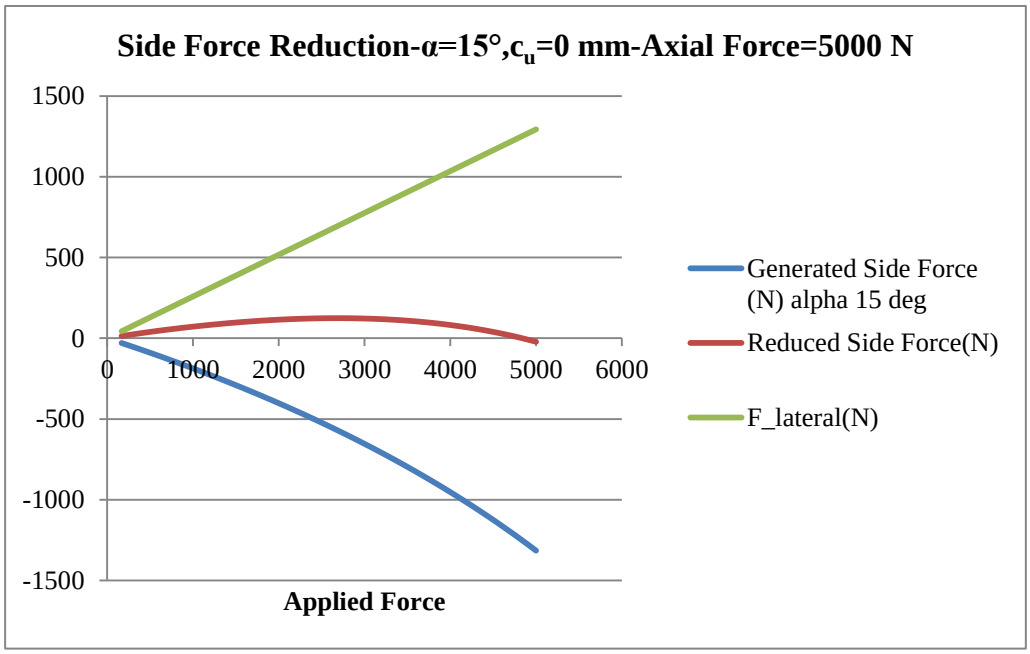

Figure 4-48: Side Force Reduction for Side Load Spring with α=15°, c_u=0 mm

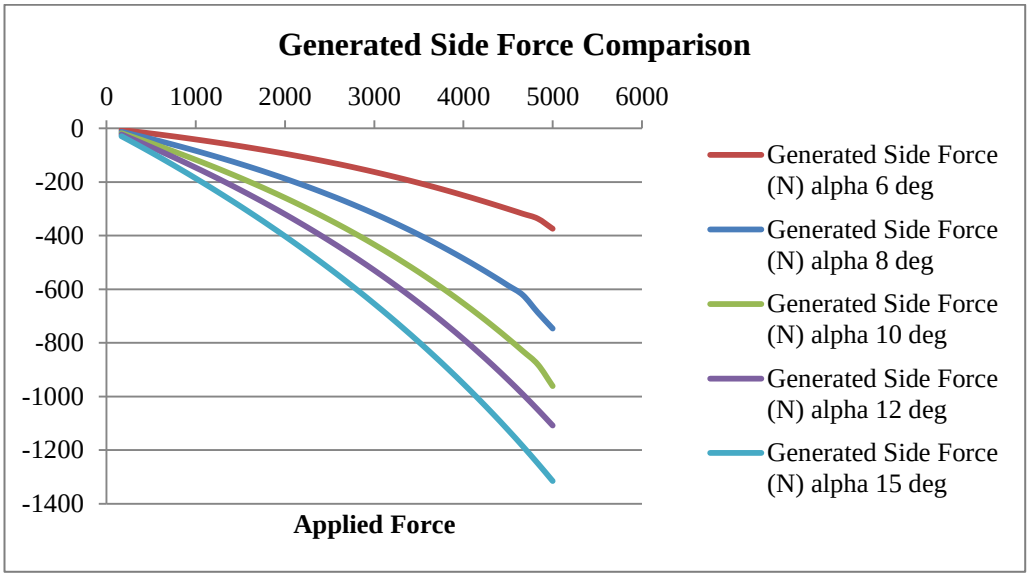

Figure 4-49: Generated Side Force Comparison of Designed Side Load Springs

4.3.3. SENSITIVITY ANALYSIS

After design and analysis of the side load springs are completed, effect of the parameters on the side load spring design is investigated. To see the influence of the parameters, design parameters; free length of the spring, mean coil diameter and wire diameter are increased and decreased by 5 and 10 percent one by one while the other parameters are remained same. Then, results are compared and effects of the parameters on the results are evaluated.

- **Center Curve According to Parameter Change**

In case of setting the other parameters same; when the free length of the spring increases, amount of the spring curvature increases, too. If the mean diameter of the coil is increased, amount of the spring curvature decreases. These expressions can be seen in Figure 4-50 and Figure 4-51. When these two parameters are compared, it is difficult to say one parameter is more influential than the other one for center curve. Since the effect of the free length on the center curve characteristic is variable, a healthy comparison is difficult.

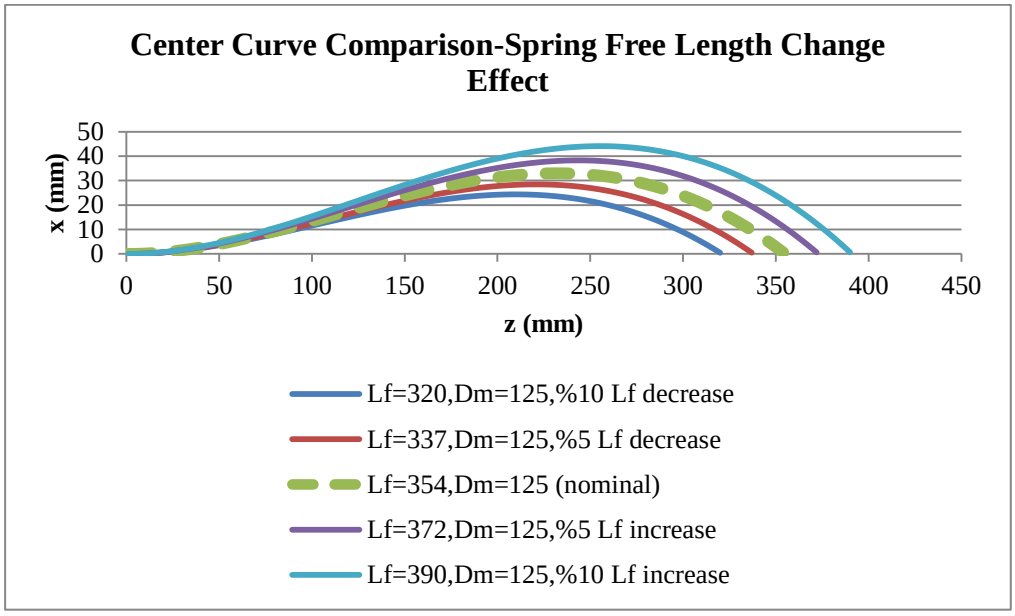

Figure 4-50: Center Curve Comparison-Effect of Spring Free Length Change

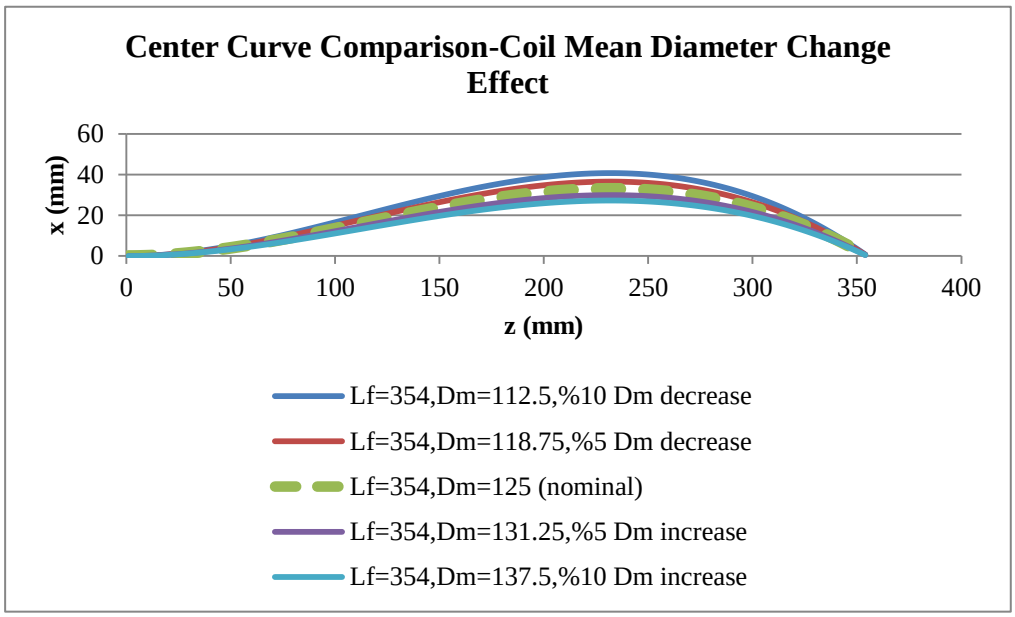

Figure 4-51: Center Curve Comparison-Effect of Coil Mean Diameter Change

According to Eq. (42), it is clear that wire diameter has no effect on the center curve.

- **Effect of the Spring Free Length Change**

Effect of the free length change of the spring on the generated and reduced side force can be seen in Figure 4-52 and Figure 4-53. Increased free length of the spring increases the generated side force and decreases the reduced side force inherently. However, it should be noted that since the free length change of the spring changes the stiffness of the spring, deformation of the spring according to applied force is also changed while maximum shear stress value does not change considerably, and related results can be seen in Figure 4-54.

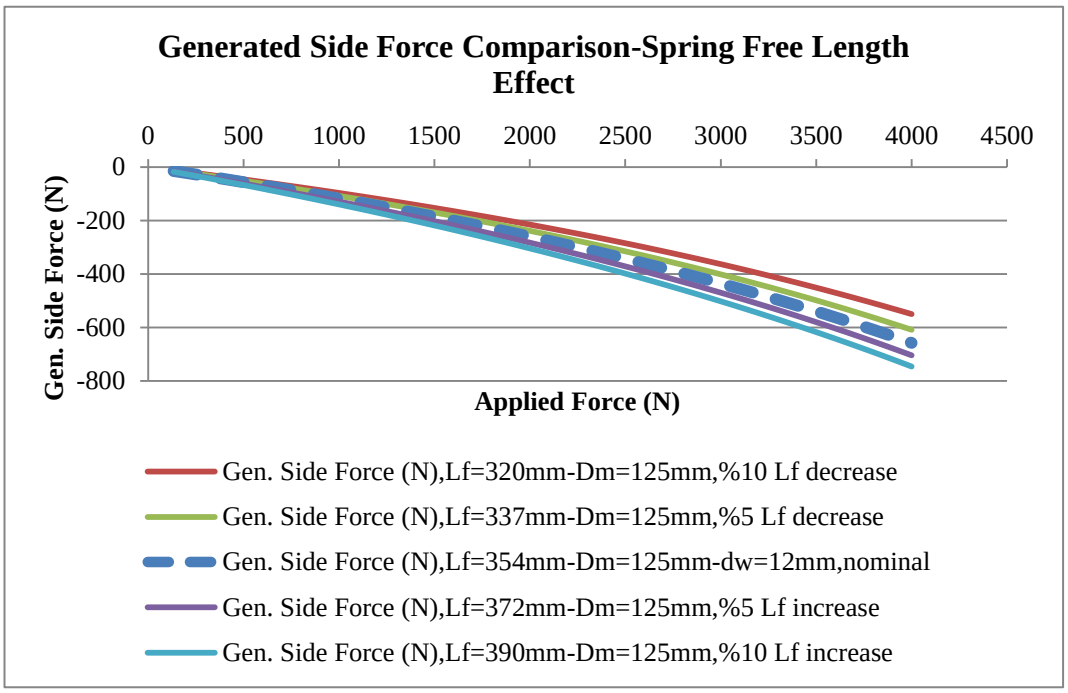

Figure 4-52: Generated Side Force Comparison-Effect of Spring Free Length Change

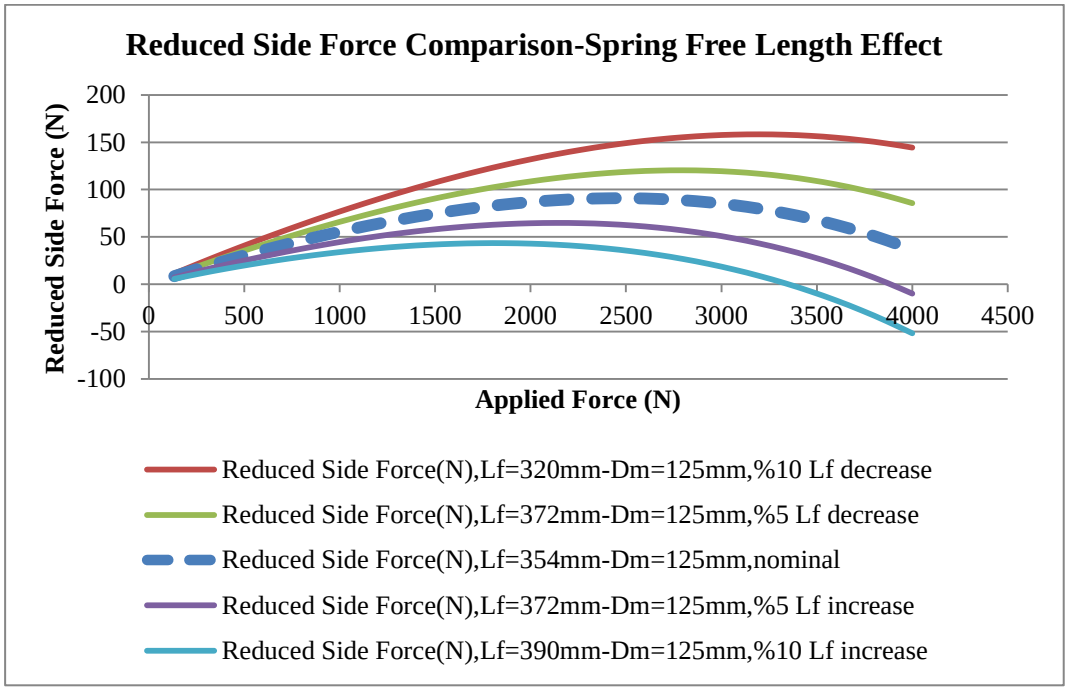

Figure 4-53: Reduced Side Force Comparison-Effect of Spring Free Length Change

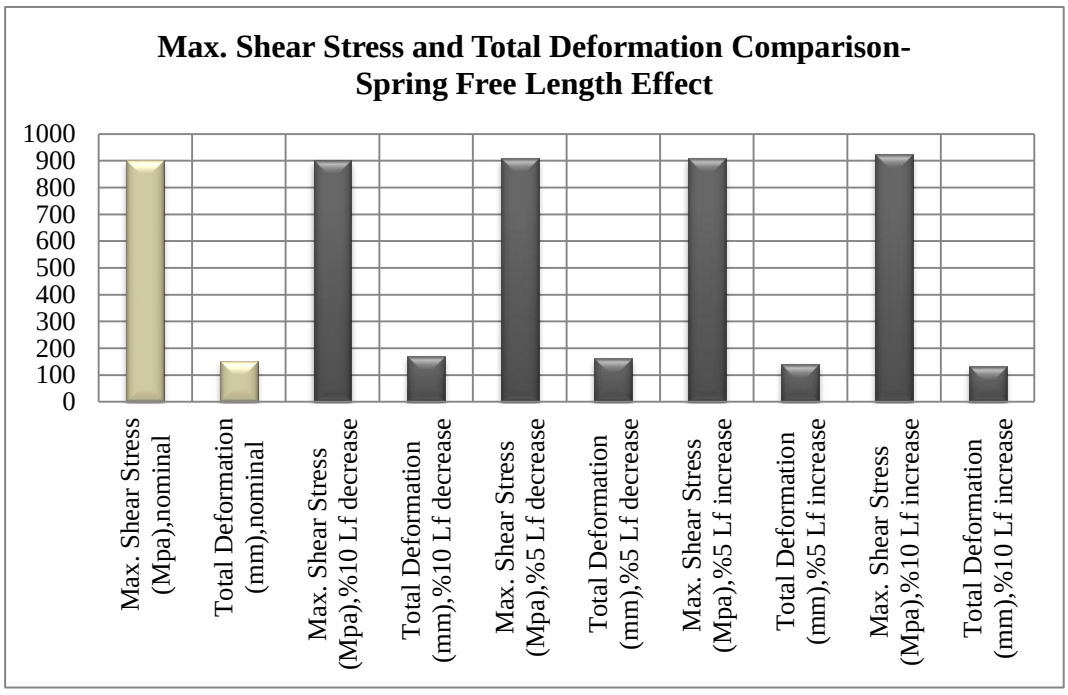

Figure 4-54: Max. Shear Stress and Deformation Comparison-Effect of Spring Free Length Change

- **Effect of the Coil Mean Diameter Change**

The effects of the mean diameter change of the coil on the generated and reduced side force is investigated and the results can be seen in Figure 4-55 and Figure 4-56. Increased mean diameter of the coil decreases the generated side force and increases the reduced side force accordingly. However, the mean diameter change of the coil changes the stiffness of the spring, deformation of the spring according to applied force is changed significantly while maximum shear stress value does not differ much, and related results can be seen in Figure 4-57.

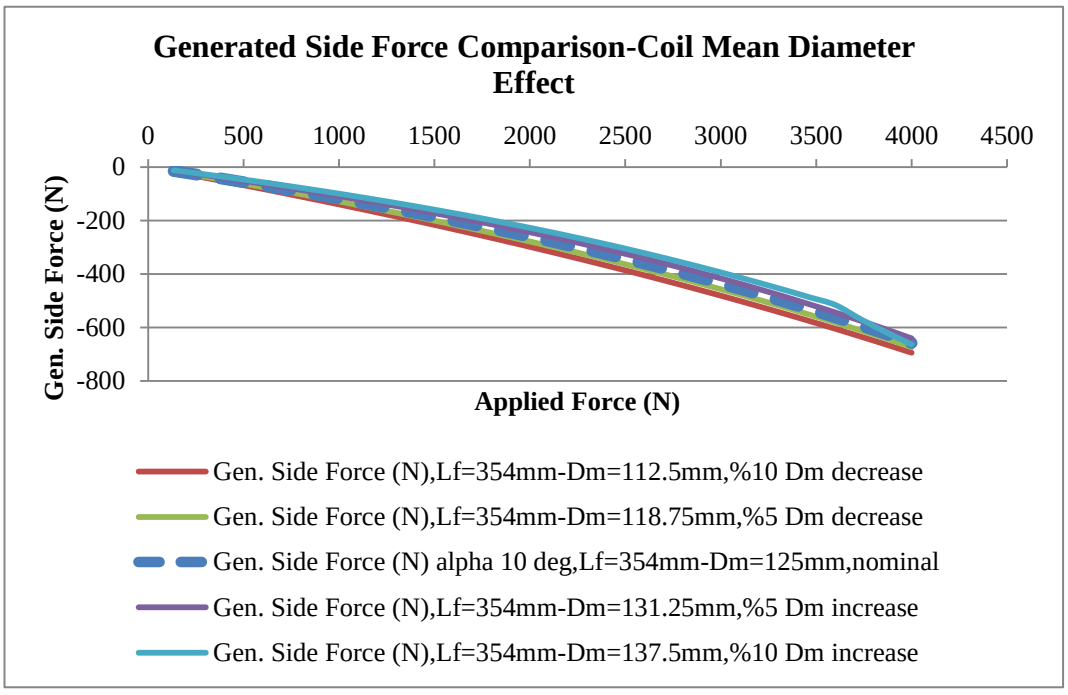

Figure 4-55: Generated Side Force Comparison-Effect of Coil Mean Diameter Change

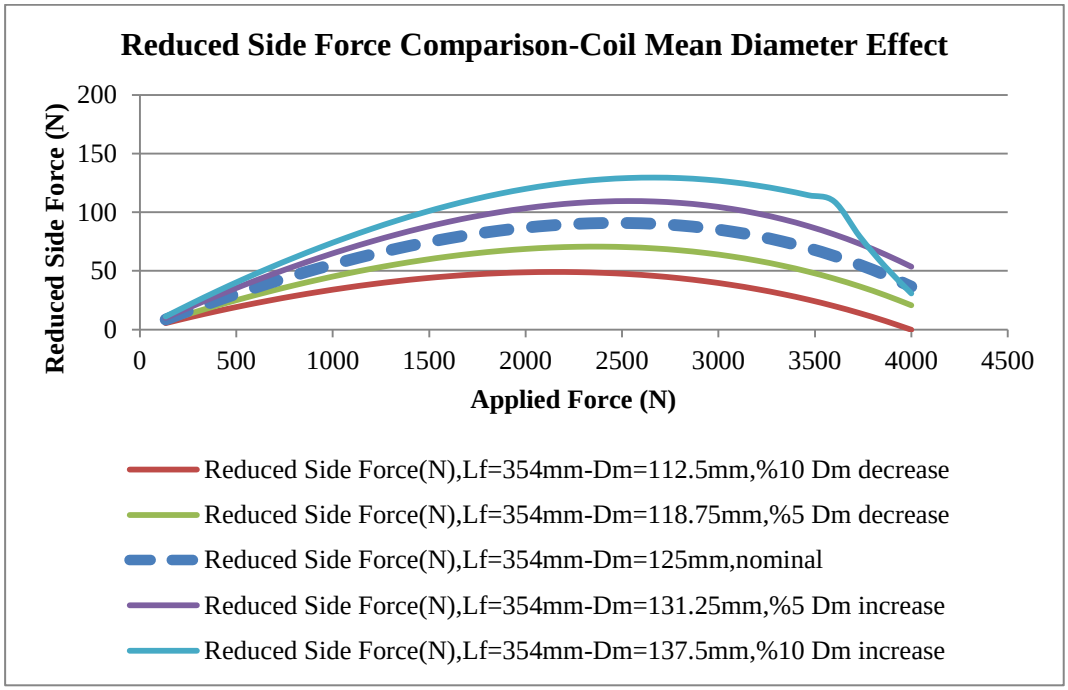

Figure 4-56: Reduced Side Force Comparison-Effect of Coil Mean Diameter Change

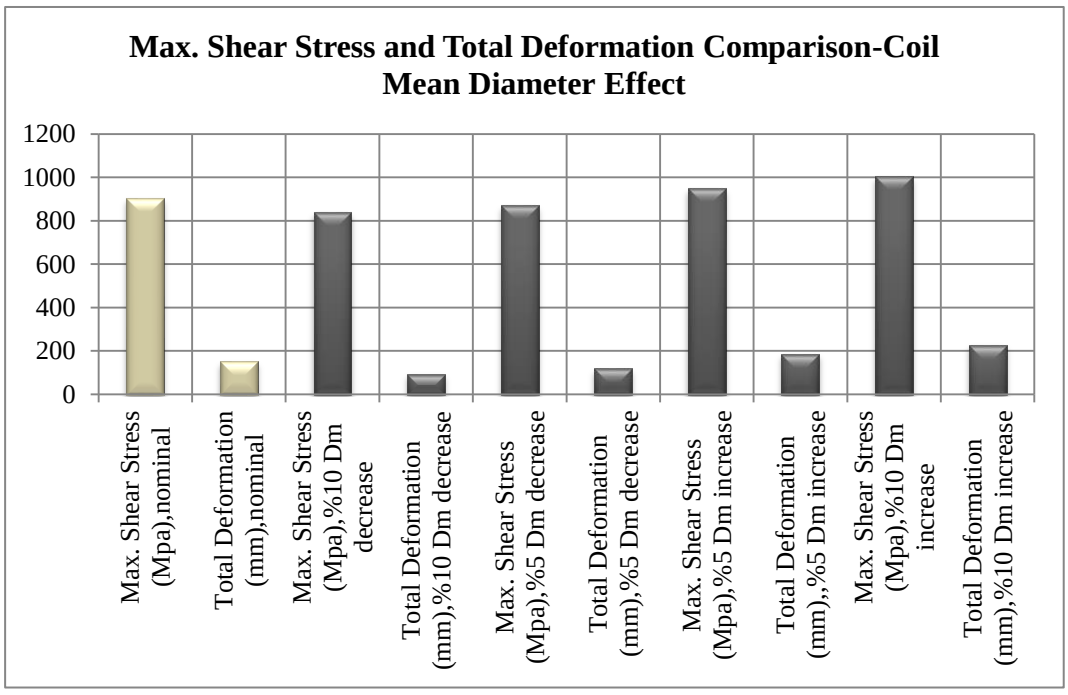

Figure 4-57: Max. Shear Stress and Deformation Comparison-Effect of Coil Mean Diameter Change

- **Effect of the Wire Diameter Change**

Lastly, effect of the wire diameter change on the generated and reduced side force is investigated and the results can be seen in Figure 4-58 and Figure 4-59. Reduced wire diameter increases the generated side force and decreases the reduced side force for specific region of the applied force. However, change of the wire diameter changes the stiffness of the spring, the maximum shear stress and the deformation of the spring according to applied force is changed significantly, and related results can be seen in Figure 4-60.

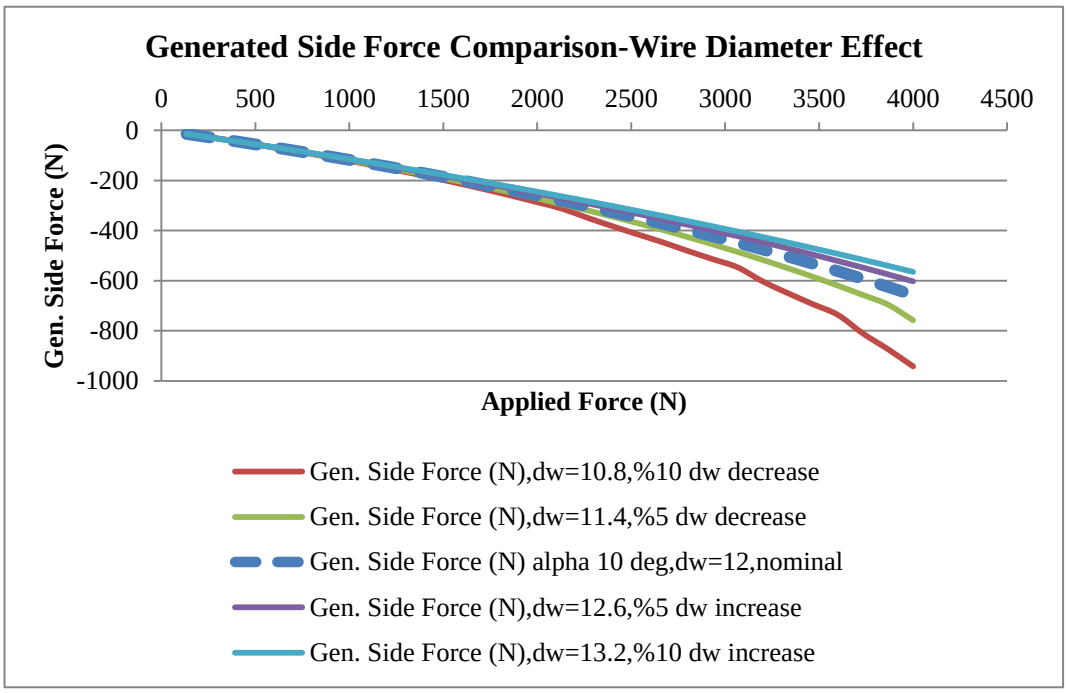

Figure 4-58: Generated Side Force Comparison-Effect of Wire Diameter Change

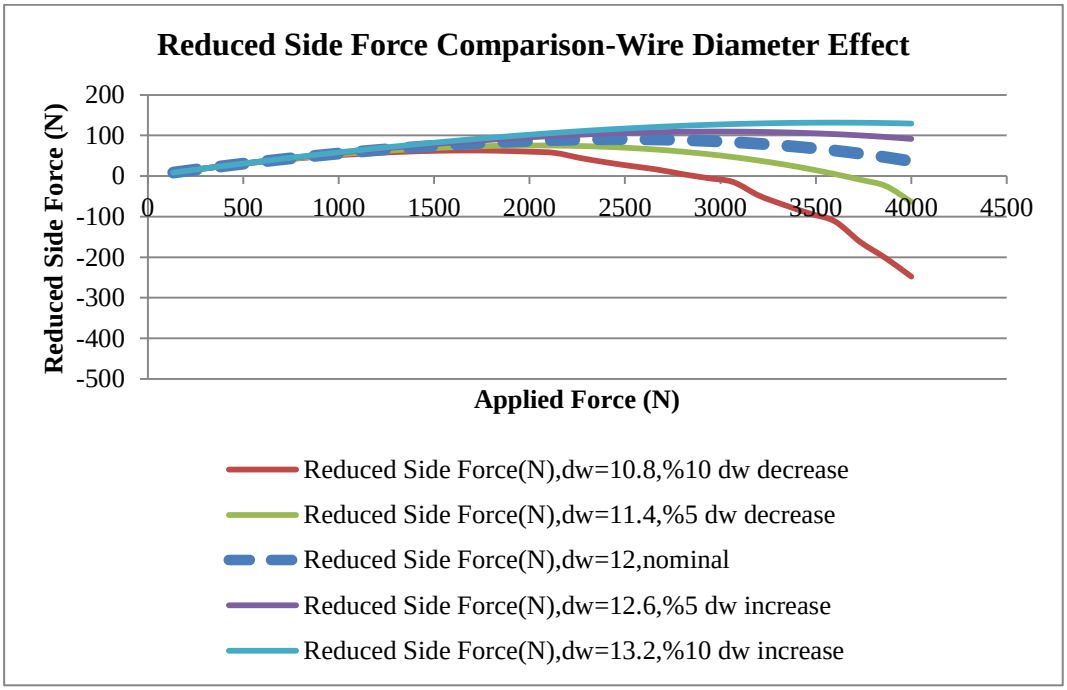

Figure 4-59: Reduced Side Force Comparison-Effect of Wire Diameter Change

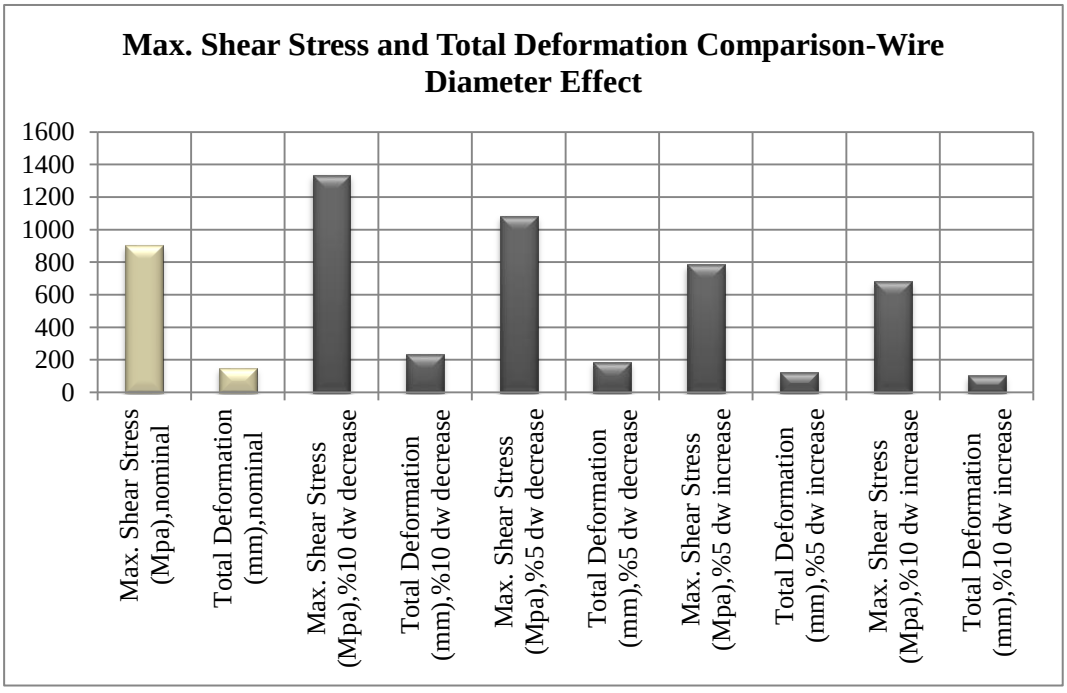

Figure 4-60: Max. Shear Stress and Deformation Comparison-Effect of Wire Diameter Change

- **Comparison of the Effect of the Parameters**

Finally, effect of the change of the all parameters is examined. Comparisons of the results can be seen from Figure 4-61 to Figure 4-64. As a result, order of importance of the effect of the parameters is; free length of the spring, mean diameter of the coil and wire diameter, respectively. However, it should be noted that this ranking is done according to the results of the generated side force. If the maximum shear stress and the deformation are examined, results will be different. Hence, this point should be taken into consideration while designing or changing the design of a side load spring. Nevertheless, this sensitivity analysis should be further developed and combined effect of the parameters should be examined.

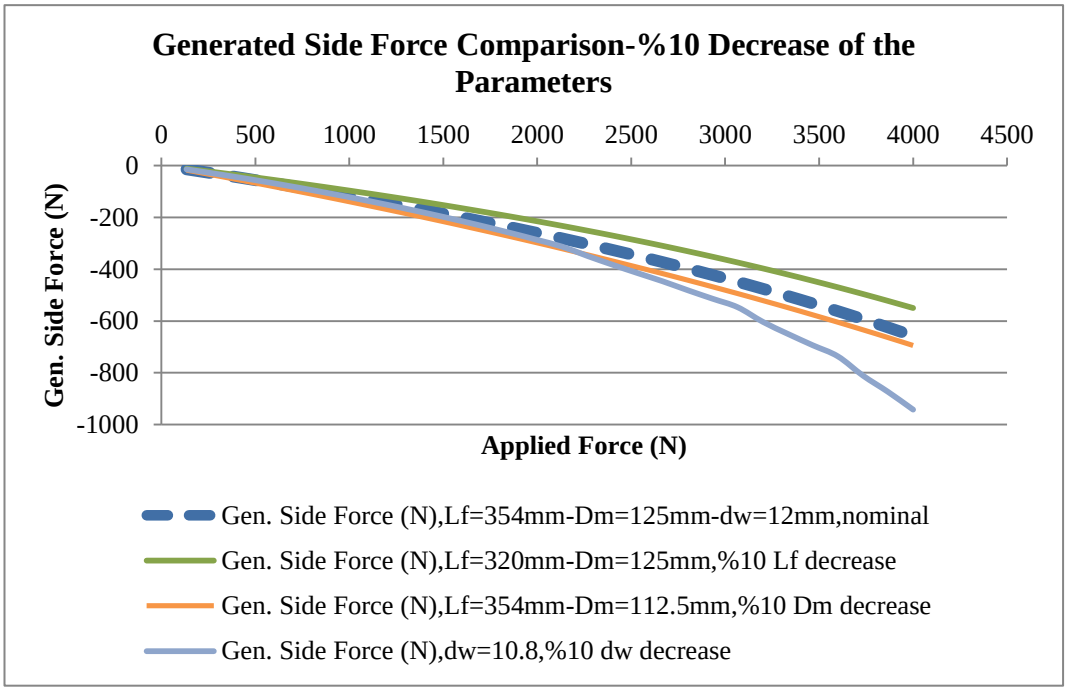

Figure 4-61: Generated Side Force Comparison-%10 Decrease Effect of Parameters

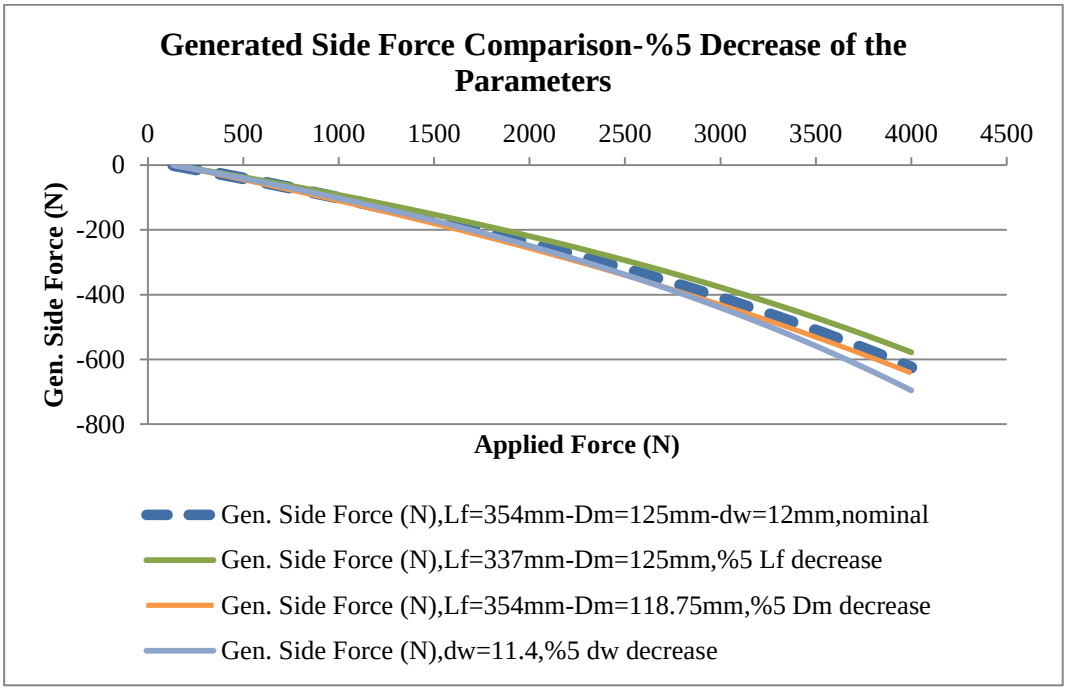

Figure 4-62: Generated Side Force Comparison-%5 Decrease Effect of Parameters

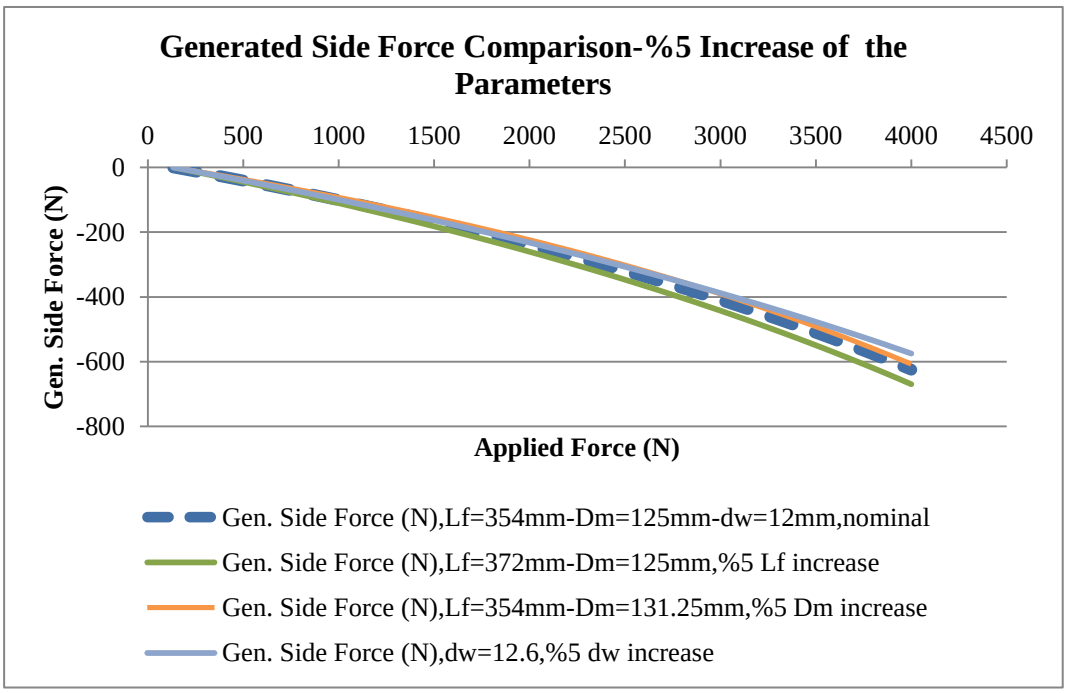

Figure 4-63: Generated Side Force Comparison-%5 Increase Effect of Parameters

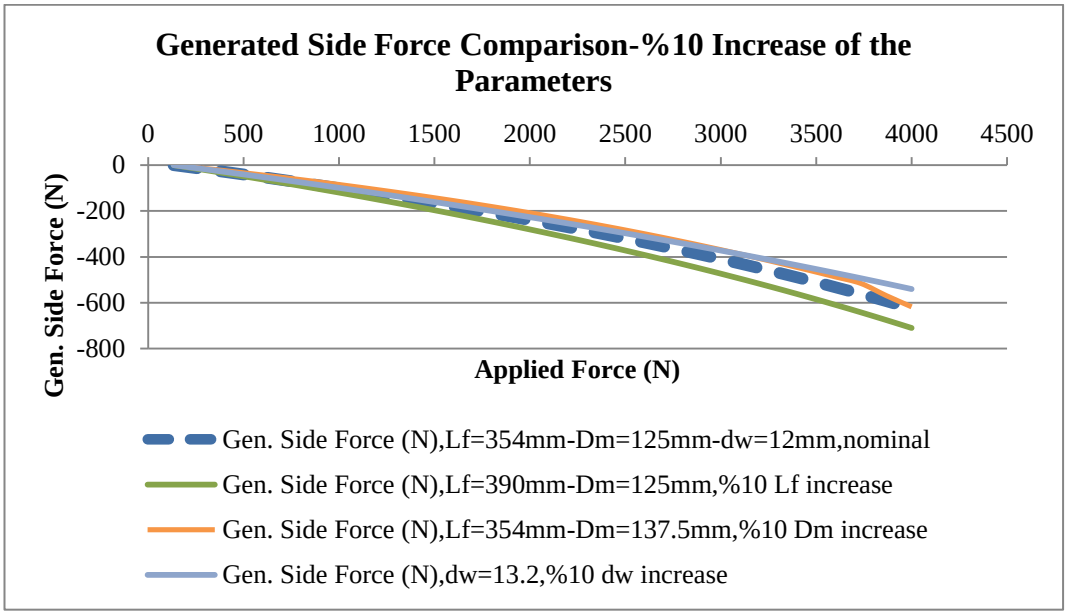

Figure 4-64: Generated Side Force Comparison-%10 Increase Effect of Parameters

4.4. GUI DESIGN

After the initial analyses of side load springs, a need for a GUI that generates side load spring centerline curvature has been realized. Therefore, a GUI which can respond to the needs is developed. The designed GUI allows the user enter the design inputs like free length of the spring, angle of the spring force action line, other spring properties and so on. In the GUI, there are two options which allow the user to enter different inputs. First option contains four parameters; offset at the top seat, force angle, mean diameter of the coil, and free length of the spring; while the second option has more parameters which are related to the stiffness of the spring. Further, illustration of the inputs can be shown in another window if it is desired, as illustrated in Figure 4-69. After the inputs are provided, GUI gives the centerline curvature as a figure in 3D or 2D view, shows the upper-lower hard points and the force action line, and also enables the user to save the data of the centerline curvature in an Excel file which will be used for modeling. The features and the illustrations of the GUI can be seen from Figure 4-65 to Figure 4-69.

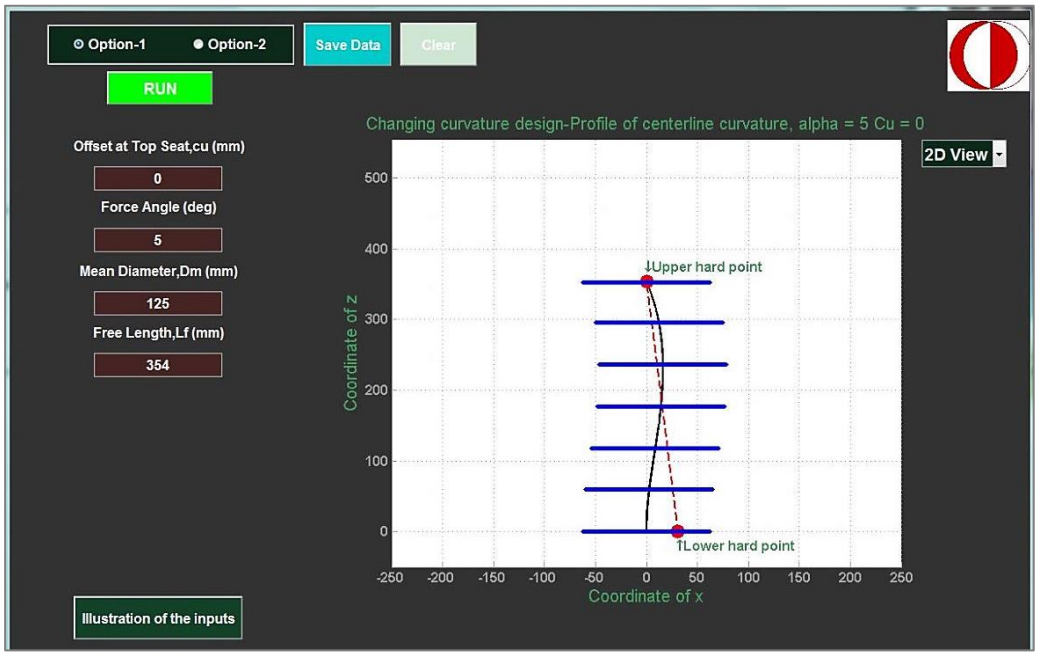

Figure 4-65: GUI View-1 (Option-1,2D View)

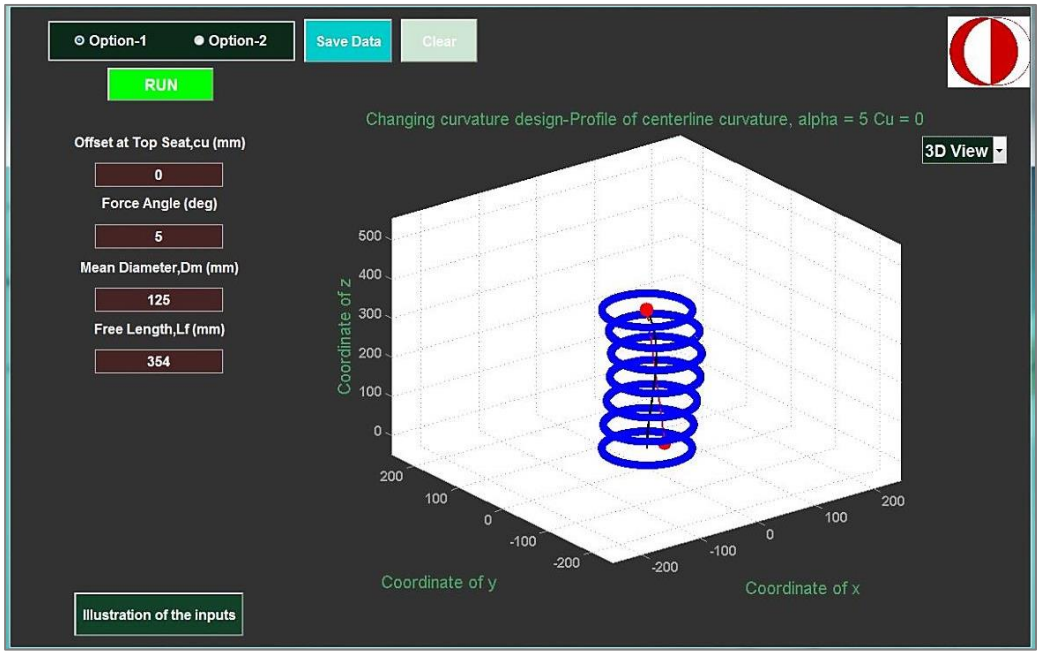

Figure 4-66: GUI View-2 (Option-1,3D View)

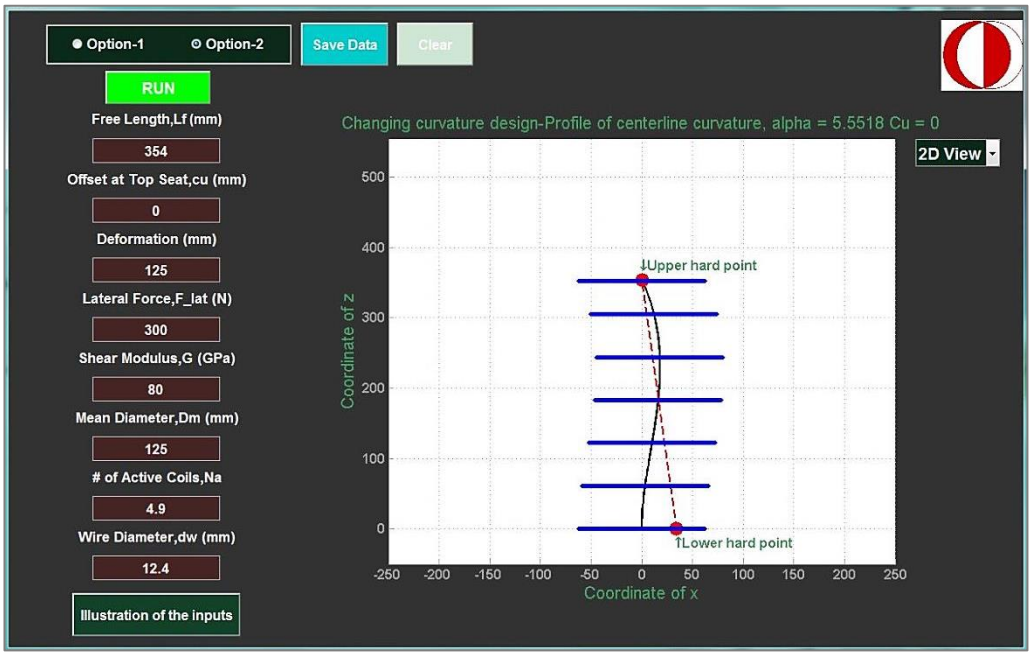

Figure 4-67: GUI View-3 (Option-2,2D View)

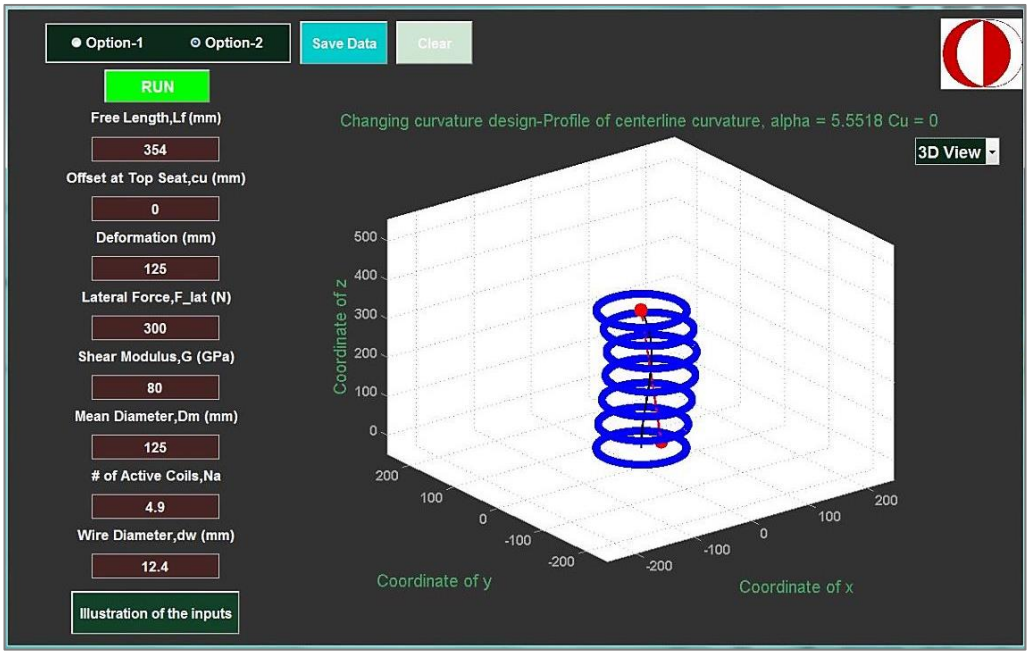

Figure 4-68: GUI View-4 (Option-2,3D View)

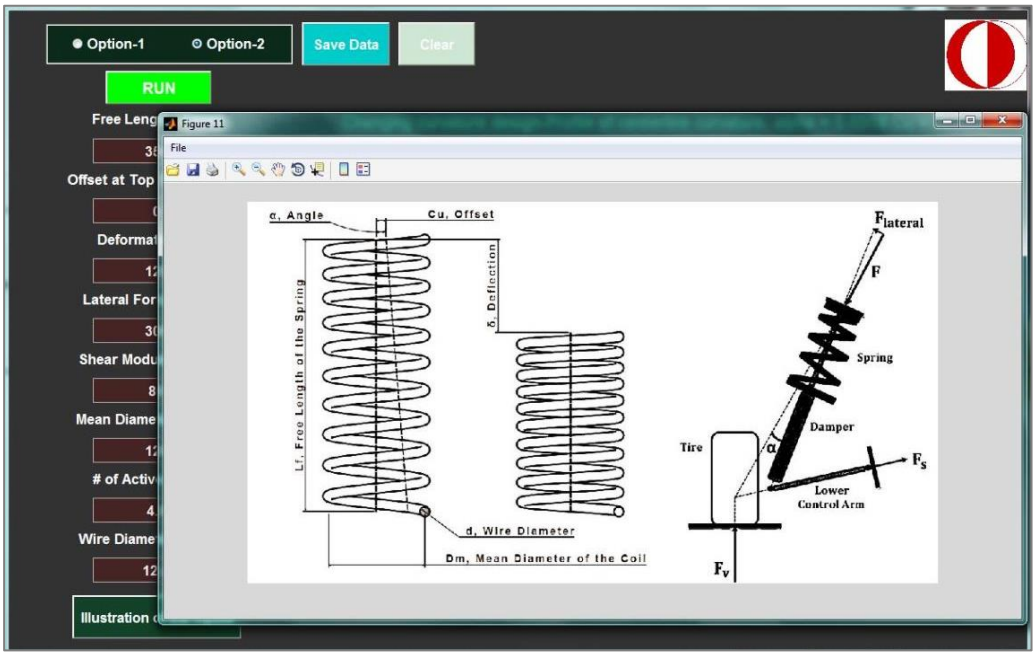

Figure 4-69: GUI View-5 (Illustration of the inputs)

The designed GUI satisfies the requirements for now, however it can be improved, more options can be added, inputs can be detailed and screen options can be changed.

CHAPTER 5

SUMMARY AND CONCLUSIONS

5.1. SUMMARY

In this study, design procedures of side load springs were examined and mathematical models for the centerline curvature of side load spring are investigated. By using this mathematical model, side load springs were modeled and analyzed.

Before starting analyses of side load spring, static analysis of a conventional helical coil spring was carried out in ANSYS to validate the analysis model with the theoretical results. While validating the analysis model; spring geometry, spring end connection types, spring seat types, and material properties were examined. After static analysis results were validated, analyses of intuitively designed side load springs were done with the same method and the results of conventional spring and side load spring were compared. In these analyses, side load springs like S-shaped, C-shaped, L-shaped, varying diameter and so forth were investigated. However, only the magnitudes of side force were investigated and compared in these analyses, no mathematical model was used or evaluated for these design options.

After intuitively designed side load springs were investigated, a mathematical formulation was obtained to design side load springs. Centerline curvatures were obtained by using this formulation and data for the curvature of the side load spring axis was exported to CATIA for modeling and then analyses of the designed side load springs were done in ANSYS. Also, a MATLAB GUI was developed to ease the design procedure.

5.2. CONCLUSIONS

Static analyses results of the conventional coil springs showed that mesh size is a critical analysis parameter for the convergence of the analysis results and the spring seat types is an important feature of the spring while the other parameters mesh type and spring end connection types are not so critical. It is also concluded that conventional coil springs are not able to generate side force, and side force reduction in the MacPherson strut suspension is not possible by using the conventional coil springs. Since, the common application of; mounting the spring in an inclined position is not always possible due to space limitations. Therefore, using side load springs is a strong alternative to reduce side force for improving ride comfort.

In order to generate side force, evaluated mathematical formulation was used to design side load springs and analyses are done with these springs. The analysis results showed that the designed side load springs have the ability of generating side force at desired level that means it can reduce lateral forces on the damper and improves the ride quality. Additionally, spring rate of the side load springs do not change very much when compared to conventional coil springs. Results of the maximum shear stress and the deflection for the applied load are very similar, that means side load springs can be replaced by conventional springs without losing performance and without requiring extra structural elements.

In the studies, the GUI was used for side load spring design and that enables user a practical way to change parameters easily and quickly and providing data for side load spring modeling. However, it can be improved and may be connected to other used software to make the operations to complete the procedure faster.

Finally, a rough sensitivity analysis was carried out and the results showed that free length of the spring and mean diameter of the coil affect the results most significantly, while wire diameter is less important. Hence, free length of the spring and mean diameter of the coil should be determined first while designing side load springs.

5.3. FUTURE WORK

In future work, an algorithm that optimizes the lateral force reduction for all spring models may be developed. Design, modeling, and analysis procedure may be integrated by automatically connecting them.

Furthermore, mathematical model can be expanded in such a way to include the other side load spring models. Especially, design of pigtail coil spring may be investigated and a mathematical model for side load spring with pigtail ends may be obtained.

In addition to these, a side load spring sample may be manufactured and experimental studies can be done with it and then, experimental test results and analysis results may compared.

Lastly, the designed GUI can be improved and expanded related to future studies.

BIBLIOGRAPHY

[1] "Double wishbone,MacPherson strut,Solid Axle and Twist beam-Aermech.com." [Online]. Available: http://aermech.com/double-wishbonemacpherson-strutsolid-axle-and-twist-beam/. [Accessed: 26-Aug-2015].

[2] T. Wünsche, K.-H. Muhr, K. Biecker, and L. Schnaubelt, "Side Load Springs as a Solution to Minimize Adverse Side Loads Acting on the McPherson Strut," *SAE Technical Paper 940862*, 1994.

[3] "Springs - Passenger Cars - GKN Land Systems." [Online]. Available: http://www.gknservice.com/global/passenger_cars/springs.html. [Accessed: 26-Aug-2015].

[4] S. Suzuki, S. Kamiya, T. Imaizumi, and Y. Sanada, "Approaches to Minimizing Side Force of Helical Coil Springs for Riding Comfort," *SAE Technical Paper 960730*, 1996.

[5] T. Gotoh and T. Imaizumi, "Optimization of Force Action Line with New Spring Design on the Macpherson Strut Suspension for Riding Comfort," *SAE Technical Paper 2000-01-0101*, 2000.

[6] T. Hamano, T. Nakamura, H. Enomoto, N. Sato, S. Nishizawa, and M. Ikeda, "Development of L-Shape Coil Spring to Reduce a Friction on the McPherson Strut Suspension System," *SAE Technical Paper 2001-01-0497*, 2001.

[7] S. Nishizawa, M. Ikeda, J. Logsdon, H. Enomoto, N. Sato, and T. Hamano, "The Effect of Rubber Seats on Coil Spring Force Line," *SAE Technical Paper 2002-01-0317*, 2002.

[8] S. Nishizawa, W. Ruiz, T. Sakai, and M. Ikeda, "Parametric Study of the Spring Force Line Effect on Vehicle Self Steer for MacPherson Strut Suspension System," *SAE Technical Paper 2006-01-1375*, 2006.

[9] J. Liu, D. J. Zhuang, F. Yu, and L. M. Lou, "Optimized Design for a MacPherson Strut Suspension with Side Load Springs," *Int. J. Automot. Technol.*, vol. 9, no. 1, pp. 29–35, 2008.

[10] Y. I. Ryu, D. O. Kang, S. J. Heo, H. J. Yim, and J. I. Jeon, "Development of analytical process to reduce side load in strut-type suspension," *J. Mech. Sci. Technol.*, vol. 24, no. 1, pp. 351–356, 2010.

[11] J. Choi, D. An, and J. Won, "Bayesian Approach for Structural Reliability Analysis and Optimization Using the Kriging Dimension Reduction Method," *J. Mech. Des.*, vol. 132, no. 5, pp. 1–11, May 2010.

[12] A. H. Joshi and H. Singh Chhabra, “Mathematical Model to Find Piercing Point in McPherson Strut Suspension and Design of profile for Side Force Control Spring,” *SAE Technical Paper 2012-28-0014*, 2012.

[13] B. J. Finn and G. R. Hawkins, “SUSPENSION STRUT WITH SIDE LOAD SUPPORT,” US 4883288, 1989.

[14] K.-H. Muhr and L. Schnaubelt, “WHEEL SUSPENSION,” US 4903985, 1990.

[15] I. J. Warmuth II, “Side load compensating air suspension,” EP 0225271 B1, 1992.

[16] I. Ivan J. Warmuth, “SIDE LOAD COMPENSATING AIR SUSPENSION,” US 4688774, 1987.

[17] D. M. Hurtubise, K. A. Perry, D. P. Kudla, and L. E. Armstrong, “STRUT ASSEMBLY WITH INTEGRAL BEARING AND SPRING SEAT,” US 5467971 A, 1995.

[18] G. D. Dronen and R. A. Hellyer, “STRUT ASSEMBLY WITH BEARING AXIS ALIGNMENT,” US 5454585 A, 1995.

[19] T. Imaizumi, T. Aoyama, S. Kamiya, T. Gotoh, and K. Irie, “HELICAL COMPRESSION SPRING FOR A VEHICLE SUSPENSION,” US 6328290 B1, 2001.

[20] T. Imaizumi, “HELICAL COMPRESSION SPRING FOR A VEHICLE SUSPENSION,” US 6712346 B2, 2004.

[21] K. Hasegawa and T. Imaizumi, “CURVED HELICAL COMPRESSION SPRING,” US 6375174 B2, 2002.

[22] J. S. Kessen and D. J. Fanson, “SPRING HAVING COILS OF VARYING DIAMETERS,” US 6481701 B2, 2002.

[23] T. Imaizumi, “HELICAL COMPRESSION SPRING FOR A VEHICLE SUSPENSION,” US 6616131 B2, 2003.

[24] M. V. Bottene, J. A. Fader, J. Steven J. Doyle, M. G. Williams, S. G. Saieg, G. N. Lasic, and T. R. King, “STRUT SPRING SEAT,” US 2004/0169324 A1, 2004.

[25] M. V. Bottene, J. A. Fader, J. Steven J. Doyle, M. G. Williams, S. G. Saieg, G. N. Lasic, and T. R. King, “MACPHERSON STRUT SPRING COIL MOUNTS,” US 2004/0169323 A1, 2004.

[26] M. V. Bottene, J. A. Fader, J. Steven J. Doyle, M. G. Williams, S. G. Saieg, G. N. Lasic, and T. R. King, “COIL SPRING WITH LATERAL BIAS,” US 6883790 B2, 2005.

[27] M. V. Bottene, J. A. Fader, J. Steven J. Doyle, M. G. Williams, S. G. Saieg, G. N. Lasic, and T. R. King, “STRUT SIDE LOADING DOUBLE WOUND TORSION SPRING,” US 2004/0178601 A1, 2004.

[28] Z. Lijun, M. Dejian, W. Shizhong, and Y. Zhuoping, “Optimization method facing lateral force of Macpherson suspension shock absorber,” CN 103310047 A, 2013.

[29] R. Budynas and K. Nisbett, “Shigley’s Mechanical Engineering Design, Ninth Edition,” *McGraw Hill Inc.*, 2009.

[30] T. M. Mulla, S. J. Kadam, and V. S. Kengar, “FINITE ELEMENT ANALYSIS OF HELICAL COIL COMPRESSION SPRING FOR THREE WHEELER AUTOMOTIVE FRONT,” *Int. J. Mech. Ind. Eng.*, vol. 2, no. 3, pp. 74–77, 2012.

[31] “Lesjöfors Automotive - Technical - Types of Spring.” [Online]. Available: http://www.lesjofors-automotive.com/springs-production/types-of-spring.asp. [Accessed: 26-Aug-2015].

[32] J. J. Tao and T. A. Bishop, “System Modeling of A Damper Module,” *SAE Technical Paper 2000-01-0727*, 2000.

[33] J. J. Tao, “MODELING SUSPENSION DAMPER MODULES USING LS-DYNA,” *7th International LS-DYNA Users Conference*. 2002.

[34] A. Ouakka and S. Gillet, “Suspension Coil Spring and Rubber Insulators : Towards a Methodology of Global Design,” *Vehicle Dynamics Expo*. 2006.

[35] S. N. Gundre and P. A. Wankhade, “A Finite Element Analysis Of Helical Compression Spring For Electric Tricycle Vehicle Automotive Front Suspension,” *Int. J. Eng. Res. Technol.*, vol. 2, no. 6, pp. 1800–1804, 2013.

[36] S. Pattar, S. J. Sanjay, and V. B. Math, “Static Analysis of Helical Compression Spring,” *Int. J. Res. Eng. Technol.*, vol. 3, no. 3, pp. 835–838, 2014.

[37] N. Lavanya, P. S. Rao, and M. P. Reddy, “Design and Analysis of A Suspension Coil Spring For Automotive Vehicle,” *Int. J. Eng. Res. Appl.*, vol. 4, no. 9, pp. 151–157, 2014.

[38] P. J. C. J and R. Pavendhan, “Design and Analysis of Two Wheeler Shock Absorber Coil Spring,” in *International Conference on Advances in Engineering and Management (ICAEM)*, 2014.

APPENDIX A

STATIC ANALYSIS OF SOME CONVENTIONAL SPRING MODELS

There are many papers about static analysis of coil springs, and several of them are investigated during static analysis studies. One of them is selected as a sample and studies are carried on with that spring model, static analysis results of the rest of the spring models are given here.

Table A-1: Spring Properties of Model-C [35]

Wire diameter, d		11 mm
Mean diameter of the coil, D		61 mm
Number of Active Coils, n		11
Number of Total Coils, n’		13
Free length of the spring, L_f		227.5 mm
Solid length of the spring, L_s		142.7 mm
Load, W		2450 N
Material (Music Wire)	Elastic Modulus, E	E=210 GPa
	Poisson Ratio, ν	ν=0.28
	Shear Modulus, G	G=80 GPa

$$Maximum\ Shear\ Stress:\ \ \tau = K \cdot \frac{8W.C}{\pi.d^2} = (1.276) * \frac{(8 * 2450 * 5.55)}{(3.14 * (11.10^{-3})^2)} * 10^{-6}$$

$$= \mathbf{365\ MPa}$$

$$Deflection:\ \ \delta = \frac{8W.C^3.n}{G.d} = \frac{(8 * 2450 * 5.55^3 * 11)}{(80.10^9 * 11.10^{-3})} * 10^3 = \mathbf{41.8\ mm}$$

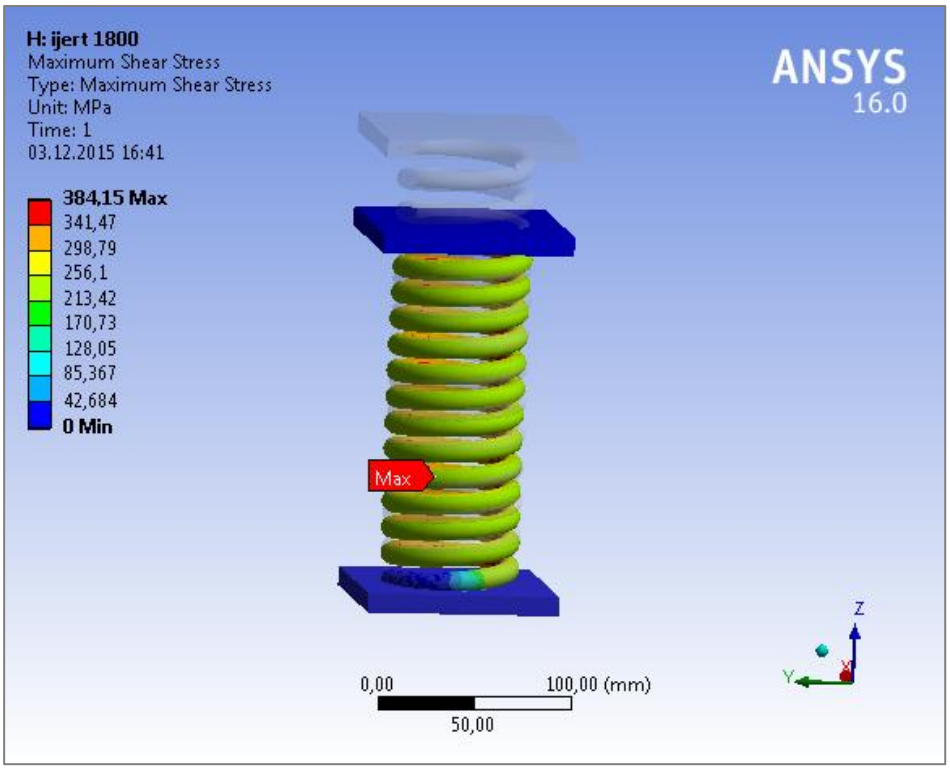

Figure A-1: Result of Max. Shear Stress Analysis of Model-C

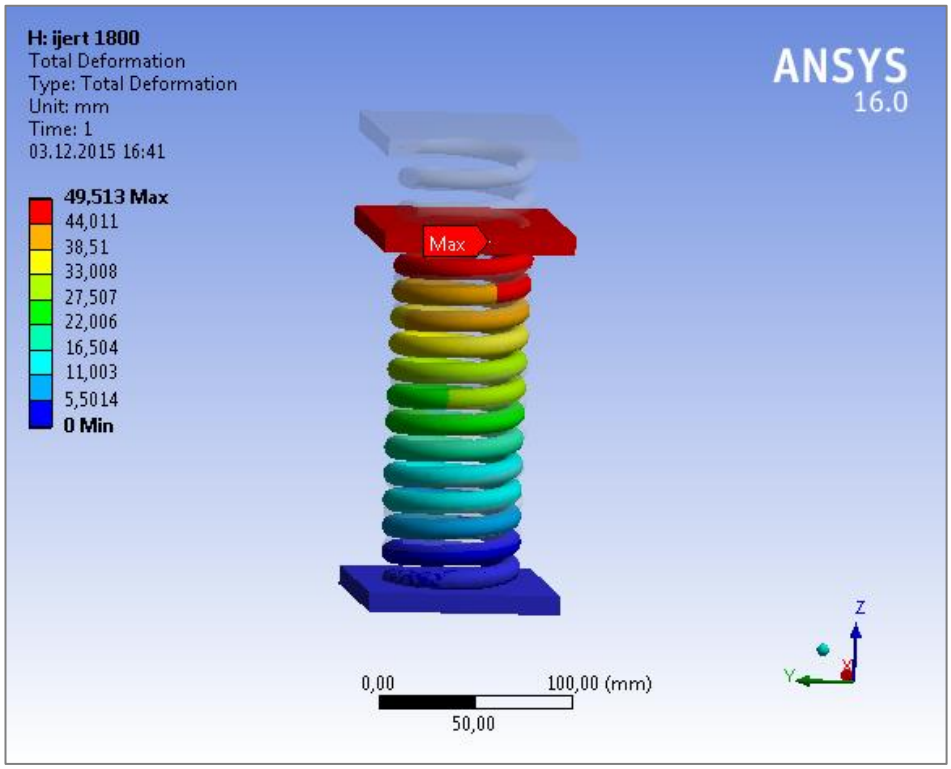

Figure A-2: Result of Deflection Analysis of Model-C

Table A-2: Spring Properties of Model-D [36]

Wire diameter, d		0.45 mm
Mean diameter of the coil, D		4.35 mm
Number of Active Coils, n		6
Free length of the spring, L_f		10.2 mm
Pitch		1.75 mm
Load, W		3 N
Material (Music Wire)	Elastic Modulus, E	E=193 GPa
	Poisson Ratio, ν	ν=0.3
	Shear Modulus, G	G=77 GPa

$$Maximum\ Shear\ Stress:\ \ \tau = K \cdot \frac{8W.C}{\pi.d^2}$$

$$= (1.15) * \frac{(8 * 3 * 9.67)}{(3.14 * (0.45 * 10^{-3})^2)} * 10^{-6} = \mathbf{420\ MPa}$$

$$Deflection:\ \ \delta = \frac{8W.C^3.n}{G.d} = \frac{(8 * 3 * 9.67^3 * 6)}{(80.10^9 * 0.45 * 10^{-3})} * 10^3 = \mathbf{3.8\ mm}$$

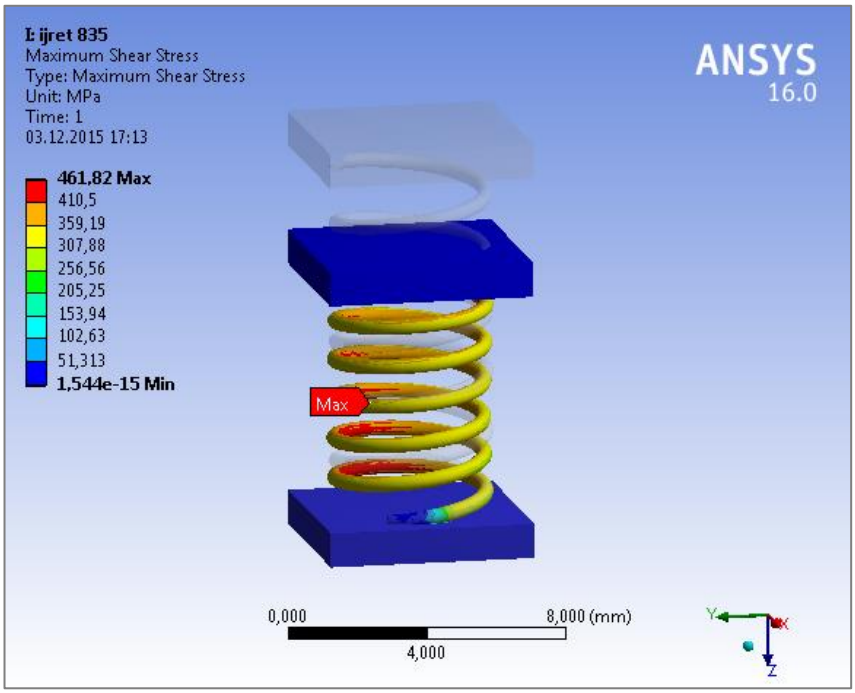

Figure A-3: Result of Max. Shear Stress Analysis of Model-D

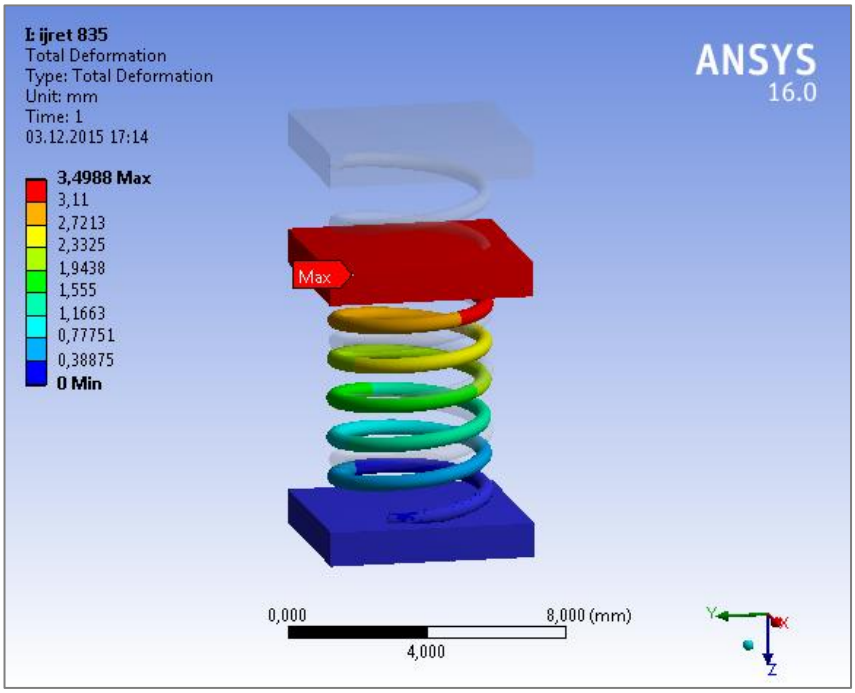

Figure A-4: Result of Deflection Analysis of Model-D

Table A-3: Spring Properties of Model-E [37]

Wire diameter, d		9.5 mm
Mean diameter of the coil, D		47.5 mm
Number of Active Coils, n		11
Free length of the spring, L_f		152 mm
Pitch		13.8 mm
Load, W		2750 N
Material (Music Wire)	Elastic Modulus, E	E=207 GPa
	Poisson Ratio, ν	ν=0.27
	Shear Modulus, G	G=80 GPa

$$Maximum\ Shear\ Stress:\ \ \tau = K \cdot \frac{8W.C}{\pi.d^2}$$

$$= (1.31) * \frac{(8 * 2750 * 5)}{(3.14 * (9.5 * 10^{-3})^2)} * 10^{-6} = \mathbf{510\ MPa}$$

$$Deflection:\ \ \delta = \frac{8W.C^3.n}{G.d} = \frac{(8 * 2750 * 5^3 * 11)}{(80.10^9 * 9.5 * 10^{-3})} * 10^3 = \mathbf{39.8\ mm}$$

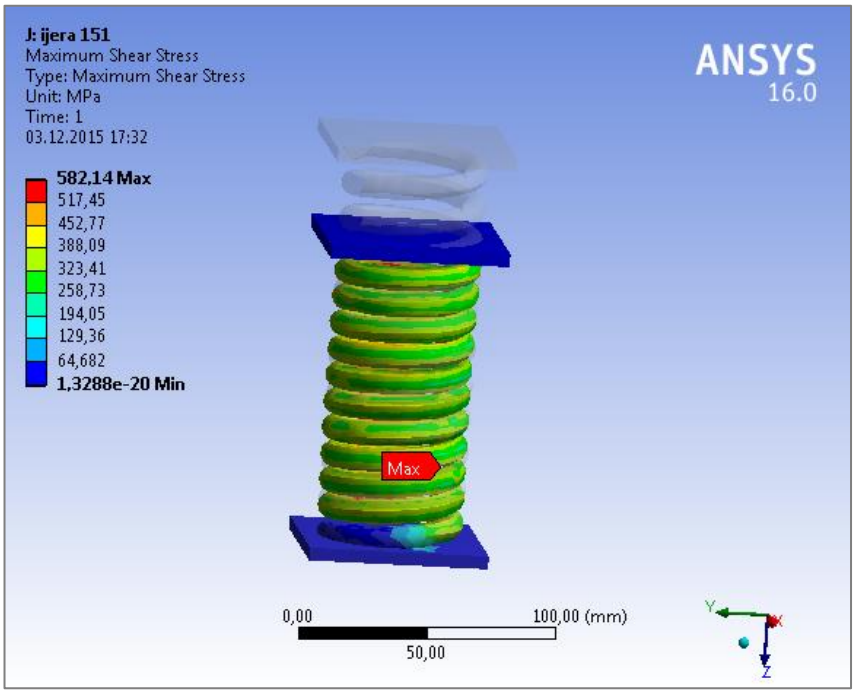

Figure A-5: Result of Max. Shear Stress Analysis of Model-E

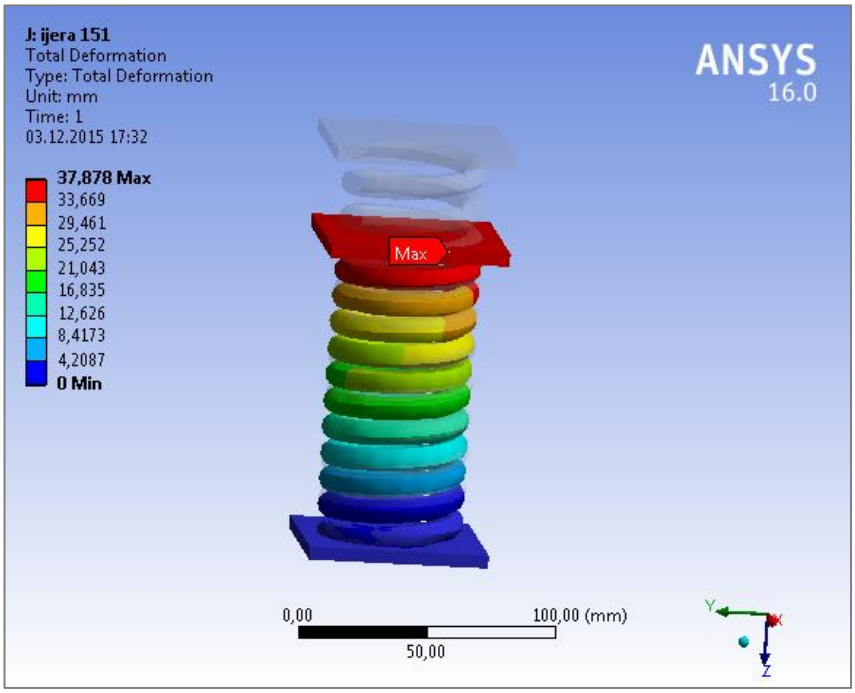

Figure A-6: Result of Deflection Analysis of Model-E

Table A-4: Spring Properties of Model-F [38]

Wire diameter, d		6.7 mm
Mean diameter of the coil, D		33.3 mm
Number of Active Coils, n		15
Number of Total Coils, n'		17
Free length of the spring, L_f		167.8 mm
Solid length of the spring, L_s		113.9 mm
Load, W		360 N
Material (Music Wire)	Elastic Modulus, E	E=200 GPa
	Poisson Ratio, ν	ν=0.25
	Shear Modulus, G	G=78.6 GPa

$$Maximum\ Shear\ Stress:\ \ \tau = K \cdot \frac{8W.C}{\pi.d^2}$$

$$= (1.313) * \frac{(8 * 360 * 5)}{(3.14 * (6.7 * 10^{-3})^2)} * 10^{-6} = \mathbf{133\ MPa}$$

$$Deflection:\ \ \delta = \frac{8W.C^3.n}{G.d} = \frac{(8 * 360 * 5^3 * 15)}{(78.6 * 10^9 * 6.7 * 10^{-3})} * 10^3 = \mathbf{10.1\ mm}$$

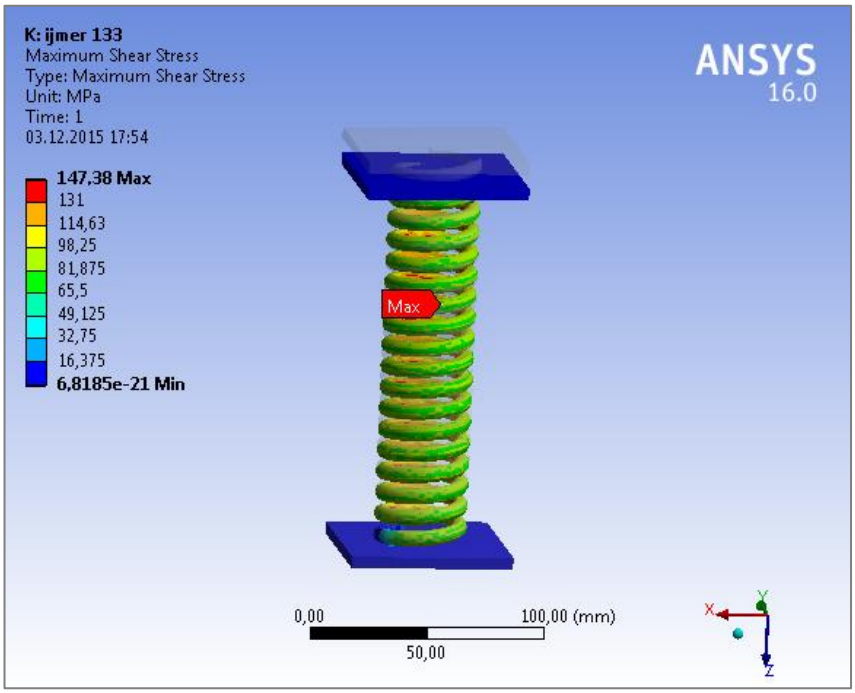

Figure A-7: Result of Max. Shear Stress Analysis of Model-F

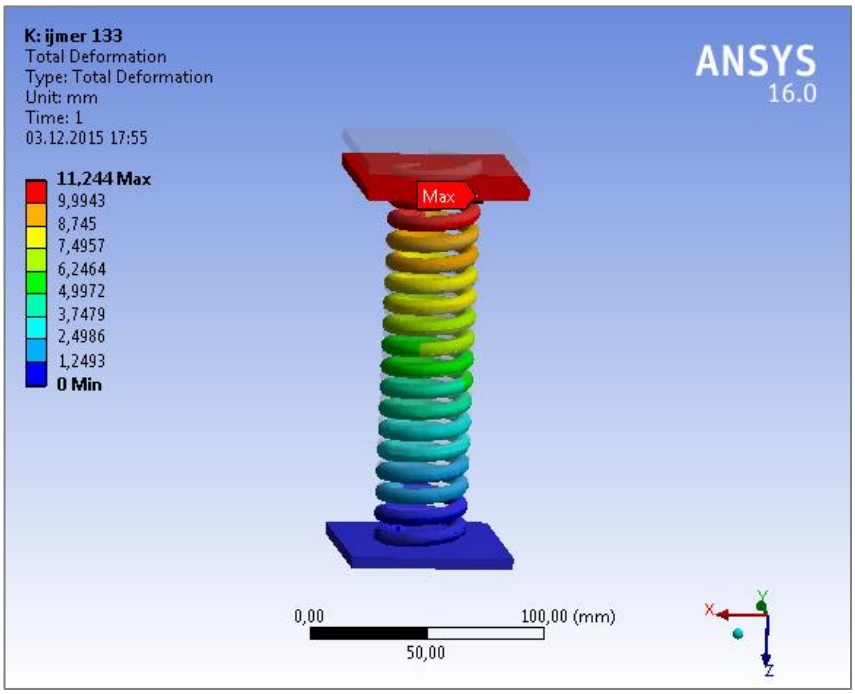

Figure A-8: Result of Deflection Analysis of Model-F